EVOLUTION OF THE JEANNE D'ARC BASIN, OFFSHORE NEWFOUNDLAND, CANADA: 3D SEISMIC EVIDENCE FOR >100 MILLION YEARS OF RIFTING

by

BEATRIZ ELENA SERRANO SUAREZ

A thesis submitted to the

Graduate School – New Brunswick

Rutgers, The State University of New Jersey

in partial fulfillment of the requirements

for the degree of

Master of Science

Graduate program in Geological Sciences

written under the direction of

Dr. Martha O. Withjack

Dr. Roy W. Schlische

and approved by

New Brunswick, New Jersey

January 2013

ABSTRACT OF THE THESIS

Evolution of the Jeanne d'Arc basin, offshore Newfoundland, Canada: 3D seismic evidence for >100 million years of rifting

by BEATRIZ ELENA SERRANO-SUAREZ

Thesis Directors:

Dr. Martha O. Withjack and Dr. Roy W. Schlische

The Jeanne d'Arc rift basin formed during the breakup of Pangea from Late Triassic through Early Cretaceous time. Previous studies concluded that rifting was episodic, occurring during two or three distinct events with intervening periods of thermal subsidence. To test these conclusions, I used 3D seismic-reflection data, well data, and restoration techniques to determine the spatial and temporal evolution of the Flying Foam region in the northwestern part of the Jeanne d'Arc rift basin. The Flying Foam region lies between the NNE-striking, E-dipping Mercury and Murre border faults of the basin. In the southern Flying Foam region, a series of basement-involved faults are present between the Mercury and Murre faults. In the north, a major anticline (the Flying Foam structure) overlies the Murre fault. I have identified three syn-rift tectonostratigraphic packages, none of which are present in the footwall of the Mercury fault. Strata within the basal Late Triassic/Early Jurassic syn-rift package thicken toward basement-involved faults. This package contains salt of the Argo Formation, which decouples the basement-involved faults from shallow structures. The overlying Jurassic package lacks evident fanning toward the Murre and Mercury faults. However, changes in thickness across the

Murre fault and along-strike thickness variations in the hanging-wall of the Mercury fault reflect displacement on the faults during deposition. The overlying Early Cretaceous package thins toward the Flying Foam anticline, a structure produced by a combination of forced folding above the Murre fault and fault-bend folding associated with a listric fault that detaches within the Argo salt. Thus, the Early Cretaceous package is also a syn-rift unit. In conclusion, my work indicates that the tectonic process of rifting in the Jeanne d'Arc basin was not episodic but rather was persistent, occurring from the Late Triassic through the Early Cretaceous. However, the intensity and the direction of the extension could have changed through time.

ACKNOWLEDGMENTS

I would like to especially thank my advisors, Dr. Martha Withjack and Dr. Roy Schlische, for their incredible patience and dedication and also for their unconditional support and contribution to this work. I would also like to thank Dr. Karen Bemis and Dr. Kevin Lyons for their continuous feedback and follow up. Additional thanks to WesternGeco for providing the seismic data, the Canada-Newfoundland offshore Petroleum Board for providing the well data, and the National Science Foundation, Husky Energy, and the Department of Earth and Planetary Sciences of Rutgers University for their financial support. I would like to thank Schlumberger and Energy Information, Software & Solutions for providing the Petrel and SMT seismic interpretation software, respectively. My gratitude also goes to my husband Andres and my parents and family for all the support to finish my studies at Rutgers. I also thank my friends and faculty from the Earth and Planetary Science Department who supported me during this time.

TABLE OF CONTENTS

LIST OF TABLES

LIST OF APPENDICES

LIST OF ILLUSTRATIONS

1. Introduction

The Jeanne d'Arc rift basin is located on the Grand Banks of Canada, offshore Newfoundland (Figs. 1 and 2). This basin is one of the most important oil provinces of Canada with four oil-producing fields: Hibernia, Whiterose, Terra Nova and North Amethyst (Appendix 1, www.cnlopb.nl.ca). The basin developed during the breakup of the supercontinent Pangea during the Mesozoic (e.g. Louden, 2002; Seton *et al.*, 2012; Withjack *et al.*, 2012a), and it is part of the more extensive eastern North American rift system (Fig. 1).

The onset of rifting in this rift system was relatively synchronous and began by the Late Triassic, but the cessation of rifting and onset of seafloor spreading was diachronous, ranging from latest Triassic in the southern segment (southeastern United States), to Early Jurassic in the central segment (northeastern United States and southern Canada) and Late Cretaceous in the northern segment (eastern Grand Banks of Canada) (Withjack *et al.*, 1998; Schlische *et al.*, 2002; Withjack and Schlische, 2005; Withjack *et al.*, 2012a). In the Jeanne d'Arc basin, some authors suggest that rifting occurred in two or three distinct episodes with intervening periods of thermal subsidence (e.g. Hubbard *et al.*, 1985; Tankard and Welsink, 1987; Hubbard, 1988; Sinclair, 1988; Grant and McAlpine, 1990; McAlpine, 1990; Sinclair and Riley, 1995; Sinclair *et al.*, 1999) (Fig. 3). My goal is to study the rift evolution of the Jeanne d'Arc basin using 3D seismic and well data from the Flying Foam area, in the northwestern corner of the basin, and to address the following questions:

- Are structures detached or basement-involved?

- When did deformation occur?
- Is rifting episodic or persistent?

The 3D seismic data available in this study provide numerous cross-sectional views and time-slices that image structures and strata relatively well in the Flying Foam area. Additionally, formation tops and unconformities from five wells provide the time frame for the interpretation.

2. Geologic and structural background

The Jeanne d'Arc basin is a funnel-shaped, 25-80 km wide, half graben that deepens and widens northward (Tankard and Welsink, 1987) (Fig. 2). The NNE-striking, E-dipping Murre fault in the south and Mercury fault in the north bound the basin on the west (e.g. Enachescu, 1987; Tankard and Welsink, 1987). Intrabasinal faults generally strike NW-SE and detach on salt (e.g. Tankard and Welsink, 1987; Withjack and Schlische, 2005). The study area, in the northwestern corner of the basin, lies between the Mercury and the Murre faults. The Flying Foam anticline overlies the Murre fault in the north; in contrast, in the south, several basement-involved faults occur between the Mercury and the Murre faults.

Pre-rift rocks consist of Paleozoic igneous and metamorphic rocks from the Avalon and/or Meguma terrains (Tankard and Balkwill, 1989) (Fig. 3). Several orogenies (Ordovician Taconic, Devonian Acadian and Carboniferous-Permian Alleghanian) preceded rifting (Naylor, 1971; Rodgers, 1971; Murphy and Keppie, 1998; Williams, 1999; Cocks and Torsvik, 2011). The overlying sedimentary section (Fig. 3) consists of

Late Triassic – Early Jurassic siliciclastic rocks from the Eurydice Formation and salt from the Argo Formation (e.g. Jansa and Wade, 1975; McAlpine, 1990). The overlying Early Jurassic to Late Jurassic section consists of dolomites, limestones, calcareous shales and some sandstones from the Iroquois, Downing, Voyager and Rankin formations (e.g. McAlpine, 1990; Sinclair *et al.*, 1999). Within the Rankin Formation, an organic-rich shale (the Egret Member) sources the hydrocarbons of the Jeanne d'Arc basin (e.g. Magoon *et al.*, 2005). The overlying latest Jurassic – Early Cretaceous section consists of sandstones, shales and some limestones from the Jeanne d'Arc, Avalon, Whiterose, Catalina, Hibernia, Nautilus and Ben Nevis formations (e.g. McAlpine, 1990; Sinclair, *et al*., 1999). Sandstones from the Hibernia and Avalon formations are the main reservoir rocks in the Jeanne d'Arc basin (e.g. Magoon *et al*., 2005). Finally, the Late Cretaceous – Cenozoic section consists of shales and some sandstones from the Dawson Canyon and Banquerau formations (e.g. Deptuck *et al.*, 2003). In general, studies suggest that the Late Triassic – Early Jurassic and the latest Jurassic – Early Cretaceous sections correspond to periods of active rifting, whereas the Early Jurassic to Late Jurassic section represents a period of tectonic quiescence (e.g. Hubbard *et al.*, 1985; Tankard and Welsink, 1987; Hubbard, 1988; Sinclair, 1988; Grant and McAlpine, 1990; McAlpine, 1990; Grant and McAlpine, 1990; McAlpine, 1990; Sinclair and Riley, 1995; Sinclair *et al.*, 1999; Welsink and Tankard, 2012). The Late Cretaceous – Cenozoic section corresponds to post-rift rocks that accumulated during the thermal subsidence of the basin (e.g. McAlpine, 1990; Sinclair, *et al*., 1999). This study focuses on the Late Triassic to Early Cretaceous sections.

3. Data and methodology

3.1 Seismic data

This study involves the interpretation of 3D seismic data from the Flying Foam area in the Jeanne d'Arc basin. The digital data, provided by WesternGeco, were acquired in 1995 and consist of 1532 E-W inlines, 3150 N-S crosslines, and 2250 time-slices (Table 1). Inlines and crosslines are generic names given to sequentially numbered orthogonal seismic profiles for 3D seismic surveys (Hart, 1999). An inline is a seismic line that parallels the movement direction of the ship acquiring the data. Crosslines are perpendicular to the inlines. A time-slice is a horizontal plane through a 3D-seismic volume at a given TWT (two-way time). Each inline and crossline is 39 km long, but the interpretable length is ~30 km for the inlines and ~36 km for the crosslines, yielding a total interpretable area of 1080 km^2. Table 1 lists the main seismic-acquisition parameters, and Appendix 2 gives the seismic processing report (Schlumberger and Geco-Prakla, 1996). The data quality is good, but the presence of peg-leg multiples commonly masks the true geometry of the reflections (Figs. 4 and 5). The displays of inlines and crosslines in this thesis have a vertical exaggeration of 1:1 assuming an average velocity of 4.0 km/s (an average velocity supported by velocity surveys from Line HBV83-195; Appendices 2 and 3).

3.2 Seismic interpretation

Tectonostratigraphic packaging (Fig. 6) provides information about the relative timing of events and the structural style of a region, and therefore, is an appropriate method to study the evolution of the Flying Foam area. The first step consists of identifying unconformity-bounded packages. For example, the rift-onset unconformity separates the pre-rift and the syn-rift packages, and the post-rift unconformity separates the syn-rift and the post-rift packages (e.g. Withjack *et al.*, 2002). Differences in the characteristics of the reflections define other packages. For example, high-ductility units lack internal reflections and decouple the deeper and shallow deformation. Fault-related growth beds thicken toward a fault on the downthrown side of a fault or exhibit differences in thickness of correlative strata on each side of a fault (e.g. Withjack *et al*., 2002). Fold-related growth beds thin toward the crest of antiforms and thicken toward the troughs of synforms (e.g. Withjack *et al*., 2002). The tie between inlines, crosslines and time-slices helped defined the 3D geometry of packages, horizons and structures in the study area. The interpretation also included the mapping of major and some minor structures (e.g., detached faults).

3.3 Well data and correlation with seismic data

Formation tops and unconformities from five wells in the study area are available from the Canada-Newfoundland Labrador Offshore Petroleum Board (CNLOPB) website (www.cnlopb.nl.ca/well_alpha.shtml) (Table 2 and Appendix 5) and the BASIN database website (http://basin.gdr.nrcan.gc.ca/wells/index_e.php). To tie the well data (in depth) to the seismic data (in two-way time), I used the velocity information from 2D seismic line HBV83-195 (Appendices 3 and 6). This line is close to the West Flying Foam L-23 and Flying Foam I-23 wells. For the other wells in the study area, I also used the velocity surveys from line HBV83-195 because they have the same lithologic formations as the West Flying Foam L-23 and Flying Foam I-23 wells.

4. Structural framework

The N-striking, E-dipping Mercury fault bounds the Flying Foam region in the west (e.g. Enachescu, 1987; Driscoll *et al*, 1995) (Figs. 7 to 9). The Murre fault is to the east of the Mercury fault and also dips to the east (e.g. Enachescu, 1987; Tankard and Welsink, 1987). My interpretation indicates that the distance between these faults decreases to the north (Fig. 8). The zone between the Mercury and the Murre fault corresponds to a relay ramp, which is an inclined zone between two normal fault segments that overstep in map view and that have the same dip direction (Peacock and Sanderson, 1994; Peacock, 2002). This kind of structure connects the footwall of a fault segment with the hanging wall of a contiguous fault segment (Peacock, 2002). In the southern part of the study area, other N-striking, E-dipping basement-involved faults lie between the Mercury and Murre faults (Figs. 7 and 8). These faults are less well imaged in the central and northern parts of the study area. Basement-involved faults have normal separation, a listric geometry in cross section and link at depth. Part of the listric geometry of the faults could be due to the increase of stratal velocities with depth. Synthetic seismic sections made by Withjack and Pollock (1984) showed that planar normal faults appear in seismic as listric faults because each second of two-way traveltime in the seismic section represents a greater distance than the preceding second.

The Flying Foam anticline, in the central and northern parts of the study, area is a doubly-plunging anticline (Fig. 10) with a N-striking, E-dipping axial plane (Fig. 11). West of the Flying Foam anticline, a doubly-plunging syncline with a N-striking, E-dipping axial plane exists (Figs. 10 and 11). East of the Flying Foam anticline, a NE-plunging syncline is present (Fig. 10). Other minor folds are present in the central western and southeastern parts of the study area (Fig. 7). Several faults with normal separation detach within a ductile package and affect some of the overlying packages (Figs. 7, 10, 12 to 19).

The structural framework proposed in this study shows the geometry of the structures and its spatial variability in map view (Fig. 7) along-strike (Fig. 8) and along-dip (Fig. 9), whereas other studies (e.g. Hubbard *et al*., 1985; Enachescu, 1987; Tankard *et al*., 1989; Edwards, 1990; Driscoll *et al*., 1995; Withjack and Callaway, 2000) were only able to show single 2D lines to interpret the structures in the Flying Foam area. Differences in the interpretation of the basin-bounding faults and the top of the ductile package also exist. In Enachescu (1987), for example, the ductile package does not parallel the Mercury fault and the position of the Murre fault in the Flying Foam area is not clear. In Edwards (1990) the Murre fault is not present and most of what in this study corresponds to a ductile package corresponds to basement in his work. Driscoll *et al*. (1995) do not interpret a ductile package and the geometry of the Mercury fault corresponds to what in this study is the geometry of the top of the ductile package. The interpretation of this study mostly agrees with the one in Withjack and Callaway (2000). Finally, previous works were not able to map the multiple detached faults shown in this study.

5. Tectonostratigraphic packages - observations

The Flying Foam area has five tectonostratigraphic packages, labeled from A to E, bounded by four horizons, labeled H1 to H4. Package A is the oldest package, and Package E to the youngest. Horizon H1 is the oldest boundary, and Horizon H4 is the youngest. Table 3 summarizes the seismic characteristics of the packages and horizons and also includes formation names, lithologies and ages. The following sections describe the packages and the horizons in detail.

5.1 Package A

Package A has a few E-dipping reflections that gradually converge at depth. These reflections are subparallel to interpreted basement-involved faults, including the Mercury and the Murre faults. Peg-leg multiples parallel to these reflections are common in Package A (Fig. 5). Horizon 1, the top of Package A (Figs. 12 to 18), is well imaged in the footwall of the Mercury fault and reasonably well imaged in the hanging-wall in the southern part of the study area (Fig. 16); elsewhere, it is not well imaged. Horizon 1 is structurally higher in the southern part of the study area and deepens toward the north (Figs. 8, 12 to 16). No well has reached Horizon 1 within the study area.

5.2 Package B

Many reflections in Package B are chaotic, but some reflections are continuous (Figs. 16 to 18). These continuous reflections subtly diverge toward the basement-involved faults (Figs. 20 and 21). Faults above and below package B terminate within it. Horizon 2, the top of Package B, is irregular with steeply dipping segments parallel to the basin-bounding faults and gently dipping segments between them (Figs. 12 and 13). Horizon 2 is best imaged in the southeastern part of the study area (Figs. 15 and 16); elsewhere, imaging of this horizon is poor. Horizon 2 is structurally higher in the southern part of the study area and deepens toward the north (Figs. 8, 12 to 16). No well has reached Horizon 2 within the study area.

5.3 Package C

Package C has sub-parallel reflections, and its thickness varies throughout the study area. In the *northern* part of the study area, Package C is thick (Figs. 12 and 13). In the *central western* part of the study area, Package C is thinner (Fig. 14); in the *central eastern* part of the study area, Package C is thick (Fig. 14). In the *southwestern* part of the study area, Package C is absent or very thin (Figs. 15 and 16); in the *southeastern* part of the study area, Package C is thick (Figs. 15 and 16). Horizon 3 bounds the top of Package C. In the *northwestern* part of the study area, Horizon 3 separates dipping sub-parallel reflections in Package C from overlying diverging reflections in Package D (Figs. 12 and 22). In the *northeastern* part of the study area, a zone of chaotic reflections commonly exists between Packages C and D (Figs. 12, 13 and 23); Horizon 3 is not well defined here. In the *central western* part of the study area, Horizon 3 separates sub-parallel reflections in both Packages C and D (Figs. 13 and 24). In the *central eastern* part of the study area, Horizon 3 is not well defined. It lies somewhere between diverging reflections from Package D and dipping sub-parallel reflections from Package C (Figs. 14 and 25). In the *southwestern* part of the study area, Horizon 3 is not present (Figs. 15 and 16). In the *southeastern* part of the study area, Horizon 3 is not well defined; it lies somewhere between sub-parallel reflections from both Packages C and D (Figs. 15, 16 and 26). In strike view in the *western* part of the study area, Horizon 3 separates reflections that diverge toward the north in Package C from sub-parallel reflections in Package D (Figs. 18 and 27). In the *eastern* part of the study area, Horizon 3 is not well defined (Fig. 19). Only the Flying Foam I-13 well reached Horizon 3, which coincides with an unconformity with a missing section of Tithonian (Jurassic) age (CNLOPB, 2012).

5.4 Package D

Package D is present only in the hanging-wall of the Mercury fault and consists of sub-parallel and diverging reflections. In the *northwestern* part of the study area, reflections from Package D diverge toward the west (Figs. 12 and 22). In the *northeastern* part of the study area, flat-lying reflections from Package D lap onto a zone of chaotic reflections that commonly exists between Packages C and D (Figs. 12, 13 and 23). In the *central western* part of the study area, older strata are sub-parallel, whereas younger strata diverge toward the west (Figs. 13,14 and 24). In the *central eastern* part of the study area, reflections diverge toward the east (Figs. 14 and 25). In the *southwestern* part of the study area, all reflections from Package D are sub-parallel (Figs. 15 and 16). In the *southeastern* part of the study area, Package D has a variety of geometries. For example, on Line D (Figs. 15 and 26), basal reflections from Package D are sub-parallel and folded. Upper reflections from Package D lap onto the eastern limb of the fold and diverge toward a detached fault to the west. On Line E (Fig. 16), reflections from Package D are sub-parallel. Horizon 4 bounds the top of Package D. Onlap, toplap and some downlap terminations mark this horizon (Fig. 28). The Mercury K-76, Nautilus C-92 and Thorvald P-24 wells (CNLOPB, 2012) reached Horizon 4, which coincides with an unconformity with a missing section of Cenomanian age (CNLOPB, 2012). Toward the top of the Flying Foam anticline, the Flying Foam I-13 and West Flying Foam L-23 wells reached Horizon 4, which coincides with an unconformity with a missing section of early Paleogene age (CNLOPB, 2012).

5.5 Package E

Package E consists of continuous reflections that dip gently to the east; these reflections are generally undeformed (Figs. 12 to 16). In the northern part of the study area, reflections are sub-parallel (Figs. 12 to 14). In the southern part of the study area, some basal reflections are sigmoidal, whereas overlying reflections are sub-parallel (Figs. 15 and 16).

6. Tectonostratigraphic packages - interpretation

6.1 Package A

Package A likely corresponds to pre-rift rocks (Table 3) because primary reflections related to stratification are absent. Basement-involved faults with normal separation offset this package. Rocks in Package A are likely igneous or metamorphic rocks because: 1) the Murre G-67 well in the southern Jeanne d'Arc basin encountered metasedimentary rocks of Middle to Late Devonian age (McAlpine, 1990) (Fig. 29, Appendix 1). The Spoonbill C-30 and Hibernia G-55 wells (Appendix 1) encountered low-grade metasedimentary rocks and metamorphic basement, respectively (McAlpine, 1990). 2) Onshore studies in Newfoundland indicate that the eastern part of the island corresponds to the Avalon terrain, which consists of upper Precambrian metasedimentary and volcanic rocks and associated intrusions and overlying Cambrian-Ordovician shales and sandstones (Keen *et al*., 1990; Williams, 1999). In the south in Nova Scotia, rocks assigned to the Meguma terrain correspond to latest Neoproterozoic or Early Ordovician siliciclastic rocks overlain by volcanic rocks and granitic plutons (Keen *et al.*, 1990; Williams, 1999; Cocks and Torsvik, 2011). Horizon 1 is an unconformity, according to data from the Murre G-67 well (Appendix 1), with Devonian rocks below the unconformity and Triassic rocks above it.

6.2 Package B

Thickening of strata from Package B toward basement-involved faults indicates that Package B is a syn-rift unit (Fig. 21). Additionally, Package B is a highly ductile unit because: 1) the upper and lower boundaries commonly have very different geometries, 2) faults above and below Package B terminate within it, and 3) Package B decouples the deep from the shallow deformation (Figs. 12 to 19) as evidenced by the differences in the structural geometries above and below Package B. Specifically, few basement-involved faults offset Package A (Fig. 14), whereas several detached faults offset Packages C and D (Figs. 14, 17 to 19). No folding occurs in Package A, whereas several folds deform strata from Packages C and D (Figs 12 to 14).

Based on these observations, Package B likely corresponds to sedimentary rocks of the Eurydice and Argo formations, the oldest syn-rift rocks encountered in the Jeanne d'Arc basin. The Murre G-67 well in the southern Jeanne d'Arc basin encountered siliciclastic rocks from the Eurydice Formation unconformably overlying metasedimentary rocks from Package A (see section 6.1, McAlpine, 1990). The Spoonbill C-30 and Cormorant N-83 wells (Appendix 1), also in the southern Jeanne d'Arc basin, encountered salt-rich rocks from the Argo Formation overlying rocks from the Eurydice Formation (McAlpine, 1990). The ductile behavior of Package B agrees with the presence of salt in the Argo Formation. Palynomorphs from the Eurydice Formation, recovered in the Cormorant N-83 and Spoonbill C-30 wells, indicate ages from Carnian-Norian to Rhaetian. For the Argo salt, samples in the Spoonbill C-30 well indicate ages from Rhaetian -Early

Hettangian to late Hettangian-early Sinemurian (McAlpine, 1990). Therefore, the age of Package B is Late Triassic – Early Jurassic.

6.3 Package C

The following stratigraphic patterns characterize Package C: 1) absence of Package C in the footwall of the Mercury fault and, in the *southwestern* part of the study area, absence of Package C in the footwall of the Murre fault (Fig. 8); 2) thickness changes in the hanging-wall of the Mercury fault; specifically strata diverging toward the north (Figs. 8, 9 and 18). These patterns suggest that Package C is a syn-rift unit because: 1) Movement along the Mercury fault explains the absence of Package C in the footwall of the Mercury fault and in the *southwestern* part of the study area. 2) Thickening of strata toward the north (Figs. 18 and 27) indicates differential movement along the Mercury fault because displacement along normal faults typically increases from the tips toward the center (e.g. Barnett *et al.*, 1987; Schlische and Anders, 1996; Kim and Sanderson, 2005). As a consequence, the syndepositional packages are thicker in the center and thinner toward the tips of the fault-bounded basin (Fig. 30) (e.g. Schlische and Anders, 1996; Withjack *et al*., 2002). Also, an increased displacement on the Mercury fault to the *north* explains the northward thickening of Package C (Fig. 27).

Alternatively, faulting and later erosion of Package C in the footwall of the Mercury fault, and salt mobilization could explain the stratigraphic patterns of Package C. However, strata from Package C are sub-parallel in dip sections (Figs. 12 to 16), which suggests little or no salt movement. Also, in the southern Jeanne d'Arc basin (Fig. 29), published seismic profiles indicate that strata equivalent to Package C thicken toward basement-involved faults. This thickening is not evident in the Flying Foam area because thickening of syn-rift strata toward the basin-bounding faults is subtle during the latter stages of rifting in many of the rift basins of eastern North America. For example, in the Newark basin, Withjack *et al.* (2012b) determined that the change in bedding dip of some of the syn-rift packages is ~3º from top to bottom. This difference in dip is only apparent in regional transects.

Only one well reached the top of Package C in the study area; the Flying Foam I-13 well encountered rocks from the Rankin Formation (CNLOPB, 2012). Studies from the southern Jeanne d'Arc basin and the Hibernia oilfield report that the Voyager, Downing and Iroquois formations underlie the Rankin Formation (McAlpine, 1990; Sinclair *et al.*, 1999). McAlpine (1990) indicates that these formations range in age from Late Triassic to Late Jurassic.

6.4 Package D

Package D consists of diverging and sub-parallel strata. In the *northwestern* part of the study area, strata thin toward the crest of the Flying Foam anticline and thicken toward Horizon 2, which locally parallels the Mercury fault (Figs. 12 and 22). Horizon 2 is a lithologic contact and a fault contact. The ductile rocks (Argo salt) of Package B underlie Horizon 2. This contact acted as a detachment fault with a ramp-flat-ramp geometry. The ramps are parallel to the Mercury and the Murre faults and the flat is between them (Fig. 31). Strata thickening toward this fault indicate syn-faulting deposition, and strata thinning toward the crest of the Flying Foam anticline indicate growth during folding (see section 7.1 for a complete explanation). In the *central western* part of the study area, younger strata thicken toward the detachment fault and thin toward the Flying Foam anticline, whereas older strata are sub-parallel (Figs. 13, 14 and 24). Therefore, folding and movement along the detachment fault started in the north and propagated later to the south. The boundary between diverging reflections and flat-lying reflections on Line B (Fig. 24) coincides with an unconformity with a missing section of Aptian age (West Flying Foam L-23 well; CNLOPB, 2012). Above this unconformity, the West Flying Foam L-23 well encountered rocks from the Nautilus and Ben Nevis formations, and below this unconformity, it encountered rocks from the Avalon, Whiterose, Catalina and Hibernia formations (CNLOPB, 2012; Appendix 4). The Fortune Bay and Jeanne d'Arc basin underlie the Hibernia Formation (McAlpine, 1990; Fig. 3). The formations that conform Package D range in age from Latest Jurassic to Early Cretaceous (McAlpine, 1990).

In the *southwestern* part of the study area, all strata from Package D are sub-parallel (Figs. 15, 16 and 28). The Mercury K-76 well encountered rocks from the Nautilus and Ben Nevis formations (CNLOPB, 2012; Appendix 4), therefore, the oldest strata from Package D did not accumulate; alternatively, they accumulated but were later eroded away. The discussion section describes in more detail other stratigraphic patterns in Package D and their tectonic significance.

6.5 Package E

Package E is present in the entire area. The Mercury fault cuts part of strata of Package E, but, in general, no significant faulting or folding deforms this package. Strata do not thicken toward the border fault, but rather thicken gradually to the east. Therefore, Package E is a post-rift unit. All wells in the study area encountered Package E. The Mercury K-72, Nautilus C-92 and Thorvald P-24 wells drilled the basal part of this package, which corresponds to the Wyandot and Dawson Canyon formations (Appendix 4). All other wells in the study area drilled the upper part of Package E, which corresponds to the Banquereau Formation (Appendix 2). The age of the oldest rocks in Package E is Late Cretaceous (Grant and McAlpine, 1990; Sinclair *et al*., 1999; Deptuck, 2003).

7. Discussion

7.1 Are structures detached or basement-involved?

Both types of structures are present in the Flying Foam area. This is because Package B, which contains salt (Argo Formation), behaves ductilely and decouples the deeper deformation from the shallower deformation. As a consequence, the style of deformation of the cover is different than the style of deformation of the basement. Specifically, a few basement-involved faults offset Package A, whereas several detached faults affect Packages C and D. Also, no major folding occurs in Package A, whereas major and minor folds deform Packages C and D. The Flying Foam structure is the main fold in the study area. This structure is a forced fold (Withjack and Callaway, 2000) and a fault-bend fold (Tankard *et al*., 1989) that deforms rocks from Package C (see discussion below). The forced fold forms because of flexure of the sedimentary cover above the Murre fault, which is a basement-involved fault with normal separation (e.g. Withjack *et al*., 1990; Schlische, 1995). The fault-bend fold (e.g. Xiao and Suppe, 1992; Schlische, 1995) forms because of movement on the non-planar detachment fault associated with Horizon 2 and with displacement on the Murre fault (see section 6.4 and discussion below).

Experimental and geometric models provide additional insights into the development of the Flying Foam structure. Experimental models from Withjack and Callaway (2000) simulated forced folding using a precut metal base to represent a basement-involved normal fault and wet clay and silicone polymer to represent the sedimentary cover and a ductile salt layer, respectively. The models show that in the presence of a ductile layer, a basement-involved fault does not propagate to the surface, but rather produces a forced-fold in the strata above the ductile layer (Fig. 32). Growth beds in the model reflect syn-faulting and syn-folding deposition during movement along the basement-involved fault and during the folding of the package above the ductile layer. Similarly, in the Flying Foam area, the Murre fault does not propagate through Package B (Argo salt) but produces a forced fold in Package C. Growth beds from Package D reflect syn-faulting and syn-folding deposition during movement along the Murre fault and during folding of Package C, therefore, Package D is a syn-rift unit. The experimental models differ from the Flying Foam area in details and complexity. In the models, both the ductile layer and the package above it are pre-rift. In the study area, Packages B and C are syn-rift. However, during the accumulation of Package D and the corresponding displacement of the Murre fault, Package C is a pre-kinematic package, just like the pre-kinematic package of the model.

Additionally, the experimental models show that, as displacement increases on the basement-involved fault, displacement also increases on the detached fault in the footwall of the master fault. One or more of those detached faults achieves a ramp-flat-ramp fault geometry, movement on which produces a fault-bend fold anticline (Fig. 32). A geometric model from Withjack and Schlische (2006) illustrates how displacement on a ramp-flat-ramp fault produces an anticlinal fault-bend fold and a dipping diachronous unconformity. The model assumes that the hanging-wall deforms by inclined simple shear, that the footwall remains rigid, that compaction is not significant and that growth beds fill depressions developed during faulting up to a prescribed datum. The inclined-shear direction dips 70º toward the main normal fault. Their results show that syndepositional strata diverge toward the fault near the upper ramp and lap onto a diachronous unconformity above the lower ramp (Fig. 33). In the Flying Foam area, strata from Package D diverge toward the detachment fault in the *northwestern* and *central western* parts of the study area (Figs. 12, 13, 22, 24 and 31). In the *northeastern* part of the study area, strata in Package D are parallel and lap onto a zone of chaotic strata that probably correspond to the diachronous unconformity observed in the geometric model (Figs. 12, 13, 23, 25 and 31). The geometric model differs from the study area in the complexity of the Flying Foam area. In the study area, the ramp-flat-ramp fault geometry of the detachment fault results from the interaction between the Mercury and the Murre faults in the presence of a ductile layer, whereas in the geometric model only one fault exists (see following section). In the study area, changes in the stratigraphic patterns occur along strike, and the structures represent a final stage of deformation, whereas the model shows the evolution of the structure and changes only in one cross section.

7.2 When did the deformation occur?

To illustrate the evolution of the Flying Foam area, I restored the cross section of Line B (Fig. 34) using inclined shear and rigid-body rotation. I assumed plane-strain conditions, negligible compaction and negligible deformation in the footwall, that all packages have constant area through time, and that growth beds completely fill any spaces created during faulting up to a prescribed regional datum. The footwall remains fixed. Despite these simplifying assumptions, the restoration schematically shows the evolution of the Flying Foam region in the *northern* part of the study area. The restoration indicates 25 km of extension equivalent to a stretch of 60%. This is a minimum estimate because the restoration does not take into account deformation accommodated by small-scale structures or footwall deformation.

7.2.1 Paleozoic (Package A)

Several orogenies (Taconic, Acadian and Alleghanian) related to the amalgamation of the supercontinent Pangea occurred during this period (Keen *et al*., 1990; Williams, 1999; Cocks and Torsvik, 2011). Structures include low-angle thrust faults. Erosion likely removed rocks from this package.

7.2.2 Late Triassic (Package B)

Rifting started with the accumulation of siliclastic rocks of the Eurydice Formation and salt of the Argo Formation (Package B). In the southern part of the study area, the Mercury and other basement-involved faults were active. The Murre fault was active in the rest of the Jeanne d'Arc basin (Sinclair, 1995), but it is unclear if it was active in the Flying Foam area. In the rest of the study area, only the Mercury fault was active. All faults had normal separation.

7.2.3 Early to Late Jurassic (Package C)

Displacement on the Mercury fault continued, but it was greater in the *north* as evidenced by the absence of Package C in the *southwestern* part of the study area and by strata thickening toward the *north* in the *western* part of the study area. Strata do not obviously thicken toward the Mercury fault likely because, in the Flying Foam region, the basin was very wide, and differences in dip between the layers are very subtle (see section 6.3). The Murre fault was only active in the *southeastern* part of the study area, as evidenced by the absence of Package C in the footwall of the Murre fault and by the apparent lack of thickness changes in the *central* and *northeastern* parts of the study area (Fig. 35).

7.2.4 Latest Jurassic to Early Cretaceous (Package D)

The structural complexity increased during this period in the study area. The stratigraphic patterns in Package D indicate differences in the deformation style between Tithonian and Aptian times and between Aptian and Cenomanian times. Differences also exist between the *eastern* and *western* parts of the study area. For clarity the discussion starts with the *western* part of the study area.

From Tithonian through Aptian times, strata from Package D diverge toward a detachment fault in the *northwestern* part of the study area (section 6.4, Figs. 12, 20 and 32), whereas in the *central western* and *southwestern* parts of the study area, strata from Package D are sub-parallel (Figs. 13 to 16, 22 and 26). From Aptian through Cenomanian times, strata from Package D diverge toward the detachment fault in the *northwestern* and *central western* parts of the study area, whereas in the *southwestern* part of the study area, strata from Package D are sub-parallel. Differences in the displacement direction on the detachment fault in space and through time could explain the heterogeneous stratigraphic patterns observed. However, this subject requires further study.

Displacement on the detachment fault produced fault-bend folding and displacement on the Murre fault produced forced folding. As a consequence, along-strike differences in the Flying Foam anticline are the result of differences in the degree of fault-bend folding vs. forced folding. In the *northeastern* part of the study area (Figs. 12, 13 and 21), strata from Package D are parallel. This stratigraphic pattern is similar to the one in the geometric model of Figure 33. Therefore, the detachment fault was active, and fault-bend folding was greater than forced folding. In the *central eastern* part of the study area (Fig. 14 and 25), strata from Package D diverge toward the east. Displacement on the detachment decreased or was oblique and, therefore, forced folding was greater than fault-bend folding in the E-W direction. In the *southeastern* part of the study area, two stratigraphic patterns exist. On Line D (Figs. 15 and 26), displacement on the detachment occurred only on the ramp parallel to the Murre fault and along the overlying detached fault. Therefore, displacement on the detachment and fault-bend folding was minimal. Forced folding predominates. On Line E (Fig. 16), no folding occurred; therefore the Murre fault was not active. Alternatively, the Murre fault was at the surface, and thus, no forced folding occurred.

7.2.5 Late Cretaceous – Cenozoic (Package E)

A period of erosion occurred, as evidenced by toplap terminations (Fig. 28). Then, during the Paleogene and Neogene, post-rift sedimentation occurred with accumulation of Package E. Differential subsidence occurred gently tilting strata to the east. Additionally, the Mercury fault offsets the strata at the base of Package E. This could be related to either slight reactivation of the Mercury fault or differential compaction of strata of Package E.

7.3 Is rifting episodic or persistent?

The stratigraphic patterns interpreted in the Flying Foam area suggest that rifting in the Jeanne d'Arc basin lasted from the Late Triassic through the Early Cretaceous; that is, rifting lasted more than 100 m.y. (Figs. 35 and 36). In contrast, previous workers (e.g. Hubbard *et al.*, 1985; Tankard and Welsink, 1987; Hubbard, 1988; Tankard *et al.*, 1989; Grant and McAlpine, 1990; Sinclair, 1995; Sinclair and Riley, 1995; Sinclair *et al.*, 1999) suggested that rifting in the Jeanne d'Arc basin occurred in two or three different episodes with intervening periods of thermal subsidence, and that each rifting episode lasted tens of millions of years. In other words, previous studies more or less consider that Packages B and D are syn-rift units, whereas Package C is a post-rift unit.

Consensus exists about the syn-rift nature of Package B (e.g. Tankard and Welsink, 1987; McAlpine, 1990; Sinclair, 1995), despite the fact that most studies do not identify thickening of strata toward the basin-bounding faults. Consensus also exists about the post-rift nature of Package C. Grant and McAlpine (1990), for example, indicated that the presence of gradational and conformable contacts of formations within Package C indicate no syndepositional growth, even though they noted that the Egret Member from the Rankin Formation thickens northeastward in the basin. Package D, in contrast, has several unconformities within it and marked thickening of strata toward the Mercury and the Murre faults, and thus previous workers (e.g. Tankard and Welsink, 1987; Edwards, 1990; Sinclair *et al.*, 1999) consider that Package D corresponds to a period of rift reactivation in the Jeanne d'Arc basin.

This study shows that strata from Package B thicken toward basement-involved faults, and thus confirms the syn-rift nature of this package. This study also shows that Package C is a syn-rift unit, and not a post-rift unit as previous studies suggest, because of the spatial distribution of the strata and thickening of strata toward the north. Finally, this study agrees with previous studies about the syn-rift nature of Package D, but identifies and describes in more detail the complex stratigraphic patterns and the deformation associated with this package. Specifically, Package D exhibits two different stratigraphic patterns: diverging strata and sub-parallel strata. These patterns are related to displacement on the Mercury and the Murre faults and a detached fault that coincides with the top of Package B (top of the Argo salt). Displacement on the Murre fault and the detachment fault caused forced folding and fault-bend folding, which are responsible for the Flying Foam anticline.

The differences in the spatial distribution of the packages and the variety of orientation of the detached structures (folds and faults) (Figs. 7, 10 and 35) suggest that the intensity of rifting and extension direction could have changed through time. However, the prediction of the extension direction in a basin is difficult. For instance, experimental clay models with multiple episodes of extension (Henza, 2009; Henza, *et al.* 2010, 2011) show that, in areas with multiple deformational episodes, fault orientation may not reflect the direction or relative magnitude of each event. In the Jeanne d'Arc basin, several authors suggest that the border faults correspond to reactivated thrust faults (e.g. Enachescu, 1987; Tankard and Welsink, 1989; Withjack and Schlische, 2005). Therefore, a complete analysis of the extension direction and intensity of rifting needs a detailed study and falls beyond the scope of this study.

The syn-rift nature of Package C implies potential reservoir rocks near basement-involved faults, because coarser rocks accumulate close to border faults (e.g. Withjack *et al*., 2002). The Voyayer Formation within Package C contains thermally mature source rocks (e.g. Fowler and Brooks, 1990; McAlpine, 1990; Magoon *et al*., 2005) and fine-grained sandstones (McAlpine, 1990) that could be reservoir rocks. Therefore, Package C could contain important hydrocarbon accumulations that might have been overlooked because of the assumption that this package was post-rift. Additionally, persistent rifting in the Jeanne d'Arc basin implies persistent heat flow for hydrocarbon maturation and generation. That persistent heat flow could explain the existence of mature rocks in the Voyayer Formation, and the likely occurrence of deeper reservoirs not explored yet.

8. Summary and conclusions

The interpretation of 3D seismic data from the Flying Foam area indicates that rifting in the Jeanne d'Arc basin was not episodic (as previous studies suggested), but persistent from the Late Triassic through the Early Cretaceous. Persistent rifting resulted in three different packages. Strata from the basal salt-rich Package B gradually thicken toward basement-involved faults. Strata from overlying Package C do not obviously thicken toward basement-involved faults, but strata thickening toward the north indicate differential displacement on the Mercury and Murre faults. Strata from the uppermost Package D have a variety of geometries that reflect differences in displacement on the basin-bounding faults and displacement on a detachment fault (top of the Argo salt in Package B).

Folding and detached faulting occurred during the Late Jurassic-Early Cretaceous in the study area. A combination of fault-bend folding and forced folding produced the Flying Foam anticline. Forced folding occurred above the Murre fault, and fault-bend folding resulted from displacement on the detachment fault with a ramp-flat-ramp geometry on top of the Argo salt. This geometry resulted because the top of Package B (Argo salt) parallels the Mercury and the Murre faults, forming ramps and a flat between them. Along-strike differences in the displacement on the basin-bounding faults and temporal differences in the activity of these faults account for the different stratigraphic patterns observed in Package D.

References

Barnett, J. A. M., Mortimer, J., Rippon, J. H., Walsh, J. J., and Watterson, J. (1987), Displacement Geometry in the Volume Containing a Single Normal Fault, *AAPG Bulletin*, *71*(8), 925-937.

CNLOPB (2012), www.cnlopb.nl.ca/well_alpha.shtml.

Cocks, L. R. M., and Torsvik, T. H. (2011), The Palaeozoic geography of Laurentia and western Laurussia: A stable craton with mobile margins, *Earth-Science Reviews*, *106*(1-2), 1-51.

Deptuck, M. E., MacRae, A., Shimeld, J. W., Williams, G., and Fensome, R. A. (2003), Revised Upper Cretaceous and lower Paleogene lithostratigraphy and depositional history of the Jeanne d'Arc Basin, offshore Newfoundland, Canada, *AAPG Bulletin*, *87*(9), 1459 - 1483.

Driscoll, N.W., Hogg, J. R., Christie-Blick, N., and Karner, G. D. (1995), Extensional tectonics in the Jeanne d'Arc Basin, offshore Newfoundland: implications for the timing of break-up between Grand Banks and Iberia, *Geological Society, London, Special Publication, 90*(1), 1-28.

Edwards, A. (1990), The Western Margin of the Jeanne d'Arc Basin Offshore Newfounland (Eastern Canada), in *The Potential of Deep Seismic Profiling for Hydrocarbon Exploration*, edited by Pinet, B. and Bois, C., pp. 161-173, Editions Technip, Paris.

Enachescu, M. E. (Ed.) (1987), *Tectonic and structural framework of the northeast Newfoundland continental margin*, 117-146 pp., Canadian Society of Petroleum Geologist.

Fowler, M.G. and Brooks, P.W. (1990), Organic geochemistry as an aid in the interpretation of the history of oil migration into different reservoirs at the Hibernia K-18 and Ben Nevis I-45 wells, Jeanne d'Arc Basin, offshore eastern Canada, *Organic Geochemistry, 161*(1-3), 461-475.

Grant, A. C., and McAlpine, K. D. (1990), The continental margin around Newfoundland, in *Geology of the continental margin of Eastern Canada*, edited by Keen, M. J. and Williams, G. L., pp. 241-292.

Hart, B. S. (1999), Definition of subsurface stratigraphy, structure and rock properties from 3-D seismic data, *Earth-Science Reviews*, *47*(3), 189-218.

Henza, A. A. (2009), Influence of pre-existing fault fabrics on normal-fault development: an experimental study, Rutgers University, The State University of New Jersey, New Brunswick.

Henza, A. A., Withjack, M. O., and Schlische, R. W. (2010), Normal-fault development during two phases of non-coaxial extension: An experimental study, *Journal of Structural Geology, 32(11)*, 1656-1667.

Henza, A. A., Withjack, M. O., and Schlische, R. W. (2011), How do the properties of a pre-existing normal-fault population influence development during a subsequent phase of extension?, *Journal of Structural Geology, 33(9)*, 1312-1324.

Hubbard, R. J. (1988), Age and Significance of Sequence Boundaries on Jurassic and Early Cretaceous Rifted Continental Margins, *AAPG Bulletin*, *72*(1), 49-72.

Hubbard, R. J., Pape, J., and Roberts, D. G. (1985), Depositional sequence mapping to illustrate the evolution of a passive continental margin, in *Seismic Stratigraphy II*, edited by Berg, O. R. and Woolverton, D. G., pp. 79-115.

Jansa, L. F., and Wade, J. A. (1975), Geology of the continental margin off Nova Scotia and Newfoundland, *Geological Survey of Canada*, *2*(Paper 74-30), 51-106.

Keen, C., Loncarevic, B. D., Reid, I., Woodside, J., Haworth, R. T., and Williams, H. (1990), Tectonic and geophysical overview, in *Geology of the continental margin of Eastern Canada*, edited by Keen, M. J. and Williams, G. L., pp. 33-74.

Kim, Y., and Sanderson, D. (2005), The relationship between displacement and length of faults: a review, *Earth-Science Reviews*, *68*(3-4), 317-334.

Louden, K. (2002), Tectonic evolution of the East Coast of Canada, *Canadian Society of Exploration Geophysicist - Recorder*, *2*, 37-48.

Magoon, L. B., Hudson, T. L., and Peters, K. E. (2005), Egret-Hibernia(!), a significant petroleum system, northern Grand Banks area, offshore eastern Canada, *AAPG Bulletin*, *89*(9), 1203-1237.

McAlpine, K. D. (1990), Mesozoic stratigraphy, sedimentary evolution, and petroleum potential of the Jeanne d'Arc Basin, Grand Banks of Newfoundland, *Geological Survey of Canada*, *paper 89-17*, 1-50.

Murphy, J. B., and Keppie, J. D. (1998), Late Devonian palinspastic reconstruction of the Avalon-Meguma terrane boundary: implications for terrane accretion and basin development in the Appalachian orogen, *Tectonophysics*, *284*(3-4), 221-231.

Naylor, R. S. (1971), Acadian Orogeny: An Abrupt and Brief Event, *Science*, *172*(3983), 558-560.

Peacock, D. C. P., and Sanderson, D. J. (1994), Geometry and development of relay ramps in normal fault systems, *AAPG Bulletin, 78*(2), 147-165.

Peacock, D. C. P. (2002), Propagation, interaction and linkage in normal fault systems, *Earth-Science Reviews, 58*(1-2), 121-142.

Rodgers, J. (1971), The Taconic Orogeny, *Geological Society of America Bulletin*, *82*(5), 1141-1178.

Schlische, R. W. (1995), Geometry and origin of fault-related folds in extensional settings, *AAPG Bulletin*, *79*(11), 1661-1678.

Schlische, R. W., and Anders, M. H. (1996), Stratigraphic effects and tectonic implications of the growth of normal faults and extensional basins, in *Reconstructing the History of Basin and Range Extension Using Sedimentology and Stratigraphy*, edited by Beratan, K. K., pp. 183-203, Geological Society of America, Boulder, Colorado.

Schlische, R. W., Withjack, M. O., and Olsen, P. E. (2002), Relative Timing of CAMP, Rifting, Continental Breakup, and Basin Inversion: Tectonic Significance, in *The Central Atlantic Magmatic Province*, edited by Hames, W. E., McHone, G. C., Renne, P. and Ruppel, C., American Geophysical Union Monograph.

Schlumberger and Geco-Prakla (1996), 1995/6 Marine 3D survey Newfoundland Grand Banks. Final processing report for Exploration Services Geco-Prakla, 51 pp, Houston.

Seton, M., Muller, R. D., Zahirovic, S., Gaina, C., Torsvik, T., Shephard, G., Talsma, A., Gurnis, M., Turner, M., Maus, S., and Chandler, M. (2012), Global continental and ocean basin reconstructions since 200 Ma, *Earth-Science Reviews*, *113*, 212-270.

Sinclair, I. K. (1988), Evolution of Mesozoic-Cenozoic sedimentary bains in the Grand Banks area of Newfoundland and comparison with Falvey's (1974) rift model, *Bulletin Canadian Petroleum Geology*, *36*(3), 255-273.

Sinclair, I. K. (1995), Transpressional inversion due to episodic rotation of extensional stresses in Jeanne d'Arc Basin, offshore Newfoundland, in *Basin Inversion*, edited by Buchanan, J. G. and Buchanan, P.G., pp. 249-271, Geological Society Special Publication 88.

Sinclair, I. K., and Riley, L. A. (1995), Separation of Late Cimmerian rift and post-rift megasequences: comparison of the Jeanne d'Arc Basin, Grand Banks and the Outer Moray Firth, North Sea, in *Sequence Stratigraphy on the Northwest European Margin*, edited by Steel, R. J. e. a., pp. 347-363, Elsevier, Amsterdam.

Sinclair, I. K., Evans, J. E., Albrechtsons, E. A., and Sydora, L. J. (1999), The Hibernia Oilfield - effects of episodic tectonics of stuctural character and reservoir compartmentalization, in *Petroleum Geology of Northwest Europe: Proceedings of the 5th Conference*, edited by Fleet, A. J. and Boldy, S. A. R., pp. 517-528.

Tankard, A. J., and Welsink, H. J. (1987), Extensional tectonics and stratigraphy of Hibernia oil field, Grand Banks, Newfoundland, *AAPG Bulletin*, *71*, 1210-1232.

Tankard, A. J., and Balkwill, H. R. (1989), Extensional tectonics and stratigraphy of the North Atlantic Margins: Introduction, in *Extensional Tectonics and Stratigraphy of the North Atlantic Margins*, AAPG Memoir, 46, pp. 1-6.

Tankard, A. J., and Welsink, H. J. (1989), Mesozoic Extension and Styles of Basin Formation in Atlantic Canada, in *Extensional Tectonics and Stratigraphy of the North Atlantic Margins*, AAPG Memoir, 46, pp. 175-195

Tankard, A. J., Welsink, H. J., and Jenkins, W. A. M. (1989), Structural styles and Stratigraphy of the Jeanne d'arc basin, Grand Banks of Newfounland, in *Extensional Tectonics and Stratigraphy of the North Atlantic Margins*, AAPG Memoir, 46, pp. 265-282.

Welsink, H. J., and Tankard, A. J. (2012), Extensional tectonics and stratigraphy of the Mesozoic Jeanne d'Arc basin, Grand Banks of Newfoundland, in *Regional geology and tectonics: Phanerozoic passive margins, cratonic basins and global tectonic maps*, edited by Roberts, D. G. and Bally, A. W., pp. 337-381, Elsevier, New York.

Williams, H. (1999), Tectonics of Atlantic Canada, *Geoscience Canada*, *26*(2), 51-70.

Withjack, M.O., and Pollock, D. J. D. (1984), Synthetic Seismic-Reflection Profiles of Rift-Related Structures, *AAPG Bulletin, 68*(9), 1160-1178.

Withjack, M. O., and Callaway, S. (2000), Active normal faulting beneath a salt layer: An experimental study of deformation patterns in the cover sequence, *AAPG Bulletin*, *84*(5), 627-651.

Withjack, M. O., and Schlische, R. W. (2005), A review of tectonic events on the passive margin of eastern North America, in *Petroleum Systems of Divergent Continental Margin Basins: 25th Bob S. Perkins Research Conference*, edited by Post, P.J., pp. 203-235, Gulf Coast Section of SEPM.

Withjack, M. O., and Schlische, R. W. (2006), Geometric and experimental models of extensional fault-bend folds, in *Analogue and Numerical Modelling of Crustal-Scale Processes*, edited by Buiter, S. J. H. and Schreurs, G., Geological Society of London, Special Publication 253.

Withjack, M. O., Olson, J., and Peterson, E. (1990), Experimental-Models of Extensional Forced Folds, *AAPG Bulletin*, *74*(7), 1038-1054.

Withjack, M. O., Schlische, P. W., and Olsen, P. E. (1998), Diachronous rifting, drifting, and inversion on the passive margin of Central Eastern North America: An analog for other passive margins, *AAPG Bulletin*, *82*(5A), 817-835.

Withjack, M. O., Schlische, R. W., and Olsen, P. E. (2002), Rift-basin Structure and its Influence on Sedimentary Systems, in *Sedimentation in Continental Rifts*, edited by Ranaut, R. W. and Ashley, G. M., pp. 57-81. SEPM Special Publication 73.

Withjack, M. O., Schlische, R. W., and Olsen, P. E. (2012a), Development of the passive margin of Eastern North America, in *Phanerozoic Rift Systems and Sedimentary Basins*, edited by Roberts, D. G. and Bally, A. W., pp. 300-335, Elsevier, New York.

Withjack, M. O., Schlische, P. W., Malinconico, M. L., and Olsen, P. E. (2012b), Rift-basin development: lessons from the Triassic-Jurassic Newark Basin of eastern North America, in *Conjugate Divergent Margins*, edited by Mohriak, W. U., Danforth, A., Post, P. J., Brown, D. E., Tari, G. C., Nemcok, M. and Sinha, S. T., Geological Society, London, in press.

Xiao, H., and Suppe, J. (1992), Origin of rollover, *AAPG Bulletin*, *76*(4), 509-529.

Table 1. Main parameters of the 3D seismic data set from the Flying Foam area.

Number of inlines (E-W orientation)	1532
Number of crosslines (N-S orientation)	3150
Inline spacing	25 m
Crossline spacing	12.5 m
Processing record length	9 s
Processing sample interval	4 ms
Nominal fold	32

Table 2. Basic information from wells inside the area of study.

Well name	**Spud date**	**Well class**	**TD* (m)**
West Flying Foam L-23	07-Nov-1981	Exploratory	4554
Flying Foam I-13	26-Sep-1973	Exploratory	3683.2
Nautilus C-92	29-Sep-1981	Exploratory	5117
Mercury K-76	19-May-1985	Exploratory	5212
Thorvald P-24	24-Jun-1991	Exploratory	3810

* TD: Total Depth

Table 3. Summary of the tectonostratigraphic units present in the Flying Foam area, Jeanne d'Arc basin, offshore eastern Canada

Packages and horizons	**Seismic-reflection geometries**	**Name, lithology and age**
Package E	Continuous, sub-parallel, low- to high-amplitude reflections	Banquereau Fm. (shales), Dawson Canyon Fm. (shales, limestones), Wyandot Fm. (chalks and marlstones) and Otter Bay Fm. (sandstones); Early Cretaceous – Recent (?) (CNLOPB, 2012; Deptuck, *et al*., 2003)
Horizon 4	Erosional truncation surface	Base of Paleogene unconformity
Package D	Continuous, low- to high-amplitude reflections; the geometry of the reflections vary from north to south and from west to east.	Ben Nevis Fm. (shales and some sandstones), Nautilus Fm. (calcareous shales). Avalon Fm. (sandstones), Whiterose Fm. (shales and limestones), Catalina Mb. (sandstones), Hibernia Fm. (sandstones), Fortune Bay Fm. (shales) and Jeanne d'Arc Fm. (sandstones); Late Jurassic – Early Cretaceous (CNLOPB, 2012; McAlpine, 1990; Sinclair *et al*., 1999)
Horizon 3	Inferred unconformity	Late Jurassic (Tithonian) unconformity
Package C	Continuous, mostly sub-parallel, low- to high-amplitude reflections	Rankin Fm. (limestones), Downing Fm. (shales with interbedded limestones) and Iroquois Fm. (dolomites and limestones); Early to Late Jurassic (?) (McAlpine, 1990; Sinclair *et al*., 1999)
Horizon 2	Top of salt	
Package B	Chaotic and locally grading to low- to moderate-amplitude parallel reflections	Eurydice Fm. (continental red beds) and Argo Fm. (mainly salt); Late Triassic – Early Jurassic (?) (McAlpine, 1990; Sinclair *et al*., 1999)
Horizon 1	Inferred angular unconformity; poorly imaged	Late Triassic
Package A	No primary reflections	Pre-Triassic strata and basement (Sinclair *et al*., 1999)

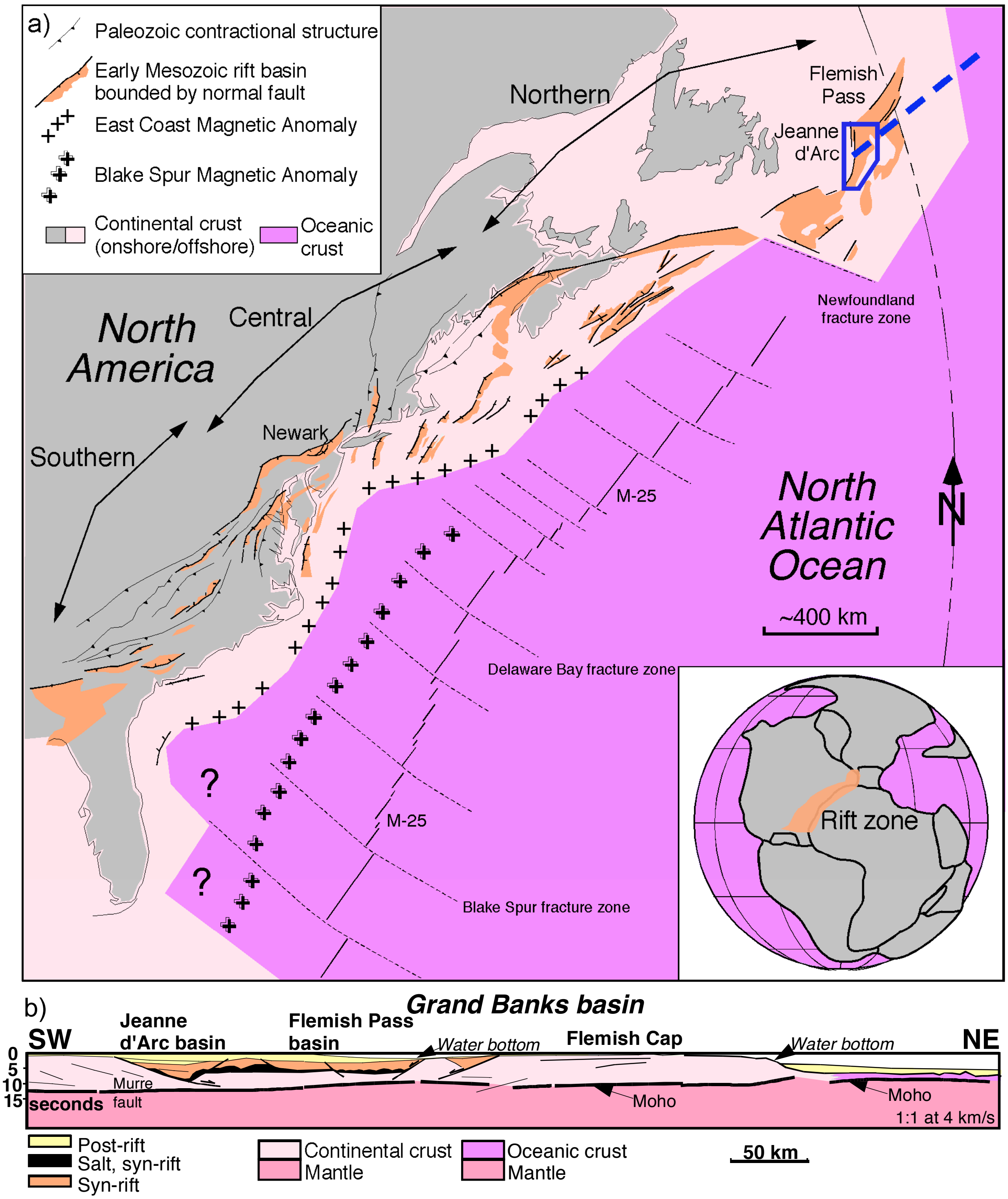

Figure 1. a) Map of the eastern North America rift system showing location of the Jeanne d’Arc basin (blue polygon) and key tectonic features. Inset shows position of the rift system relative to Pangea during Late Triassic time. b) Regional transect from offshore Canada (location given by dashed line in a) showing key tectonostratigraphic features. Modified from Withjack *et al*. (2012).

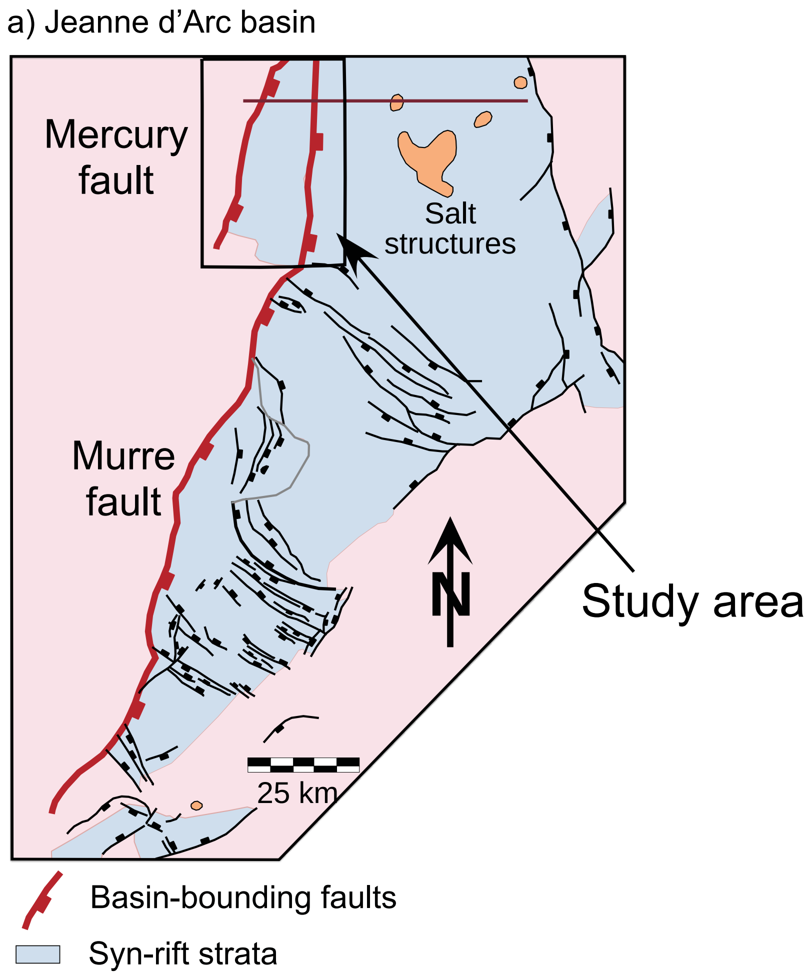

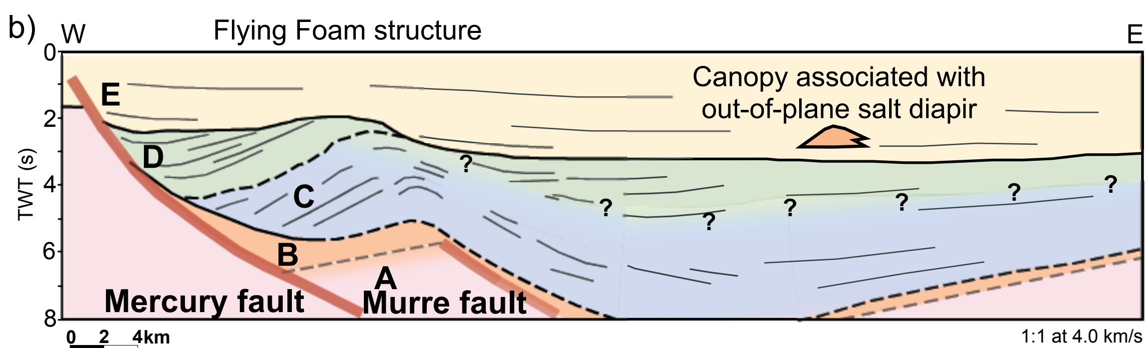

Figure 2. a) Map of the Jeanne d'Arc basin highlighting the study are. Southern half of map shows faults cutting prominent Middle Jurassic reflection, and northern half shows faults cutting Aptian/Albian sequence (modified from Withjack and Schlische, 2005). b) Regional cross section (location given by red line in a) showing tectonostratigraphic packages (capital letters and colors) and main structural features. Dashed lines and gradational colors show uncertainty. Regional cross section is based on seismic line HBV83-195 (Appendix 3), modified from Withjack and Schlische, (2005), and line B, this study. See location of line B in Figure 7 and interpreted line in Figure 13.

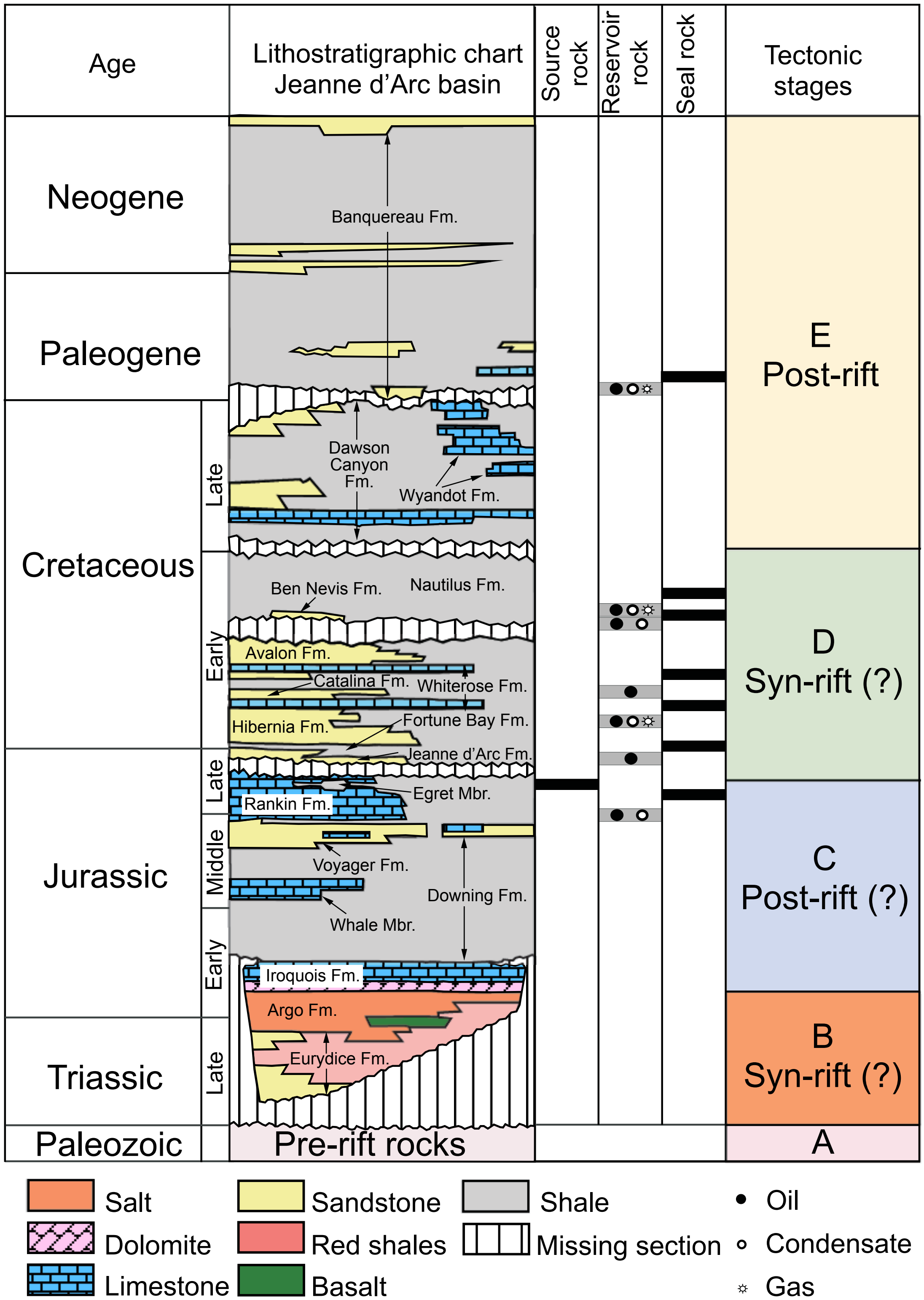

Figure 3. Lithostratigraphic chart of the Jeanne d'Arc basin highlighting tectonostratigraphic packages interpreted in this study (capital letters) and tectonic stages interpreted in previous studies. Modified from Sinclair *et al*. (1999) and Magoon *et al*. (2005). Results from my thesis work will show that Packages B, C and D are all syn-rift units.

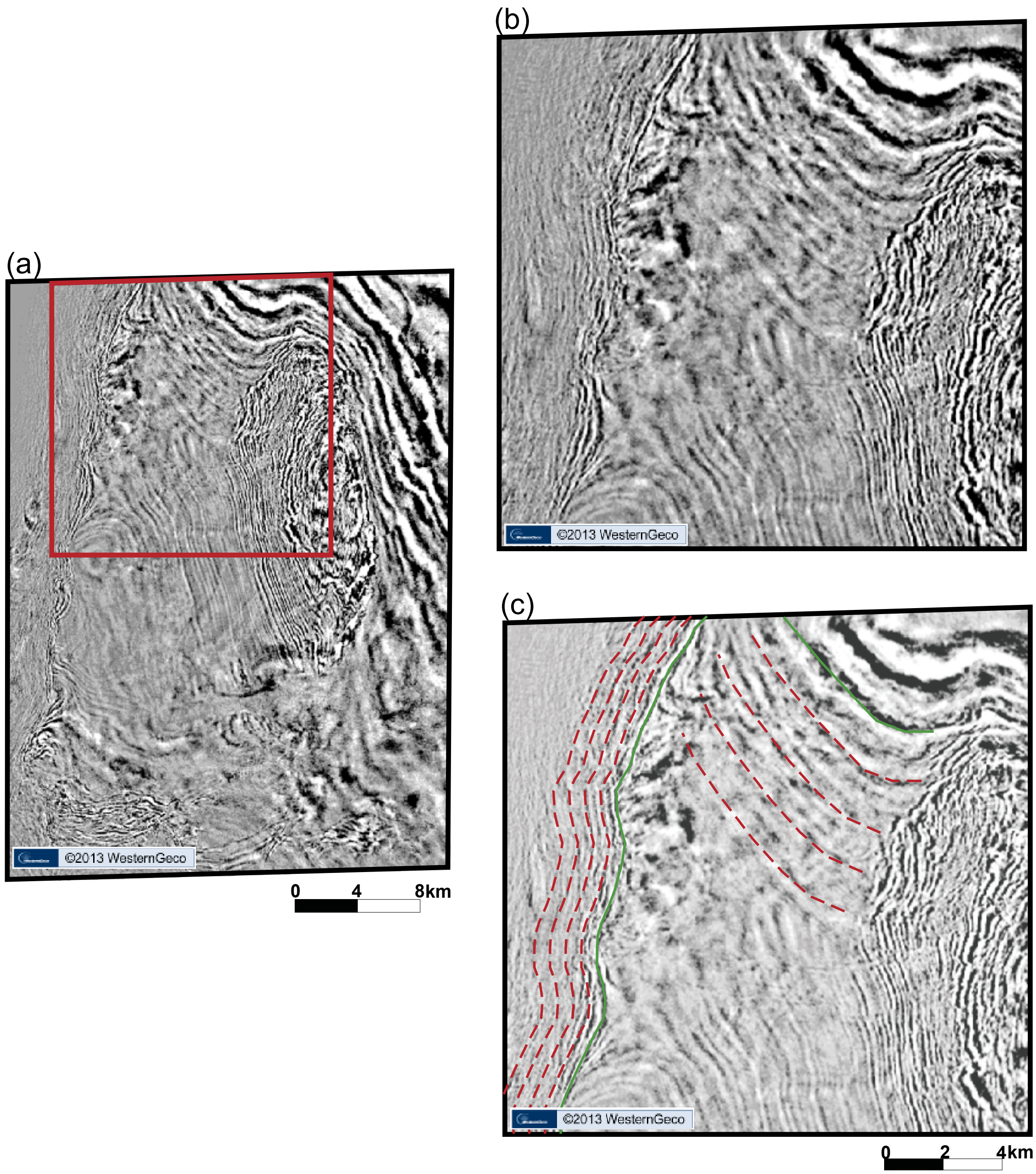

Figure 4: a) Uninterpreted time-slice at 2.720 s. Box shows location of enlargement in b. b) Uninterpreted part of time-slice. c) Interpreted part of time-slice showing true reflections (green lines) and peg-leg multiples (dashed red lines).

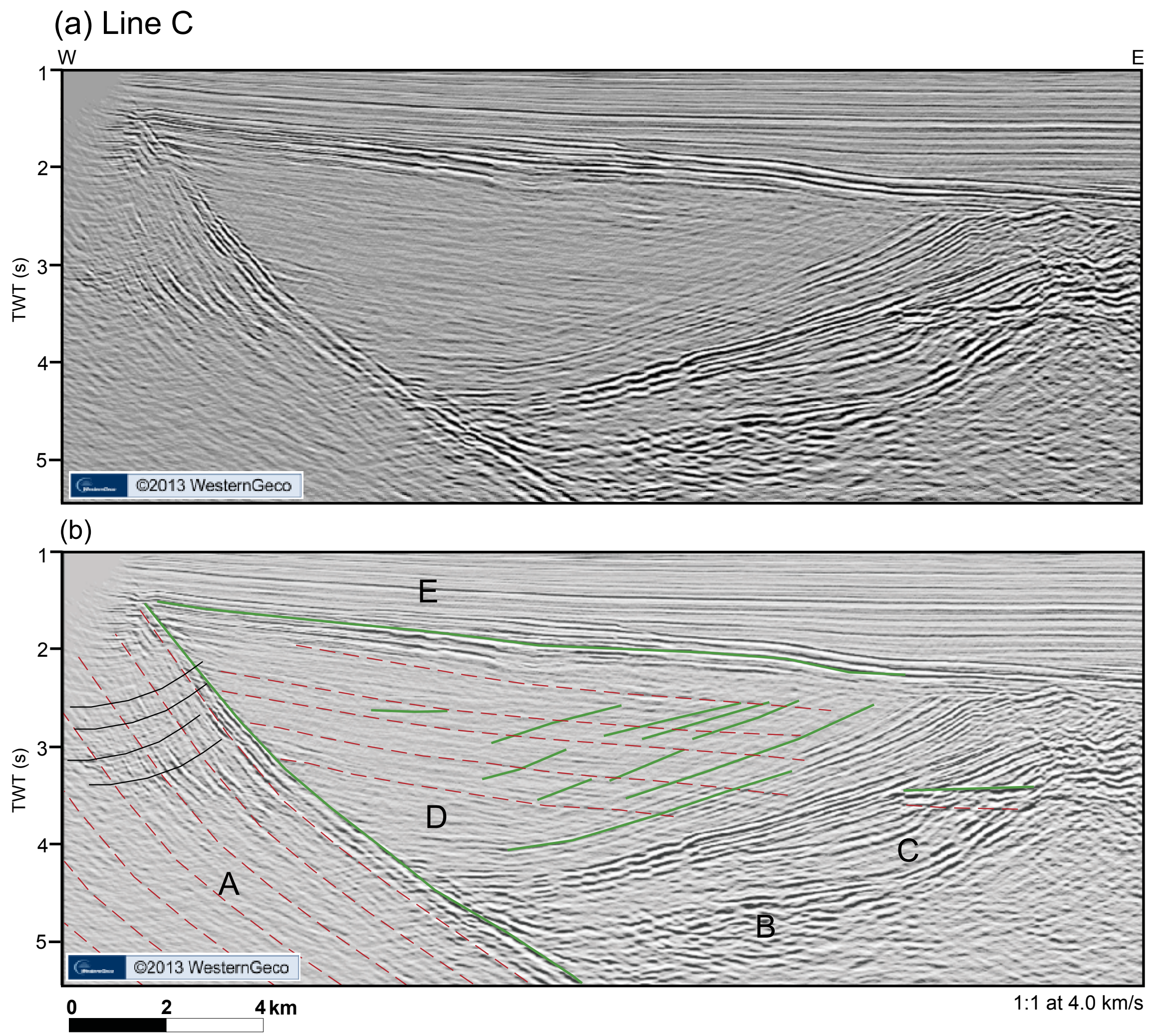

Figure 5: (a) Part of seismic line C. (b) Interpreted line showing primary reflections (green lines), multiples (dashed red lines) and migration artifacts (black lines). Capital letters are tectonostratigraphic packages. See line location on Figure 7 and complete line in Figure 14.

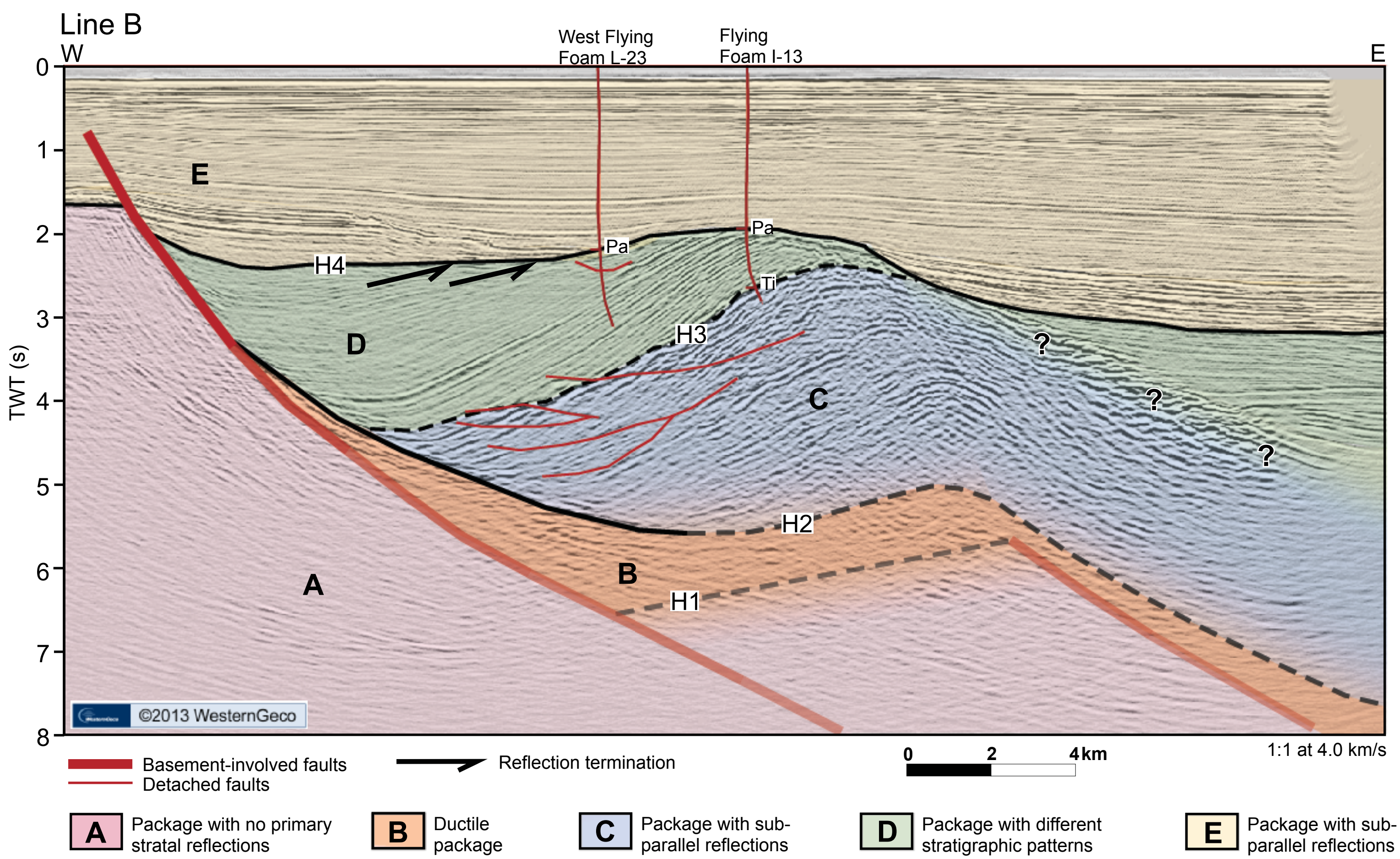

Figure 6. Interpreted seismic line B (see location of line on Figure 7) showing key features. Colors represent tectonostratigraphic packages. Detached faults dip away from the cross section. Differences in the stratigraphic patterns in Package D are described in detail in section 5. H1, H2, H3 and H4 are mapped horizons. Gradational colors, dashed lines and question marks indicate uncertainty in the interpretation. Pa (Paleogene) and Ti (Tithonian) (CNLOPB, 2012) are unconformities recognized in wells converted from depth to time (see section 3.3).

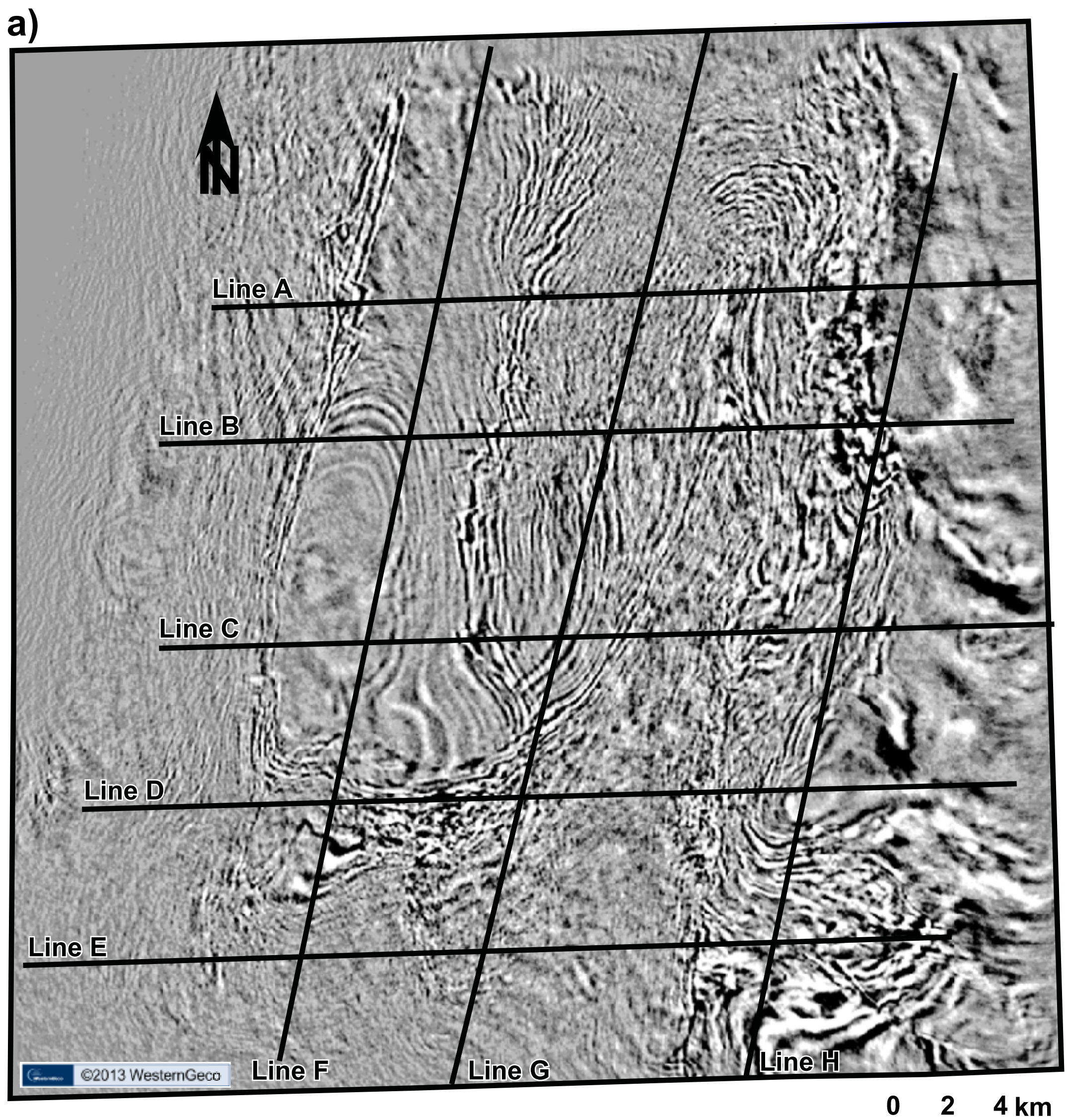

Figure 7. a) Time-slice at 3.9s without interpretation showing location of selected seismic lines presented in this thesis.

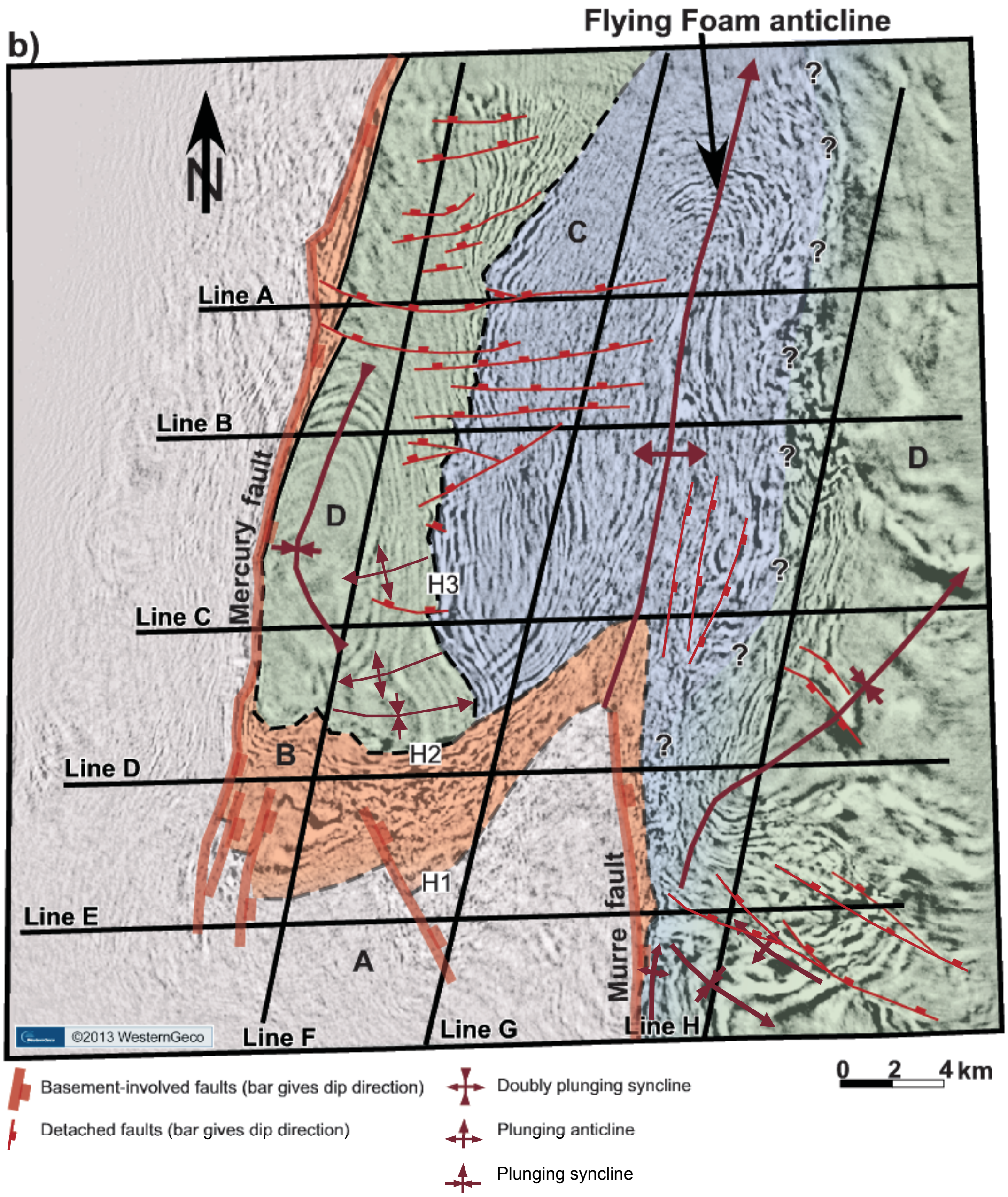

Figure 7. b) Interpreted time-slice at 3.9 s showing the distribution of the tectonostratigraphic packages and structural features. The southern part of the area is mainly fault-dominated, whereas the central and northern parts are fold-dominated. H1, H2 and H3 are mapped horizons. Other letters and colors indicate tectonostratigraphic packages. Dashed lines and gradational colors indicate uncertainty.

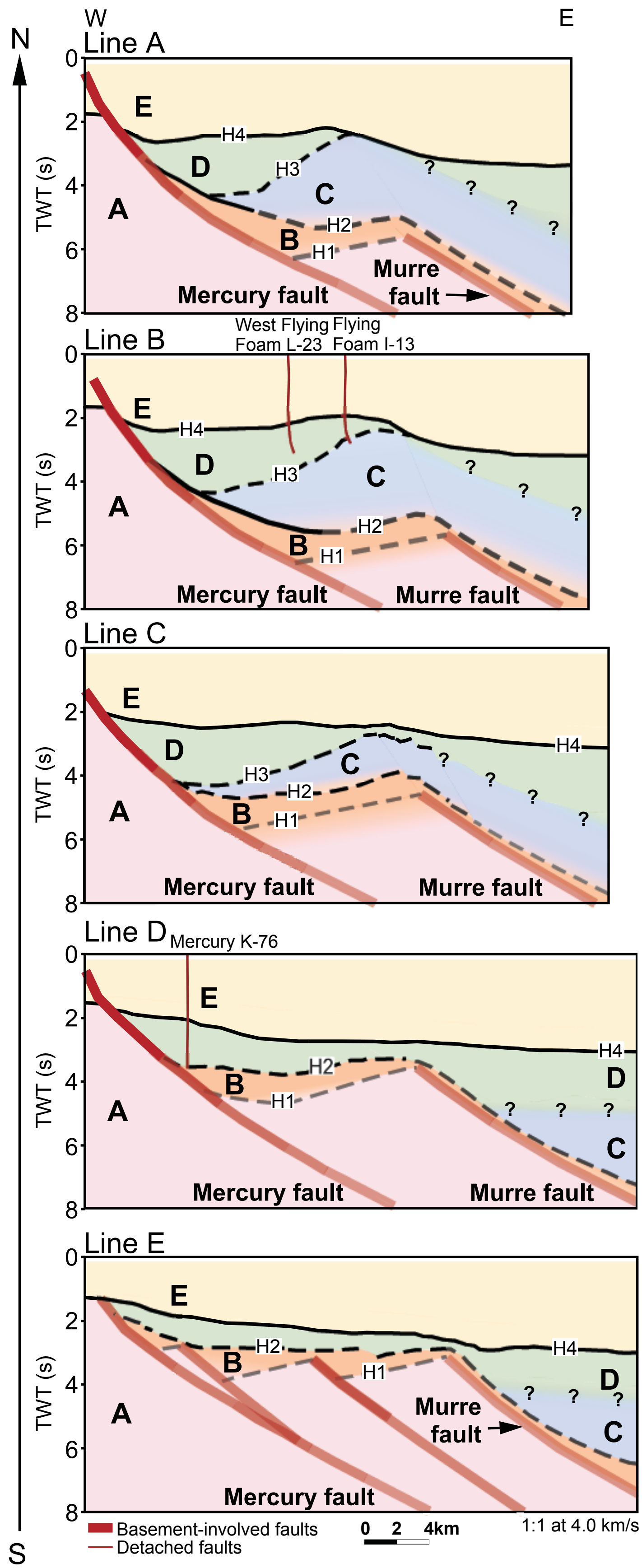

Figure 8. Line drawings of seismic lines showing the along-strike structural variability in the study area from north to south. H1, H2, H3 and H4 are mapped horizons. Other capital letters and colors indicate tectonostratigraphic packages. Dashed lines, gradational colors and question marks indicate uncertainty. See location of dip lines in Figure 7.

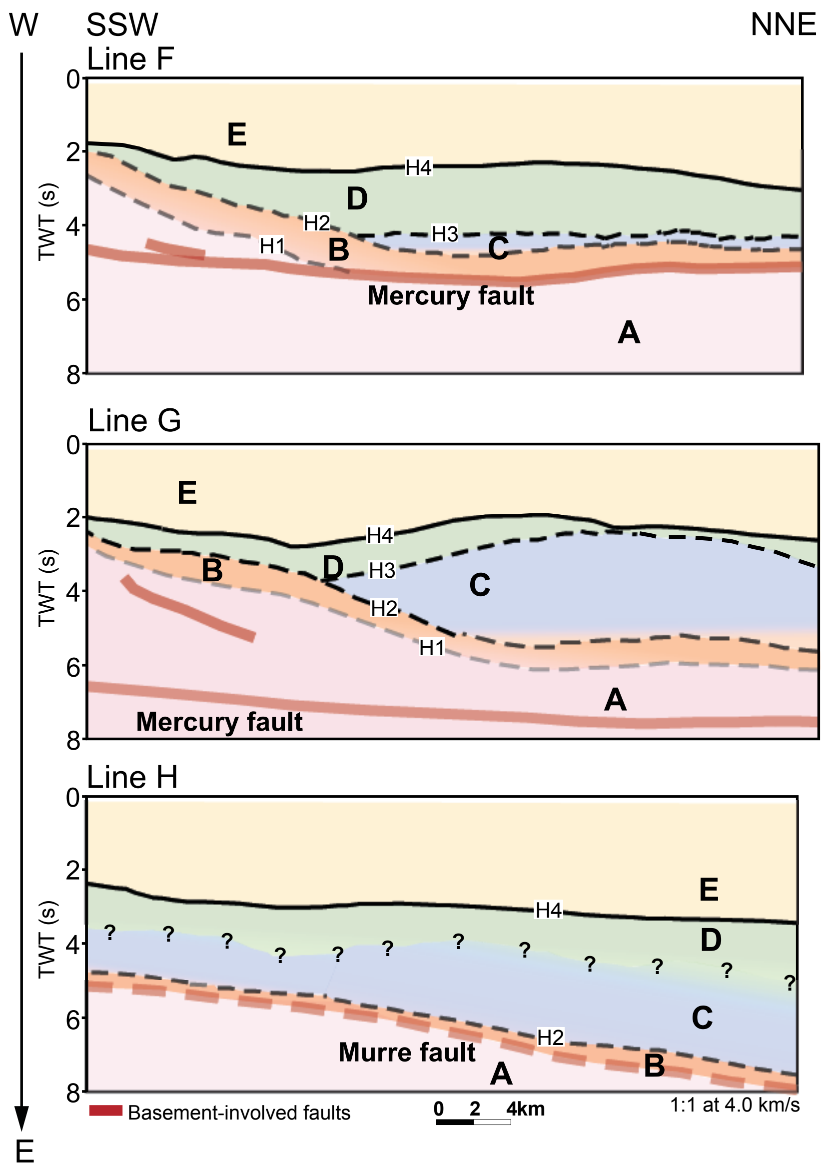

Figure 9. Line drawings of seismic lines showing along-dip structural variability in the study area from west to east. H1, H2, H3, and H4 are mapped horizons. Other capital letters and colors indicate tectonostratigraphic packages. Dashed lines, gradational colors and question marks indicate uncertainty. See location of strike lines in Figure 7.

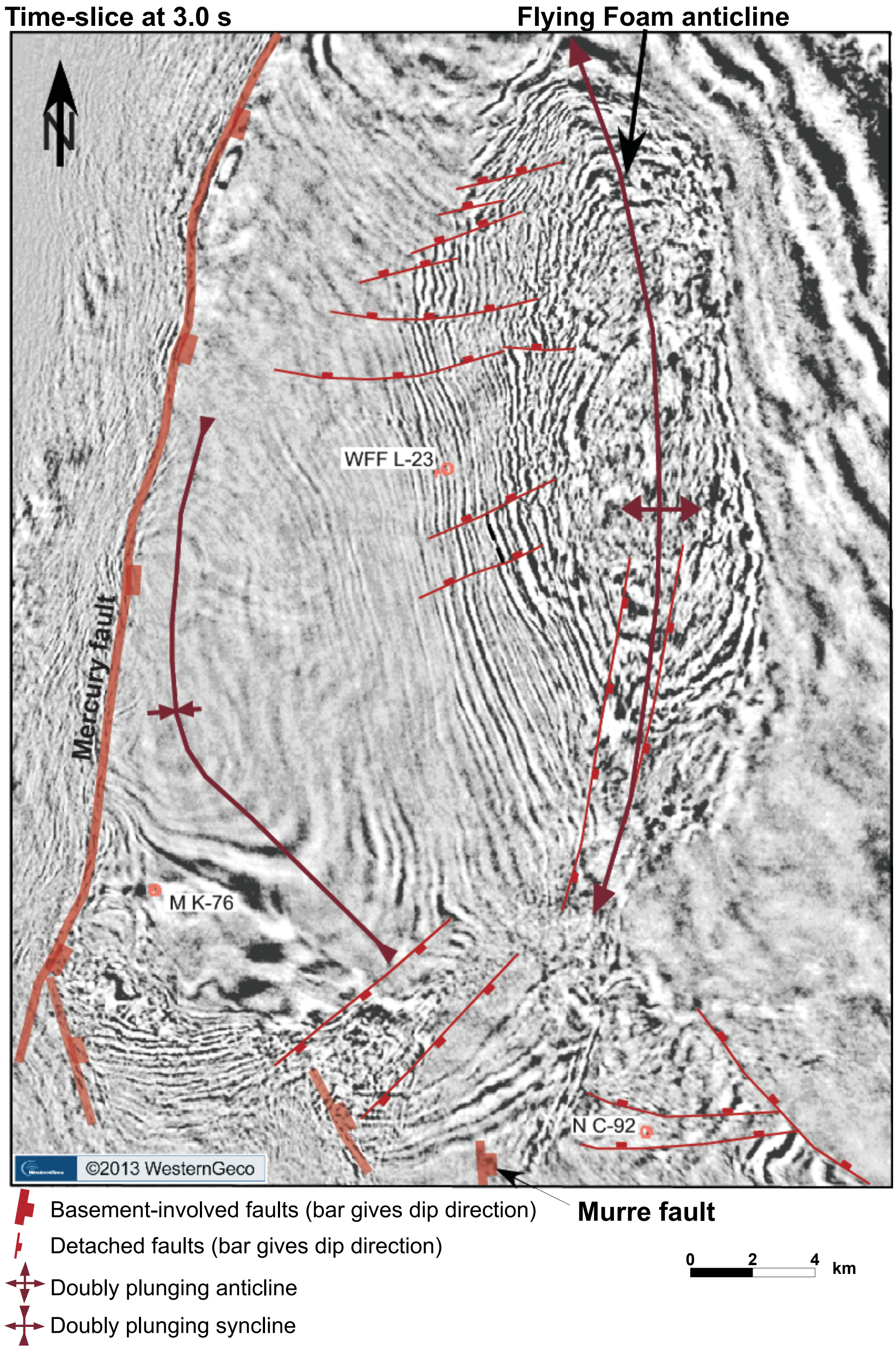

Figure 10. Time-slice at 3.0 s showing faults and folds. Gradational colors indicate uncertainty. Red circles are wells. Abbreviations for wells are: WFF, West Flying Foam; M, Mercury; N, Nautilus.

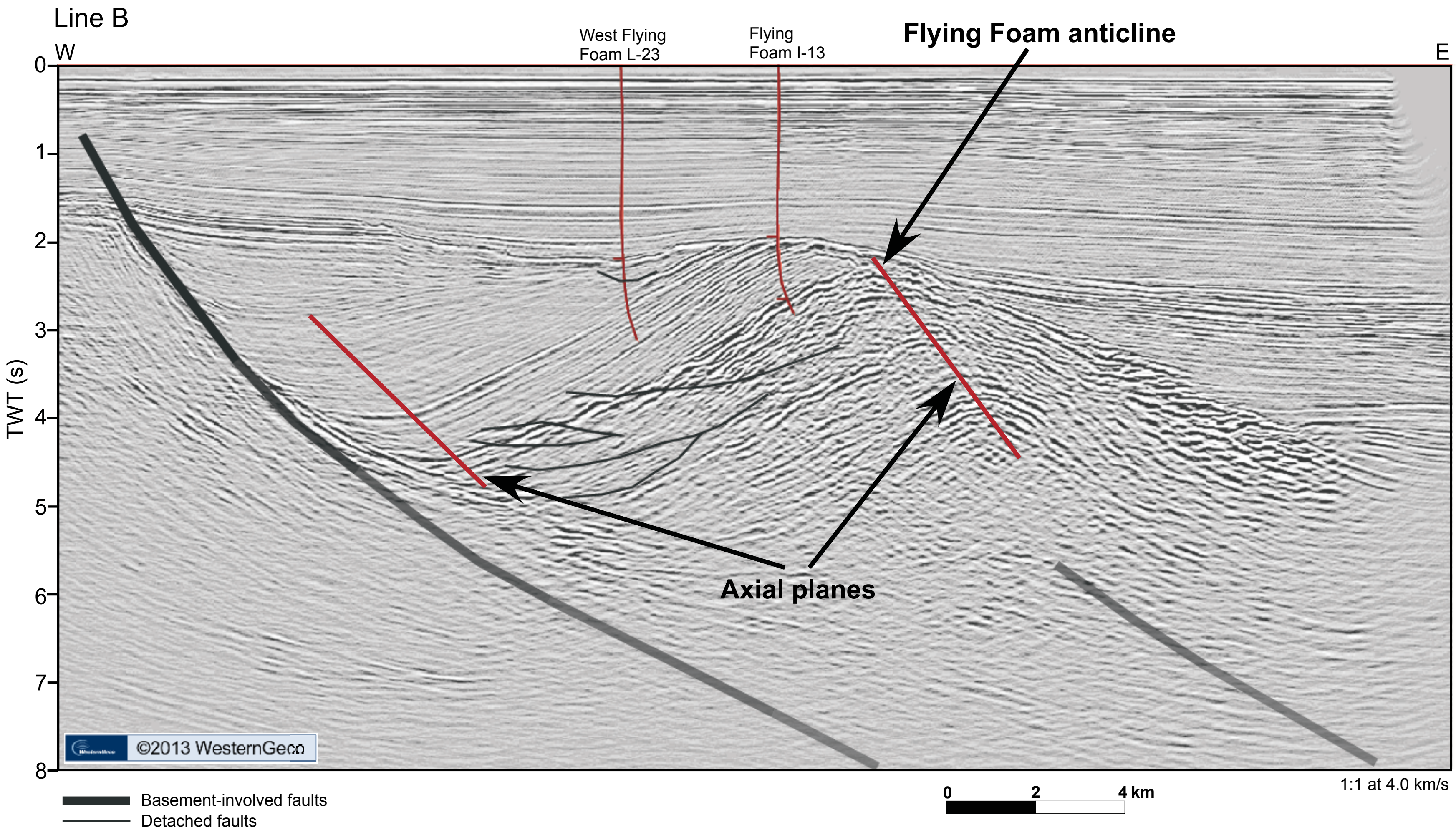

Figure 11. Seismic line B (see location of line on Figure 7) showing faults and axial planes of folds. See full interpretation of line in Figure 13.

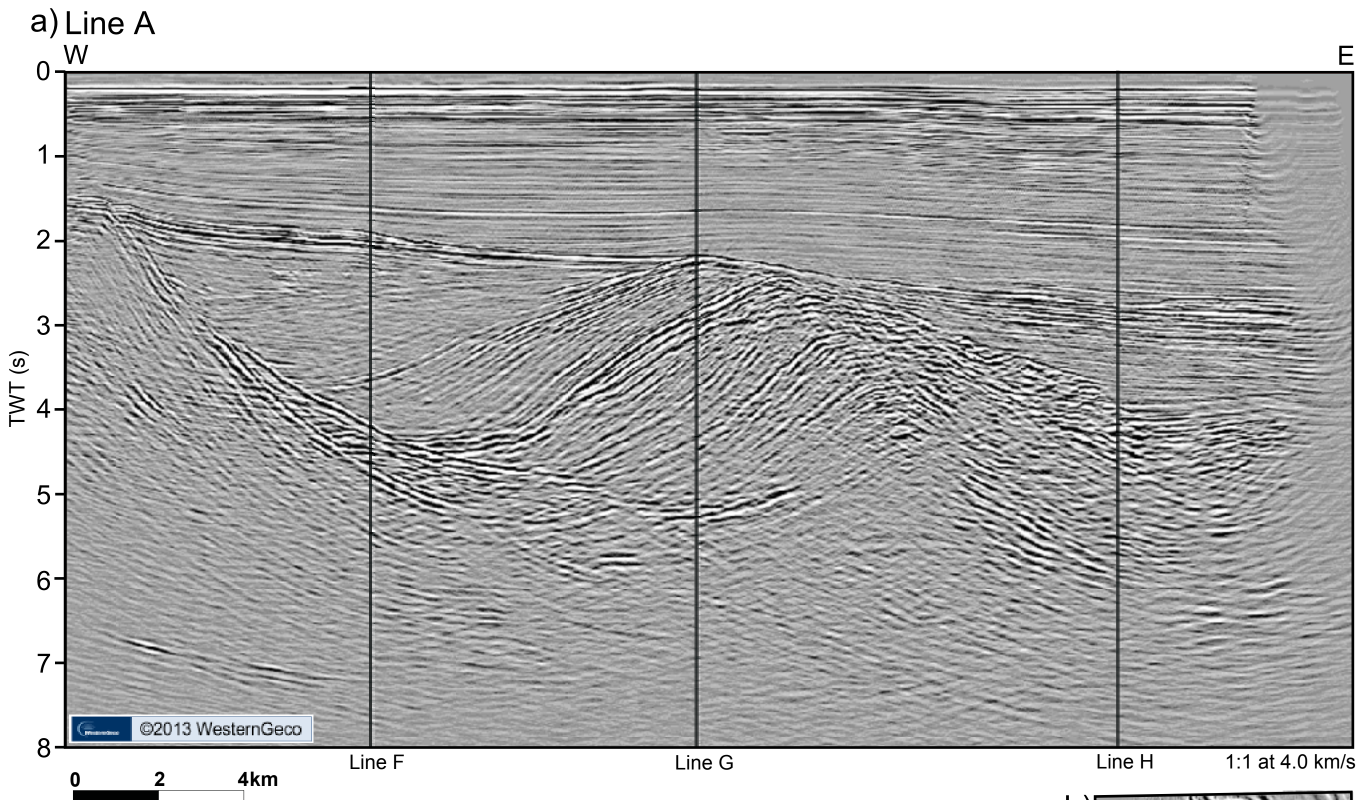

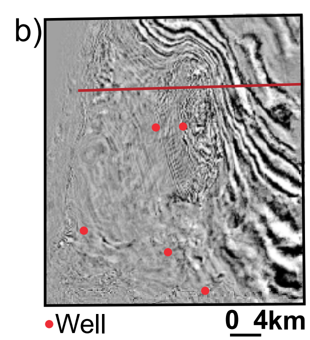

Figure 12. a) Seismic line A without interpretation showing the location of intersecting strike lines. b) Time-slice at 2.640 s showing the location of line A. The time corresponds to the maximum TWT reached by all the wells in the study area.

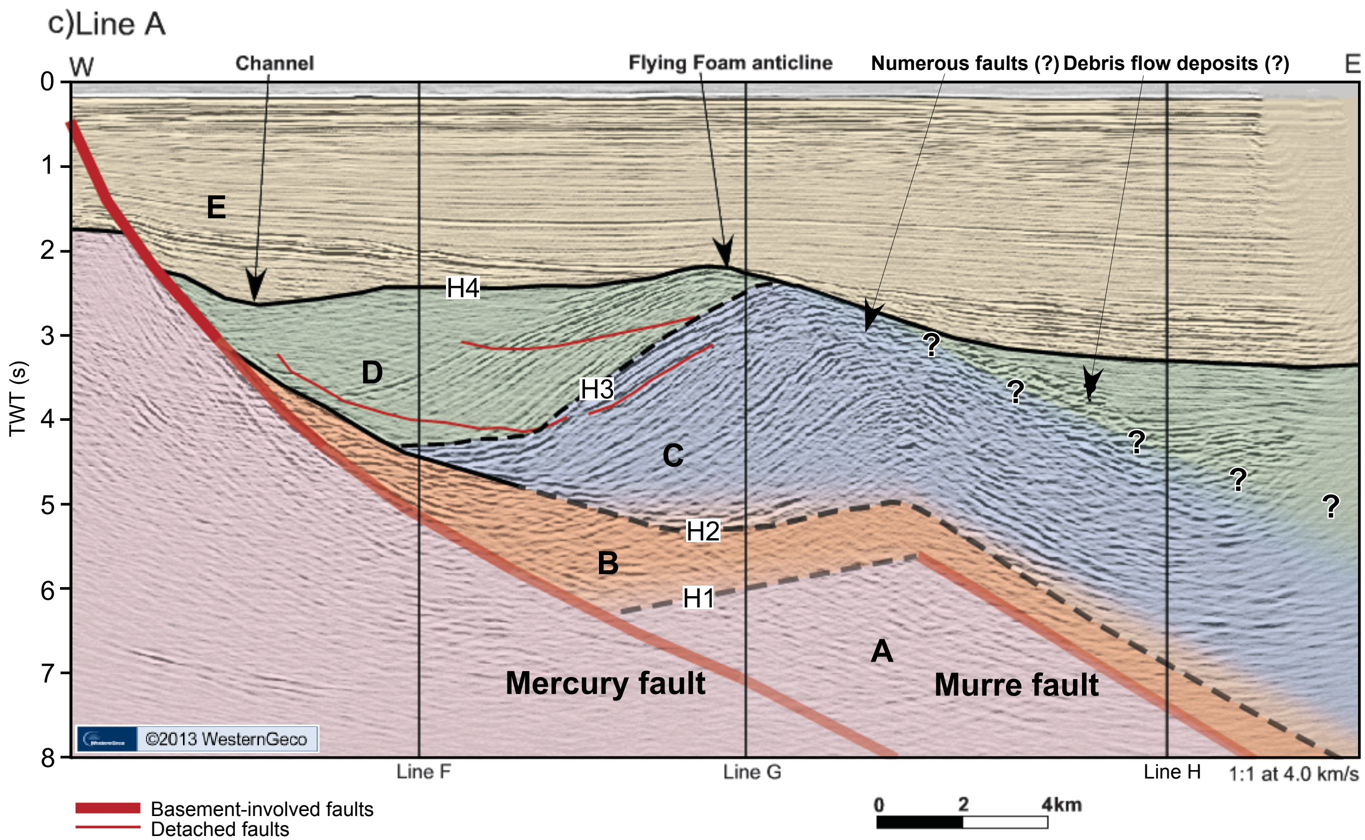

Figure 12. c) Interpreted seismic line A showing tectonostratigraphic packages (A to E and colors) and key geologic features. H1, H2, H3 and H4 are mapped horizons. Dashed lines, gradational colors and question marks indicate uncertainty.

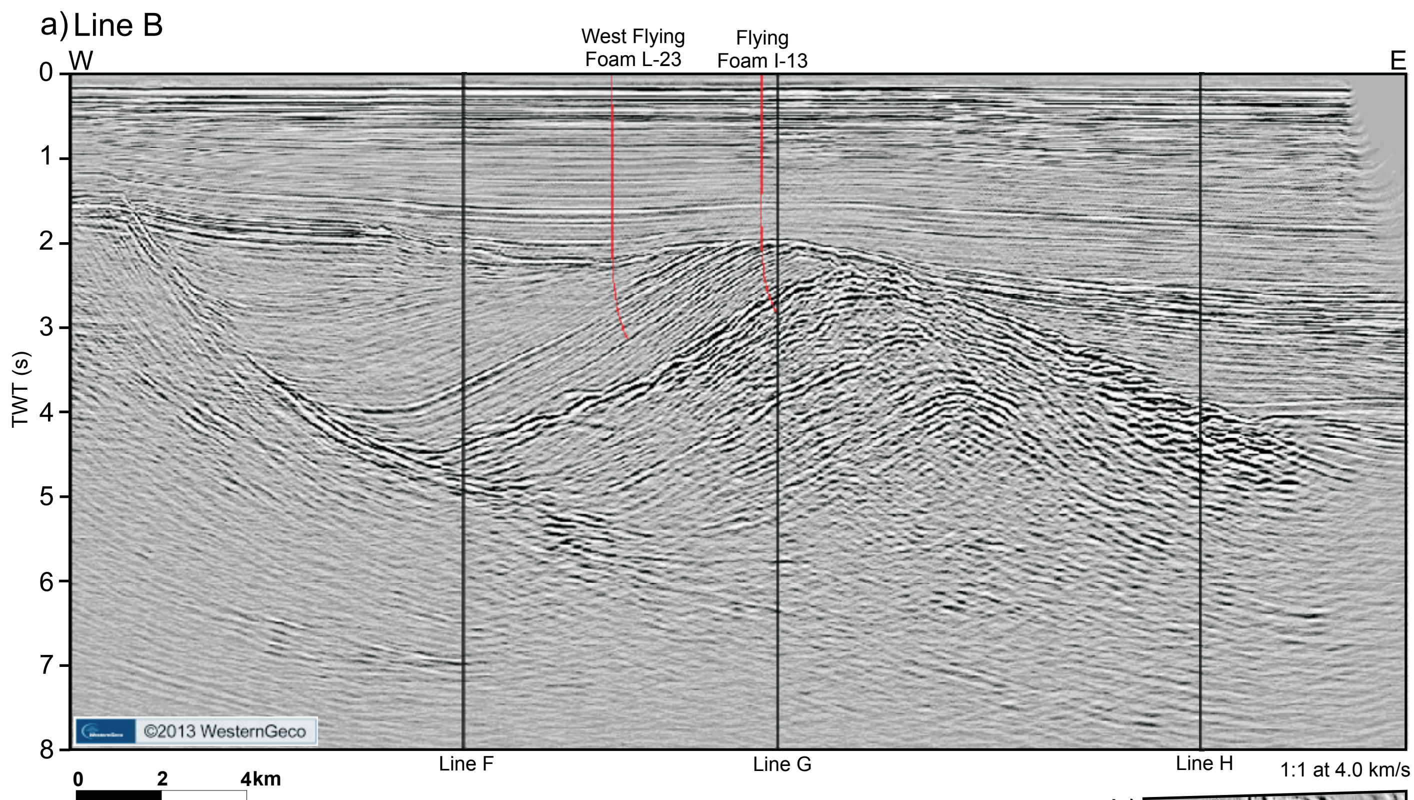

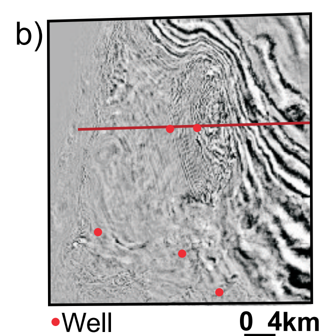

Figure 13. a) Seismic line B without interpretation showing the location of intersecting strike lines. b) Time-slice at 2.640 s showing the location of line B.

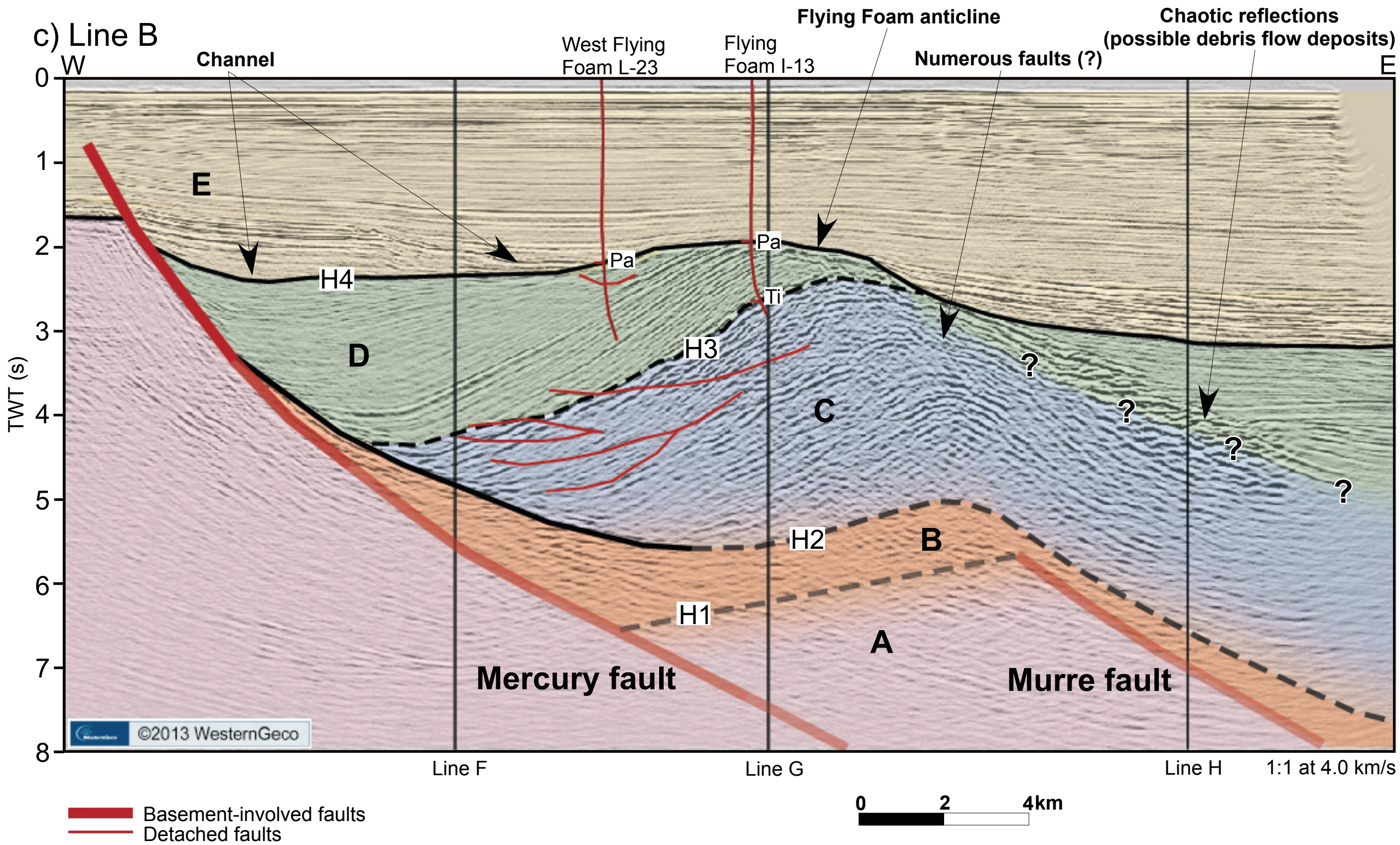

Figure 13. c) Interpreted seismic line B showing tectonostratigraphic packages (A to E and colors), key geologic features and wells with unconformities (Pa: Paleogene, Ti: Tithonian, CNLOPB, 2012). H1, H2, H3 and H4 are mapped horizons. Dashed lines, gradational colors and question marks indicate uncertainty.

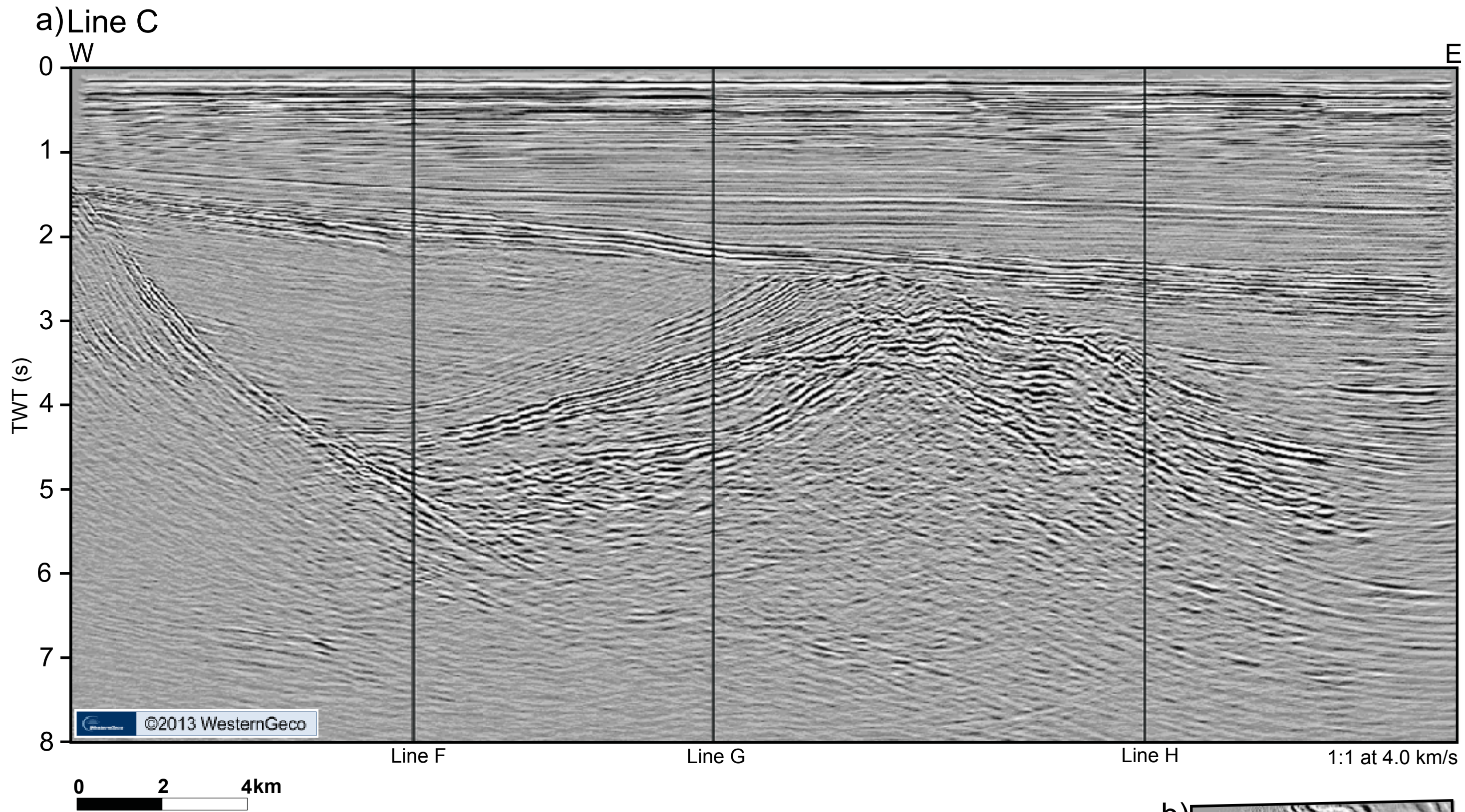

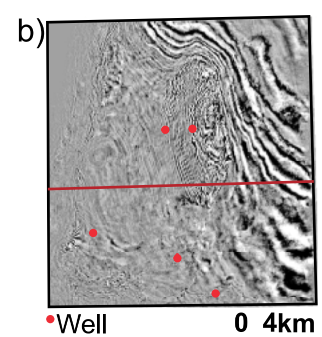

Figure 14. a) Seismic line C without interpretation showing location of intersecting strike lines. b) Time-slice at 2.640 s showing the location of line C.

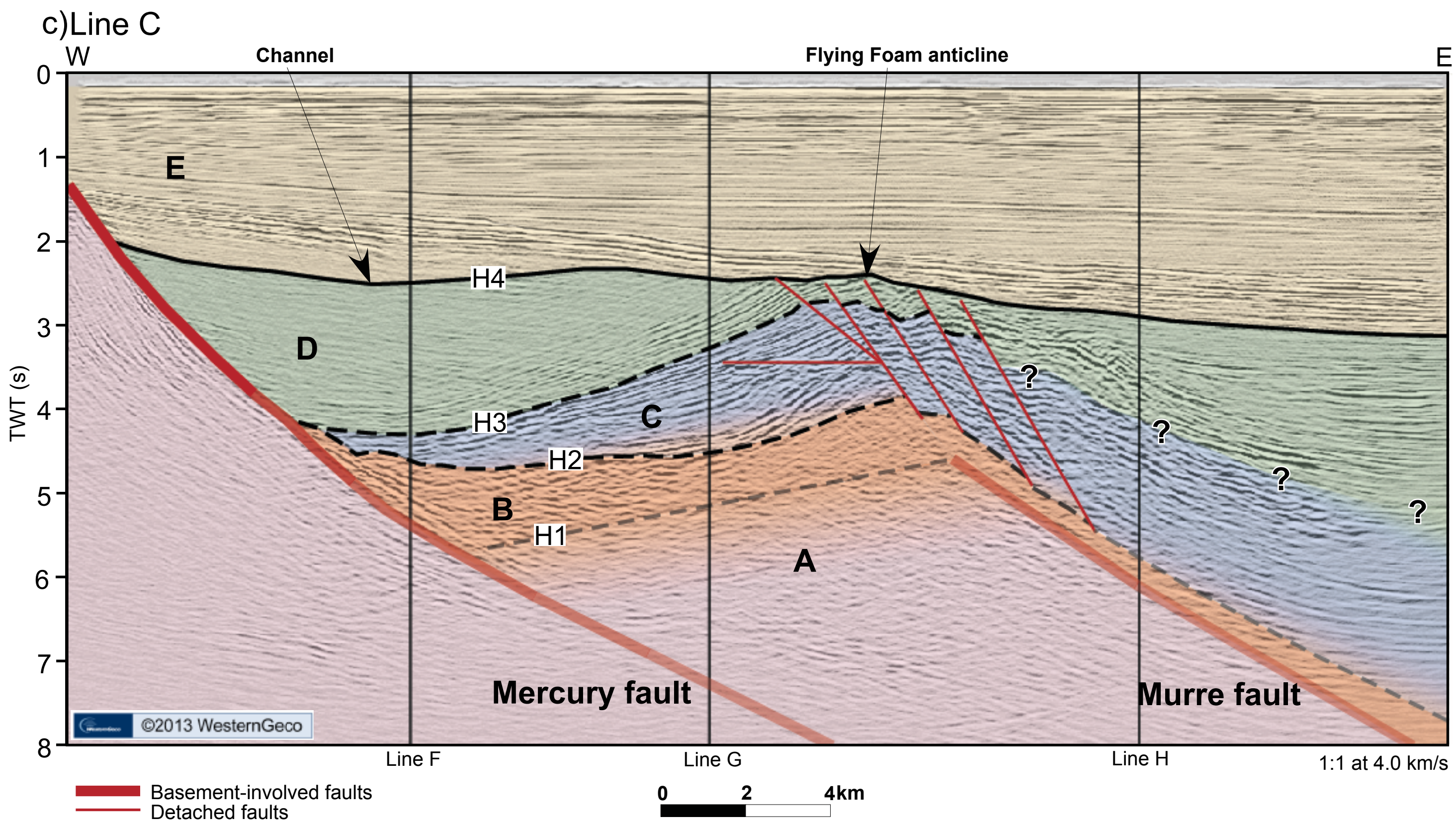

Figure 14. c) Interpreted seismic line C showing tectonostratigraphic packages (A to E and colors) and key geologic features. H1, H2, H3 and H4 are mapped horizons. Dashed lines, gradational colors and question marks indicate uncertainty.

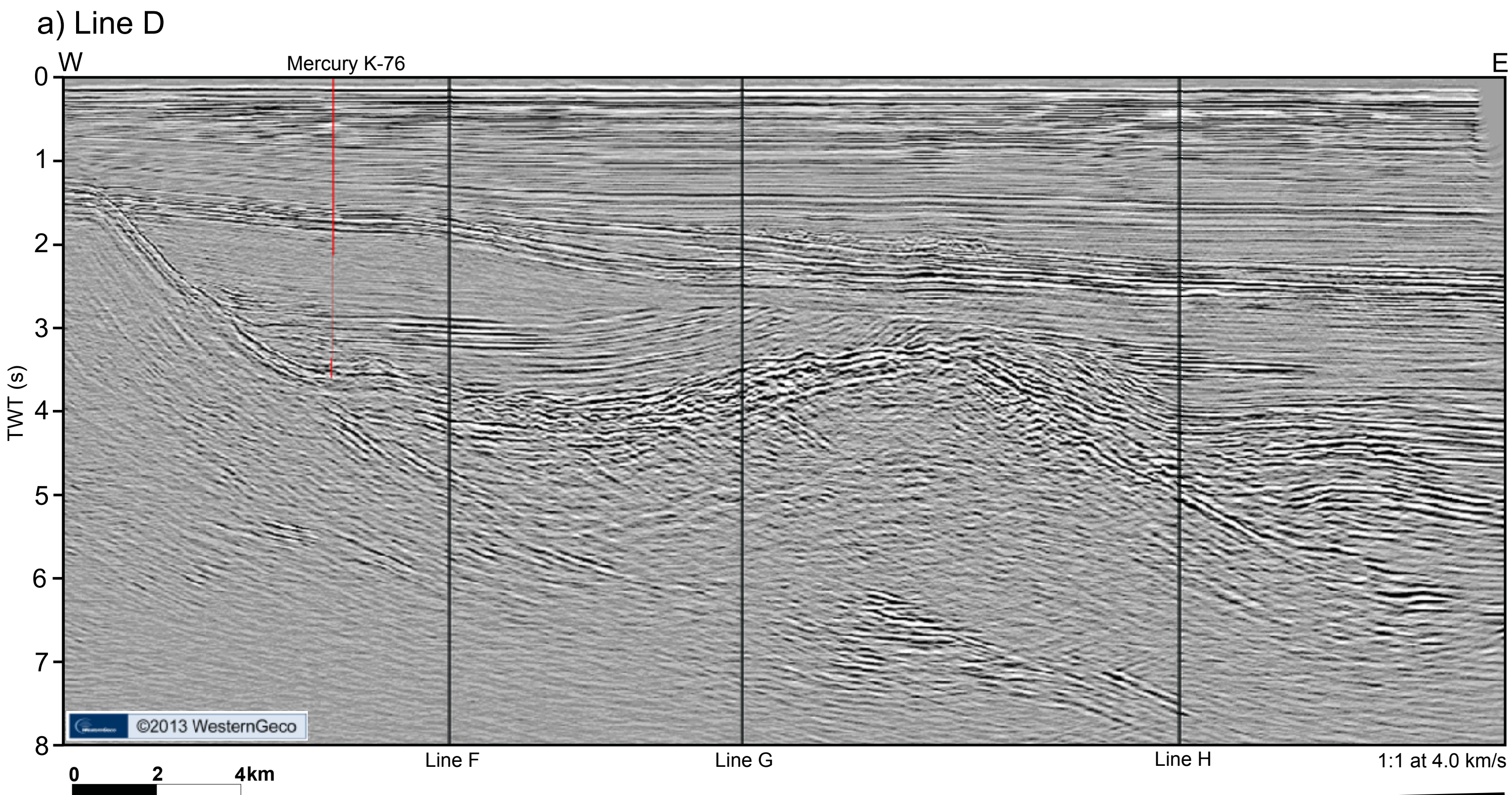

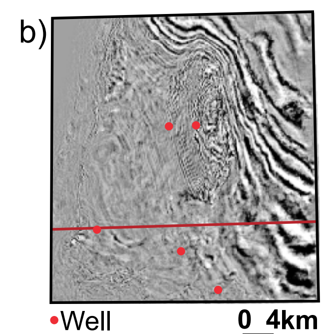

Figure 15. a) Seismic line D without interpretation showing the location of intersecting strike lines. b) Time-slice at 2.640 s showing the location of line D.

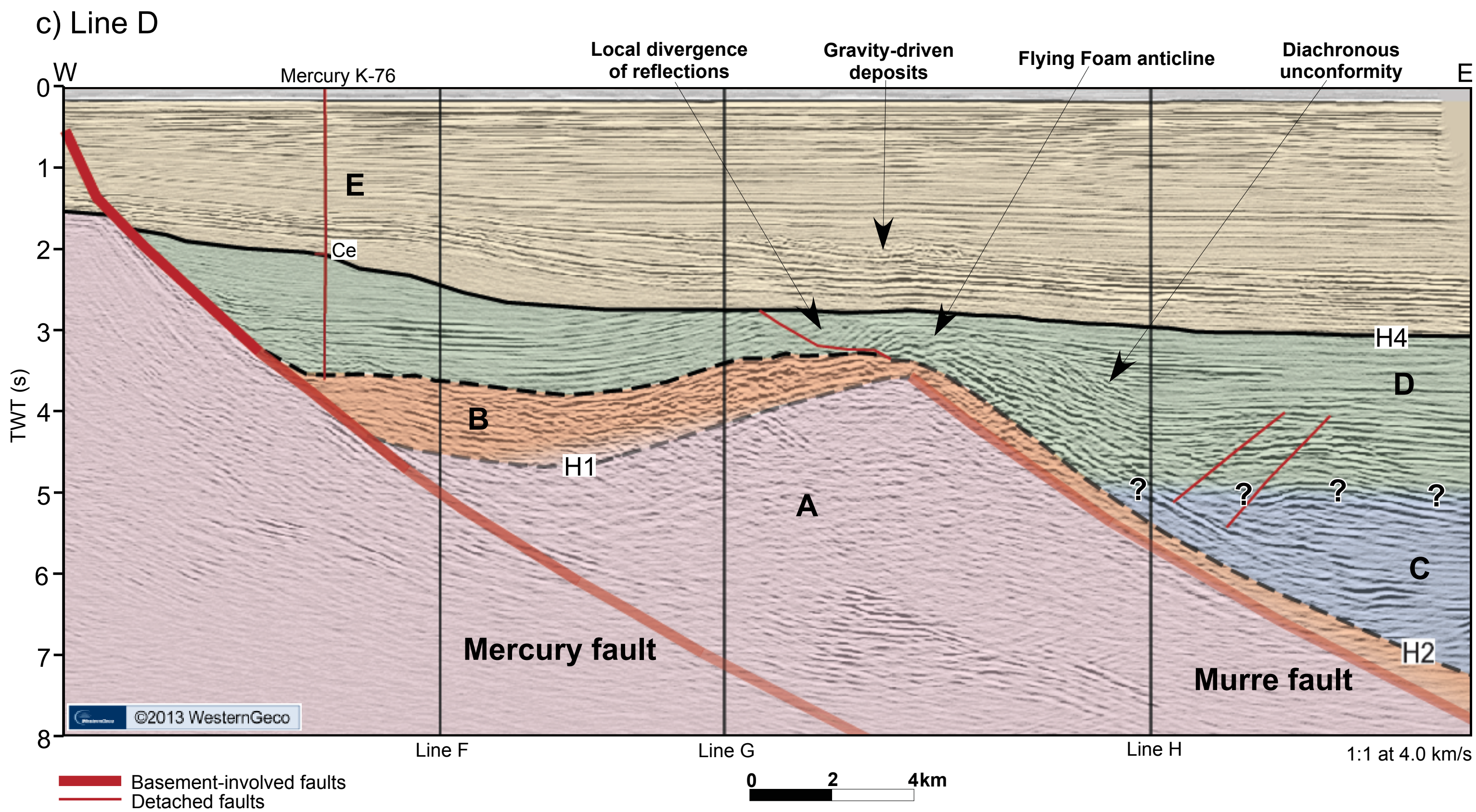

Figure 15. c) Interpreted seismic line D showing tectonostratigraphic packages (A to E and colors), key geologic features and a well with unconformities (Ce: Cenomanian, CNLOPB, 2012). H1, H2 and H4 are mapped horizons. Dashed lines, gradational colors and question marks indicate uncertainty.

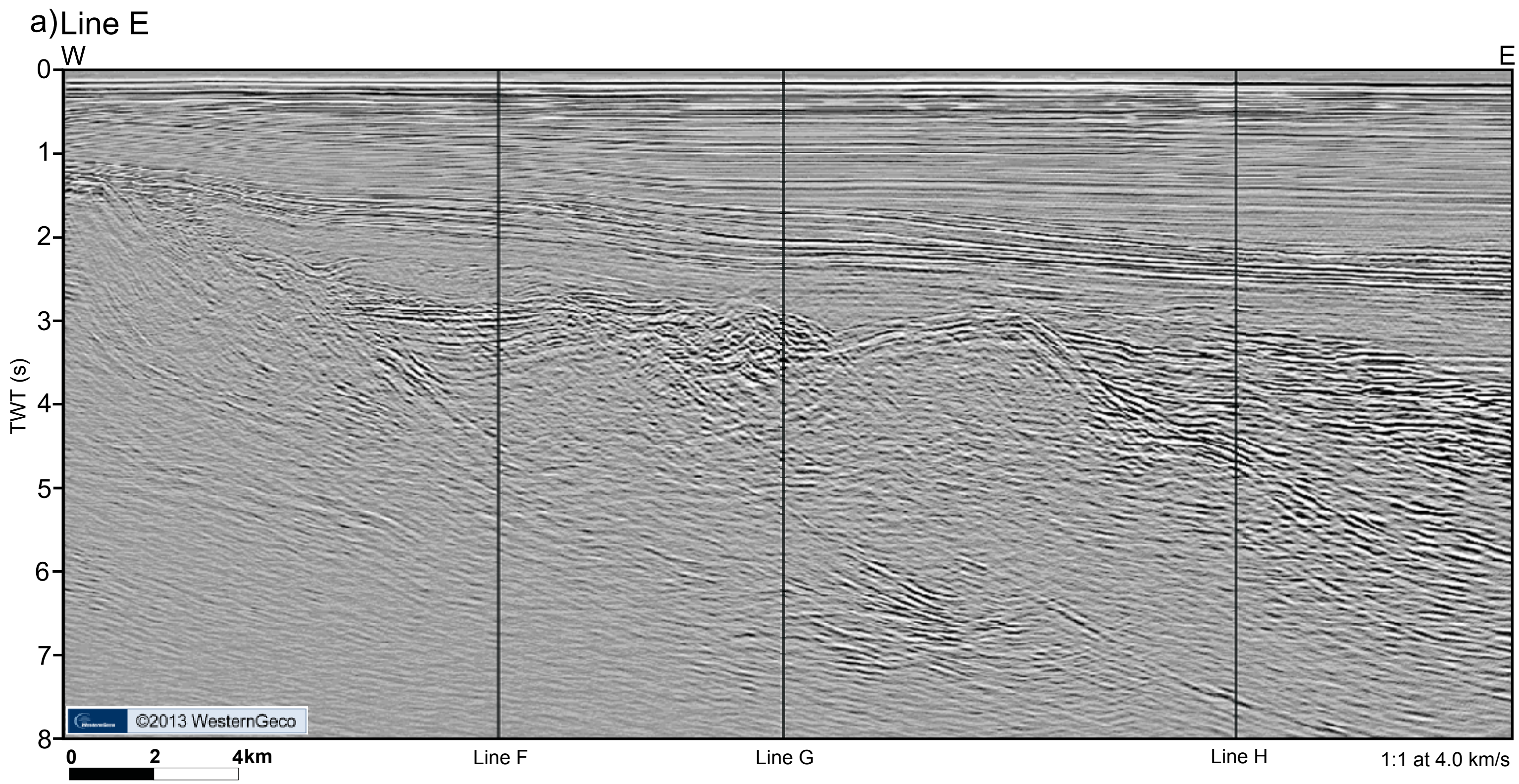

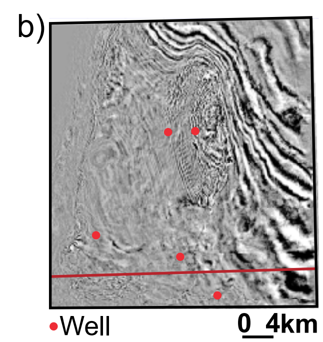

Figure 16. a) Seismic line E without interpretation showing the location of intersecting strike lines. b) Time-slice at 2.640 s showing location of line E.

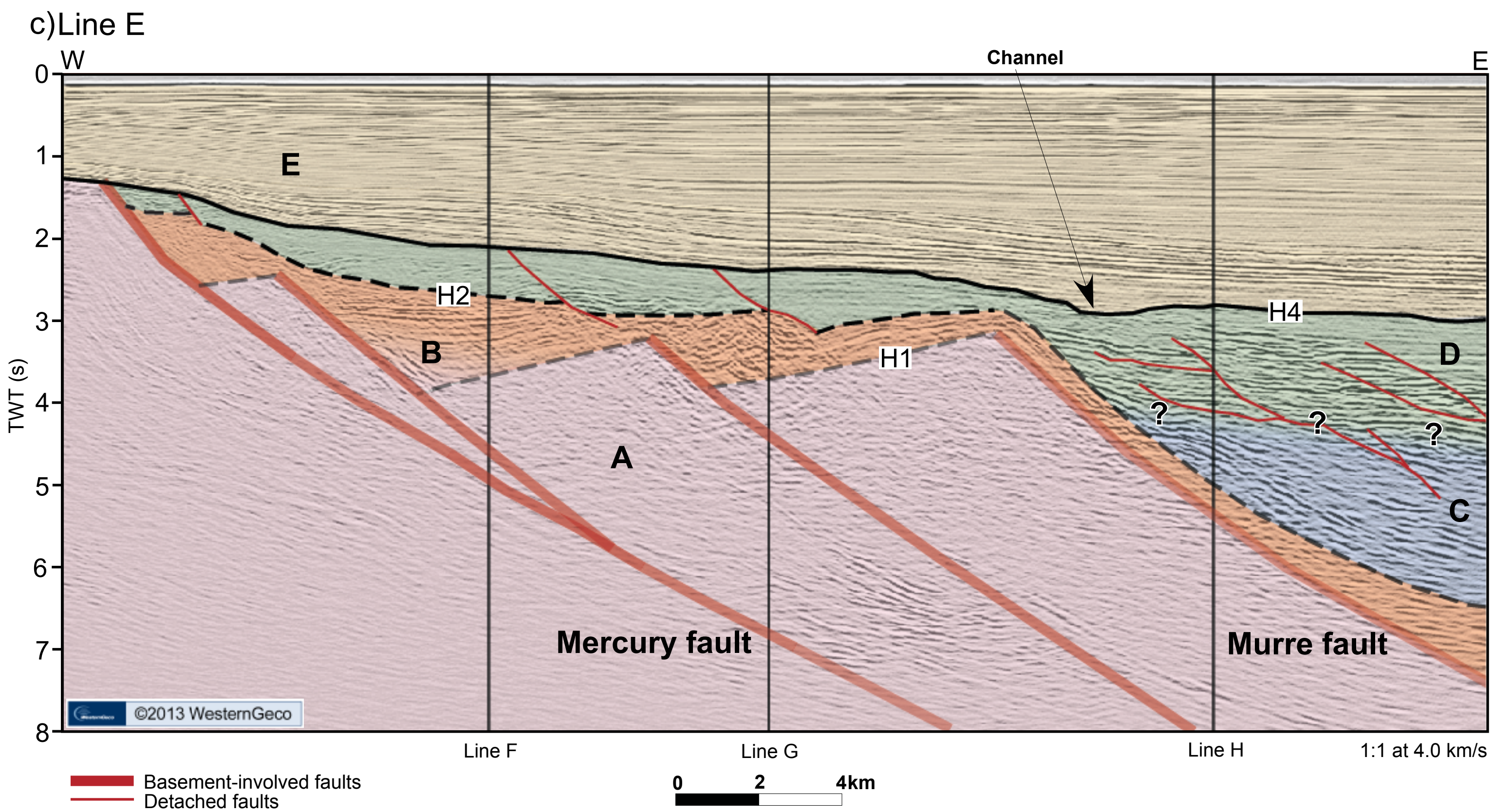

Figure 16. c) Interpreted seismic line E showing numerous basement-involved faults and detached faults. H1, H2 and H4 are mapped horizons. Other capital letters and colors indicate tectonostratigraphic packages. Dashed lines, gradational colors and question marks indicate uncertainty.

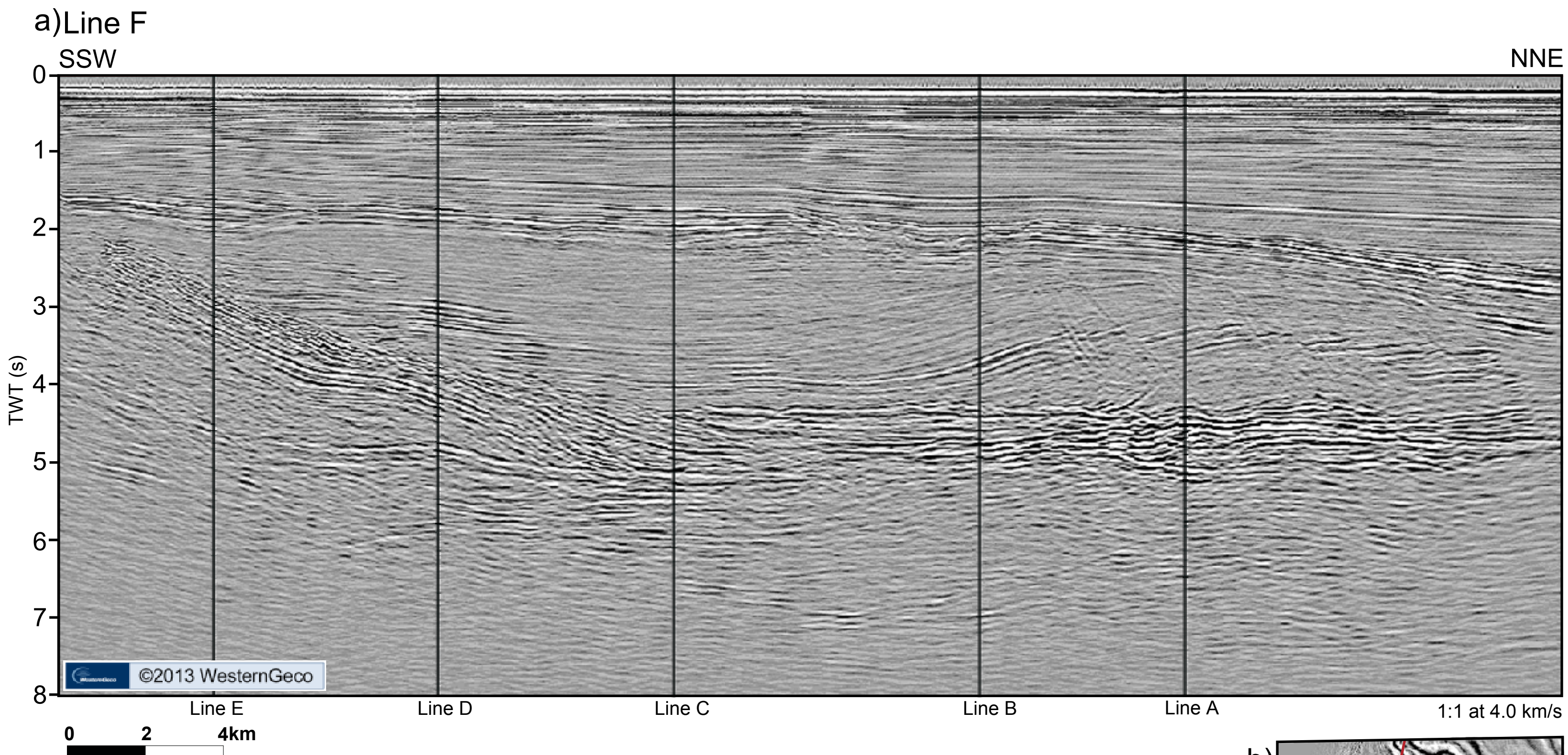

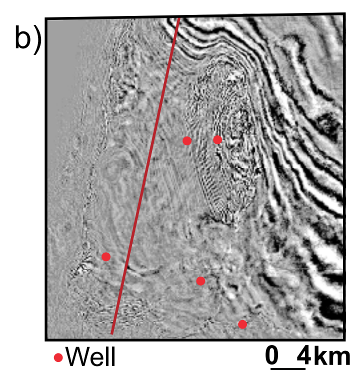

Figure 17. a) Line F without interpretation showing the location of intersecting lines.
b) Time-slice at 2.640 s showing the location of line F.

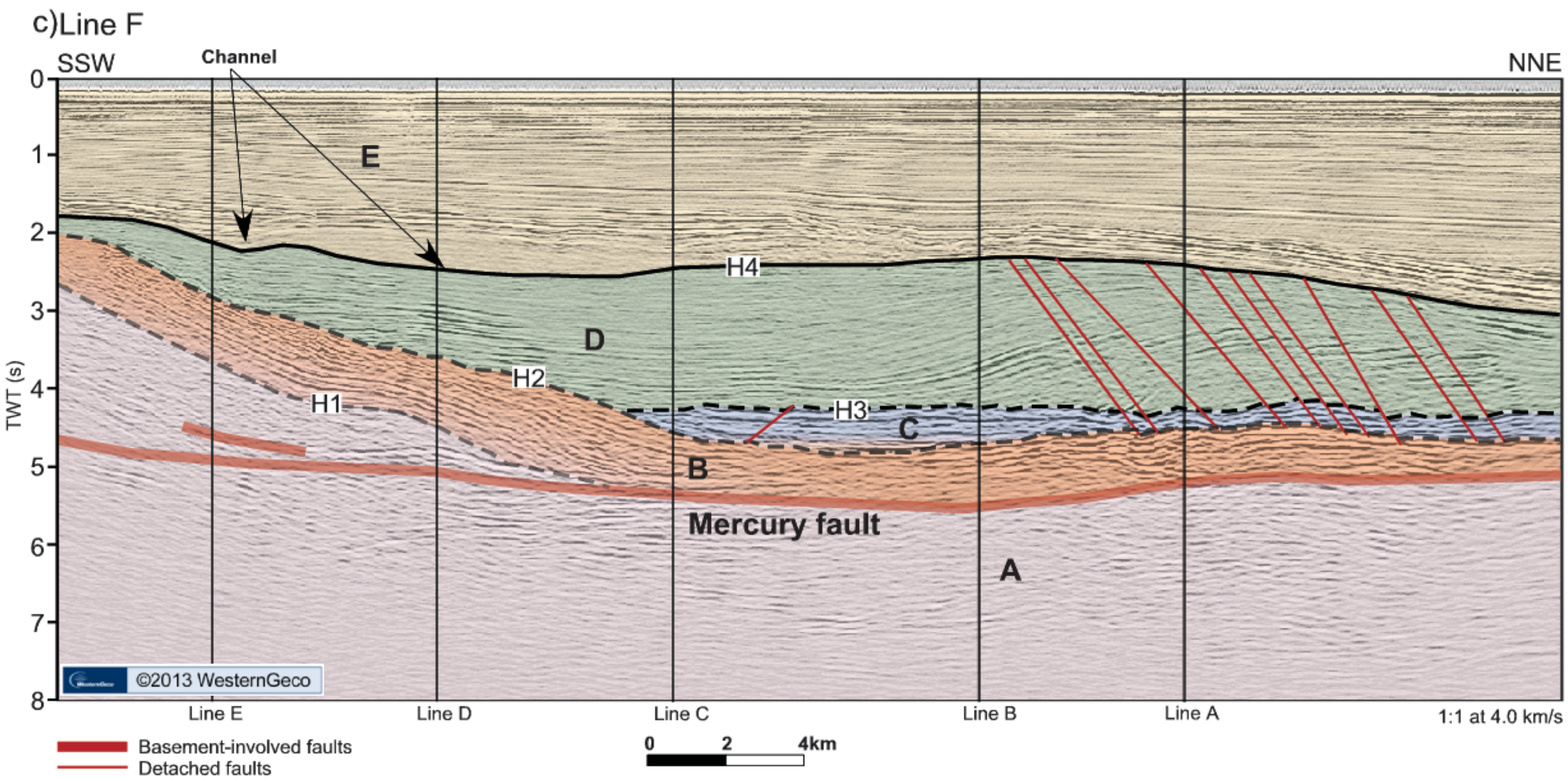

Figure 17. c) Interpreted line F showing tectonostratigraphic packages (A to E and colors) and key geologic features. H1, H2, H3 and H4 are mapped horizons. Dashed lines and gradational colors indicate uncertainty.

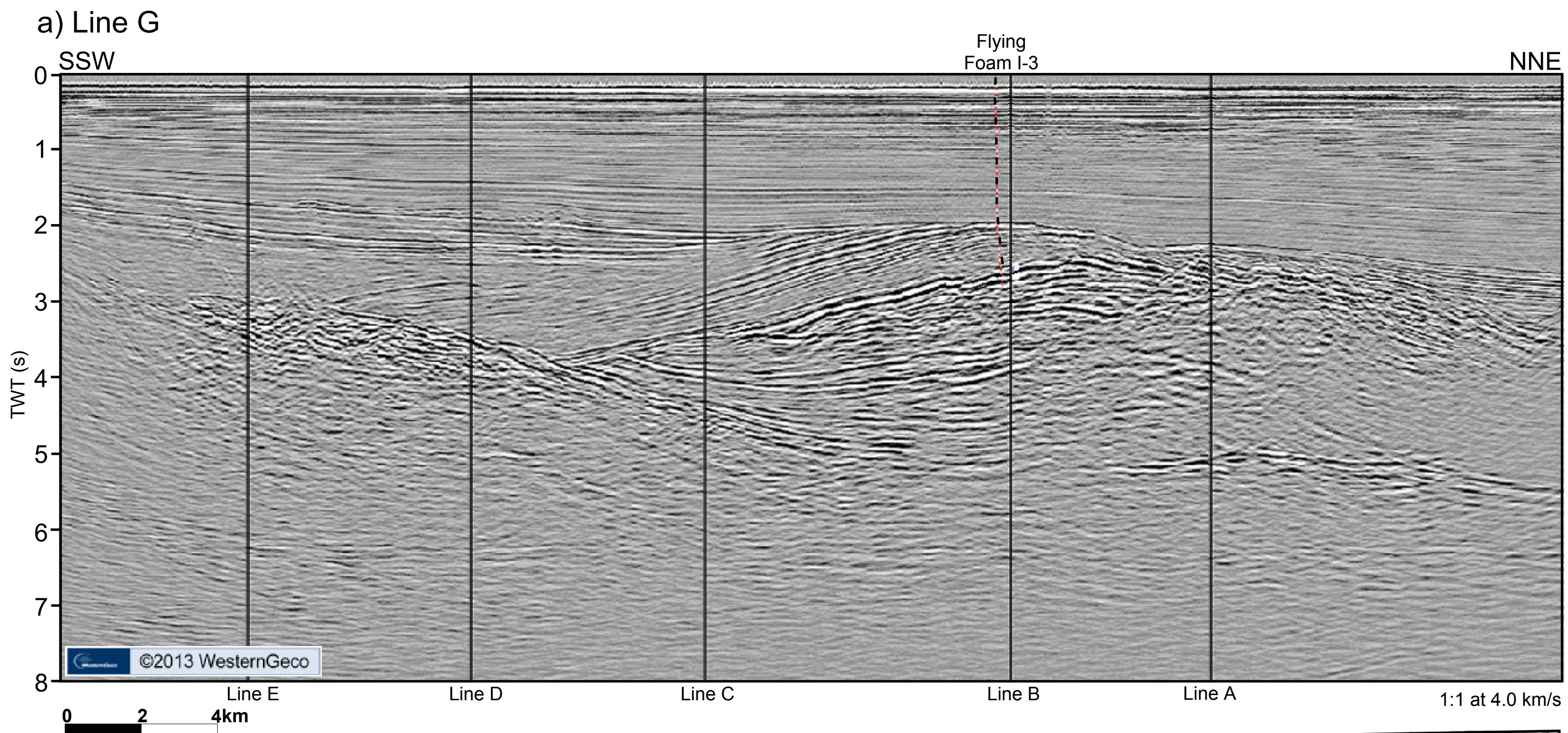

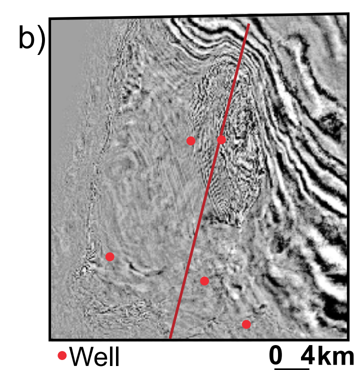

Figure 18. a) Line G without interpretation showing the location of intersecting lines.
b) Time-slice at 2.640 s showing the location of line G.

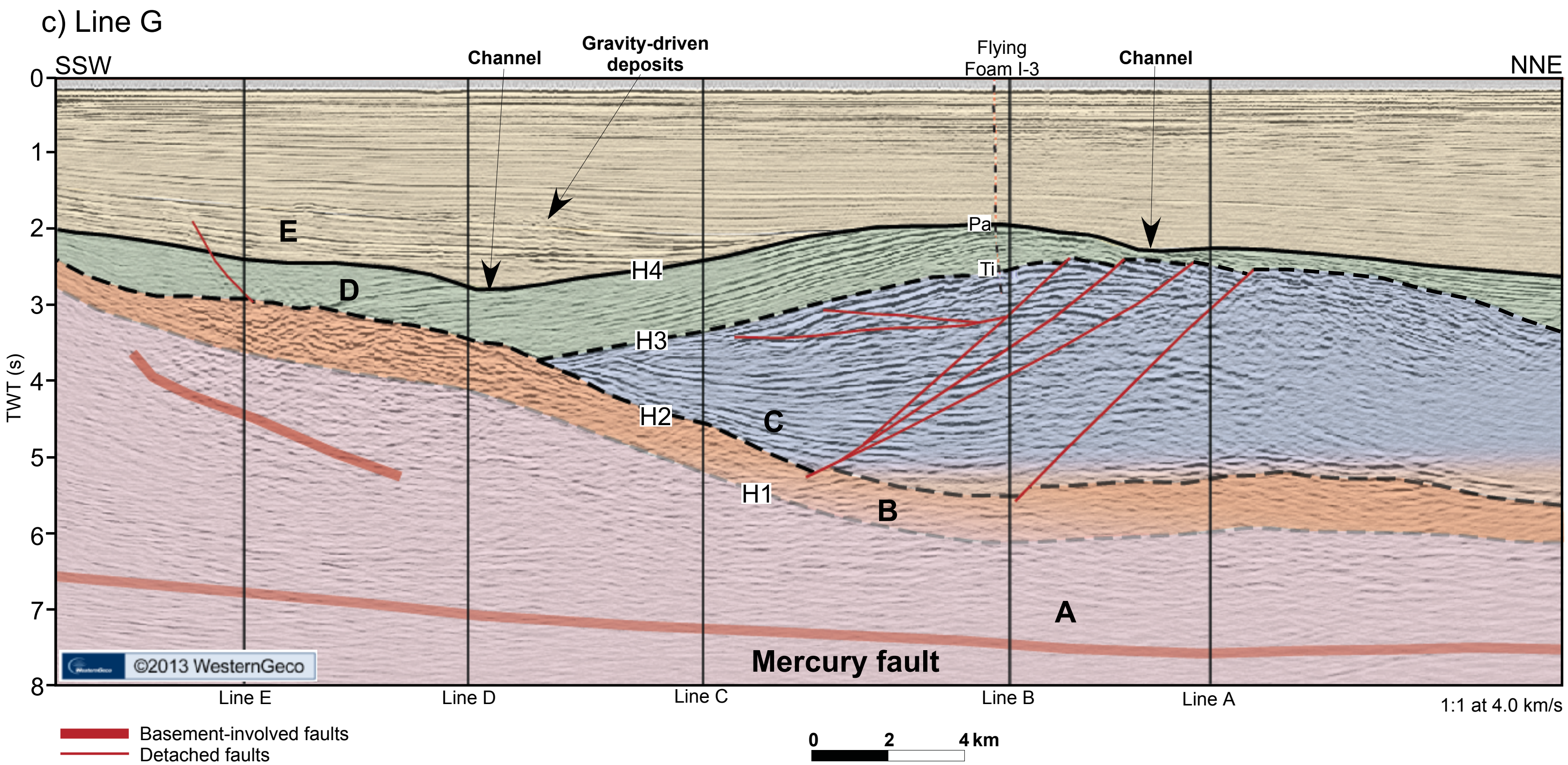

Figure 18. c) Interpreted line G showing tectonostratigraphic packages (A to E and colors), key geologic features and wells with unconformities (Pa: Paleogene, Ti: Tithonian, CNLOPB, 2012). H1, H2, H3 and H4 are mapped horizons. Dashed lines and gradational colors indicate uncertainty.

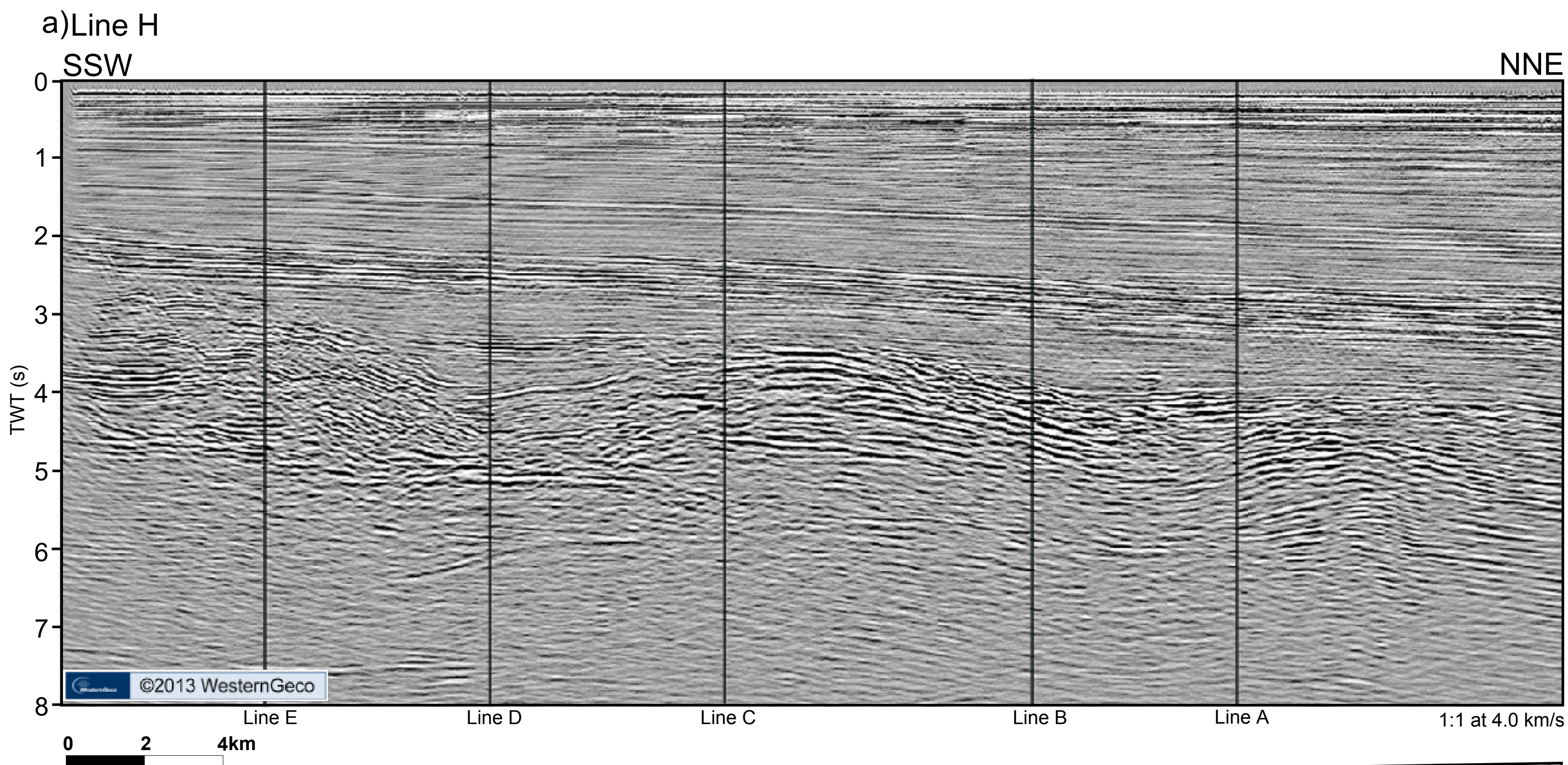

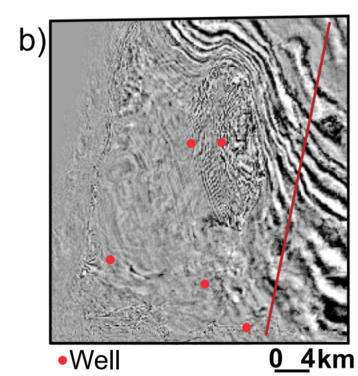

Figure 19. a) Line H without interpretation showing the location of intersecting lines.
b) Time-slice at 2.640 s showing the location of line H.

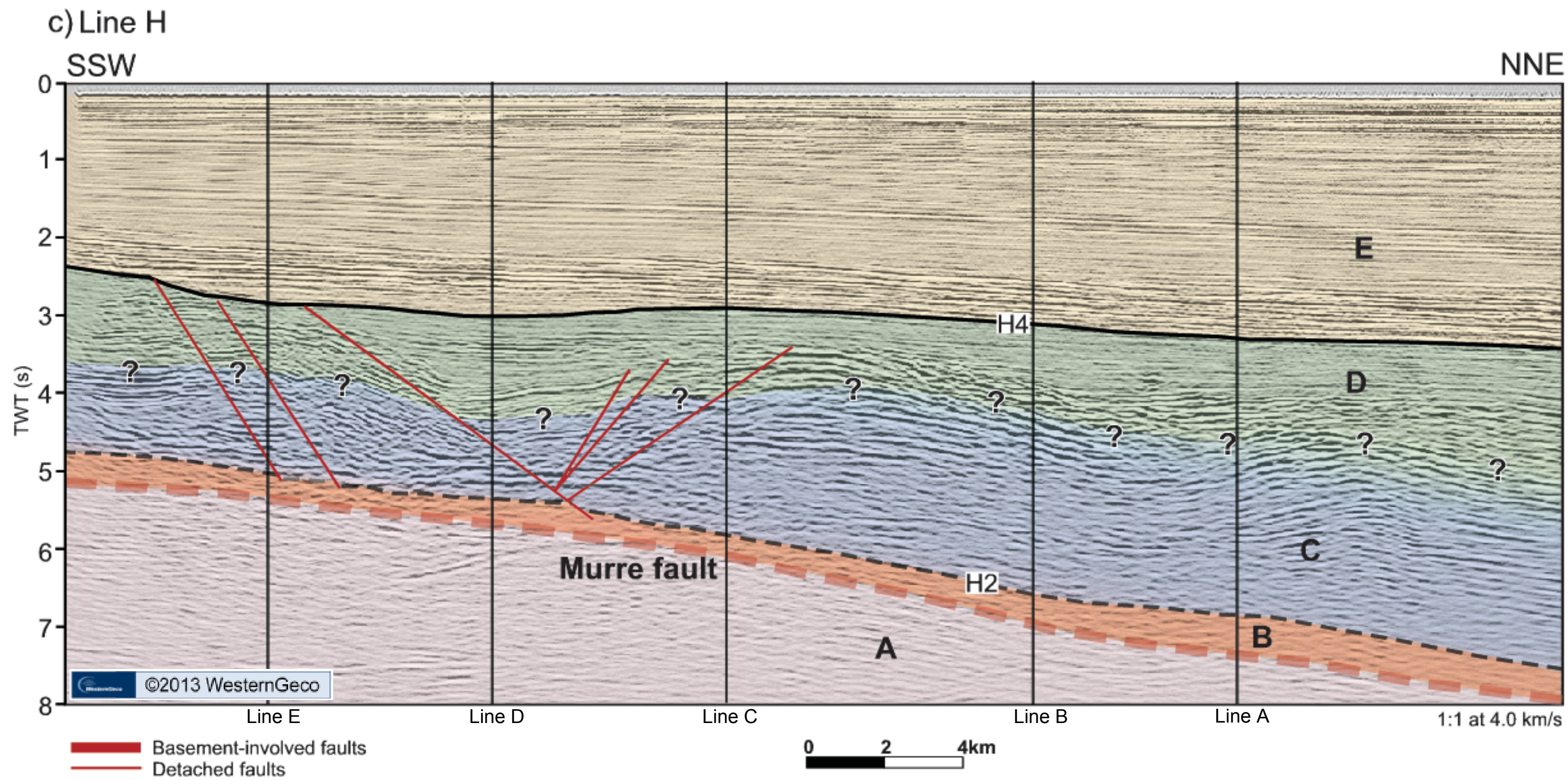

Figure 19. c) Interpreted line H showing tectonostratigraphic packages (A to E and colors) and key geologic features. H2 and H4 are mapped horizons. Dashed lines, gradational colors and question marks indicate uncertainty.

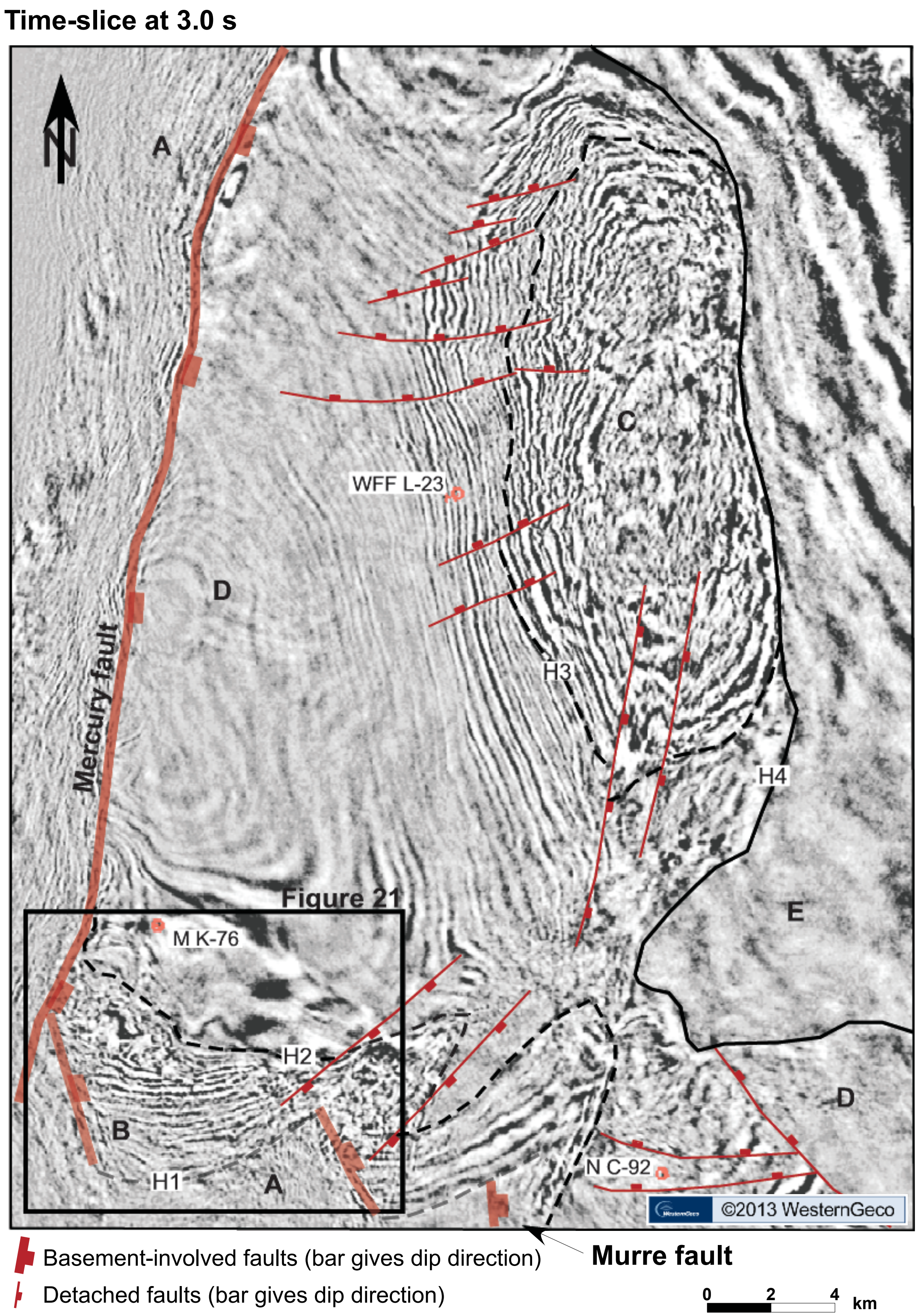

Figure 20. Time-slice at 3.0 s showing Package B in orange. H1, H2, H3 and H4 are mapped horizons. Other capital letters are tectonostratigraphic packages. Dashed black and grey lines and gradational colors indicate uncertainty. Red circles are wells. Abbreviations for wells are: WFF, West Flying Foam; M, Mercury; N, Nautilus.

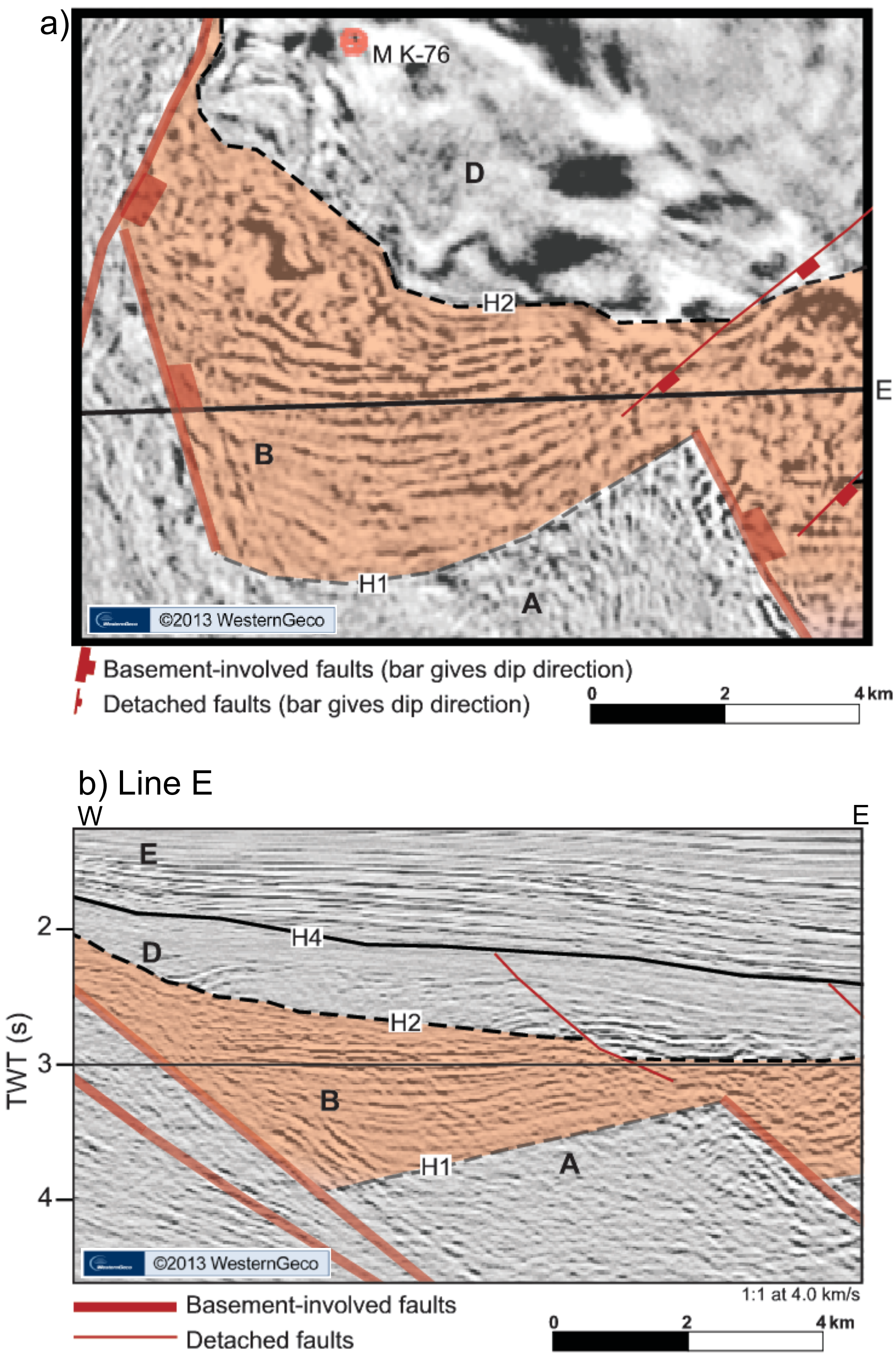

Figure 21. a) Enlarged area from Figure 20 with Package B in orange. b) Cross section showing part of Line E with Package B in orange. Reflections diverge toward basement-involved faults. H1, H2 and H4 are mapped horizons. Other capital letters are tectonostratigraphic packages.

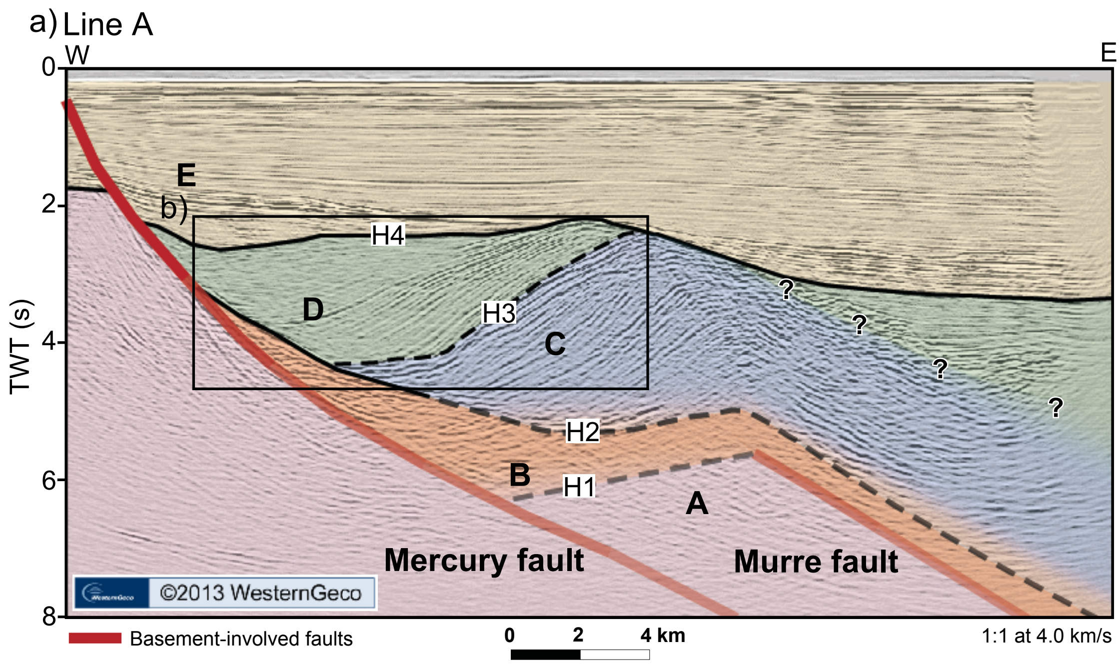

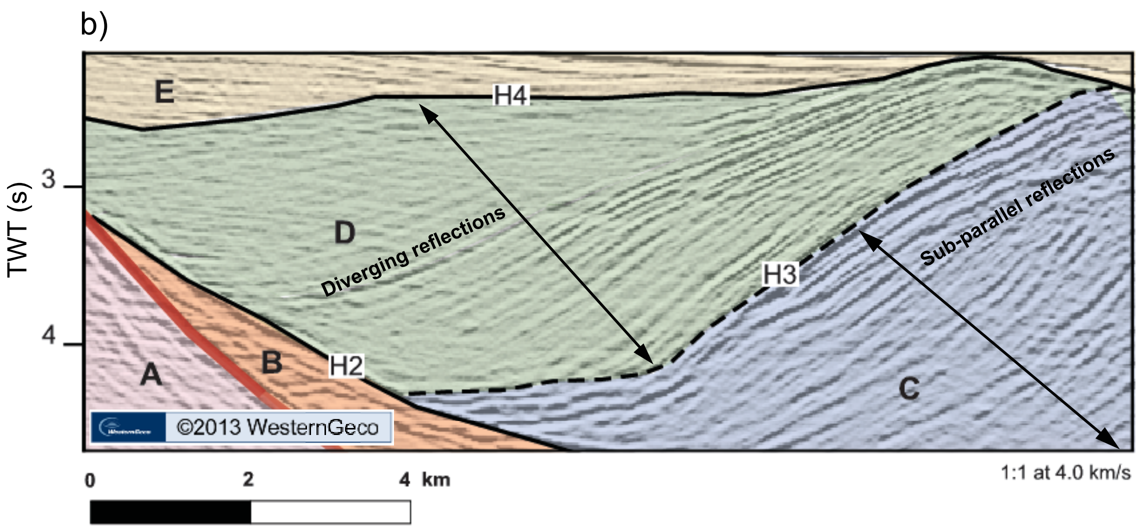

Figure 22. a) Line A interpreted with packages and faults. b) Enlargement showing diverging reflections in Package D and sub-parallel reflections in Package C. Horizon 3 separates the packages. H1, H2, H3 and H4 are mapped horizons. Other capital letters and colors are tectonostratigraphic packages. Gradational colors, dashed lines and question marks indicate uncertainty.

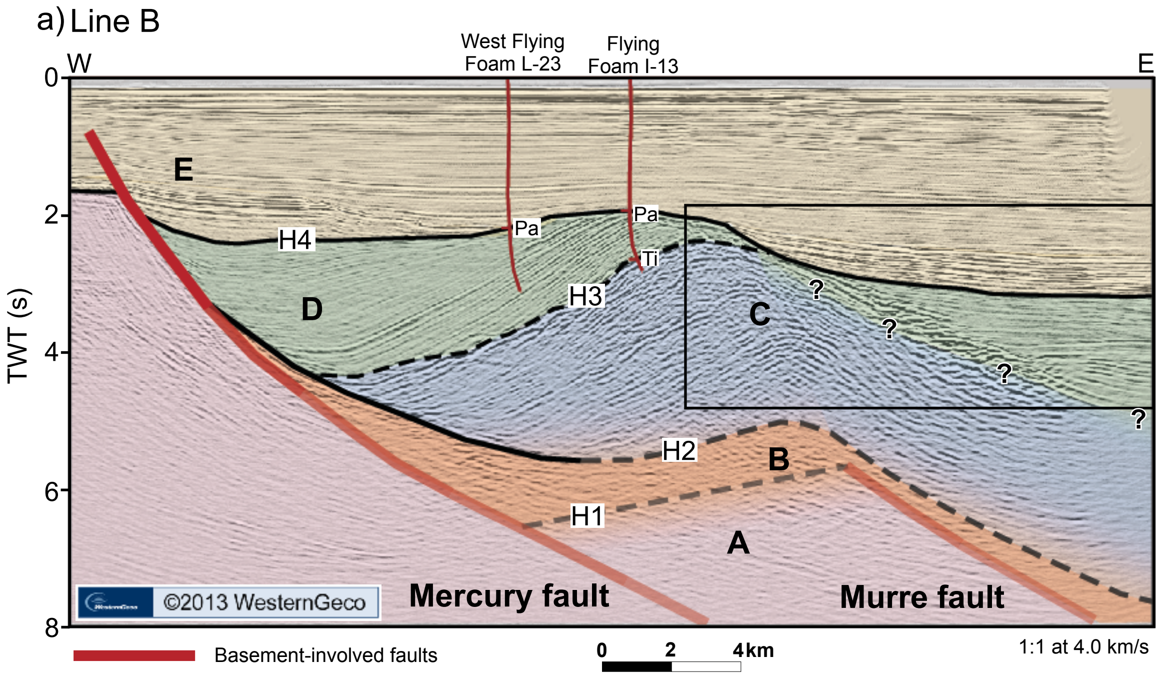

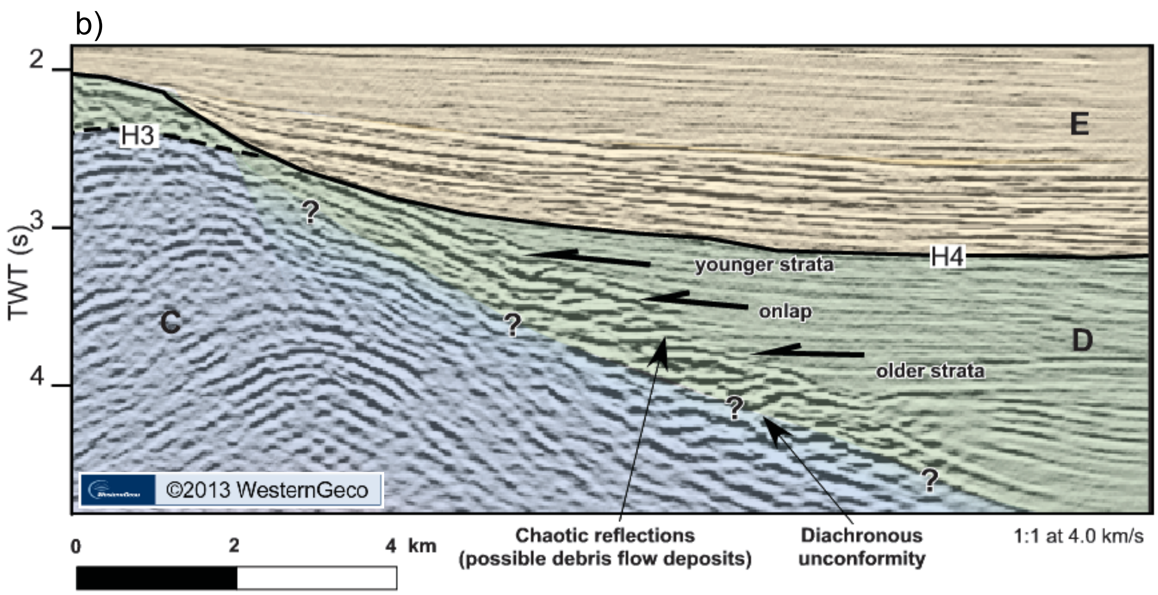

Figure 23. a) Line B highlighting Packages C and D in the hanging wall of the Murre fault. b) Enlargement shows onlap terminations (half-arrows) in Package D. H1, H2, H3 and H4 are mapped horizons. Other capital letters and colors are tectonostratigraphic packages. Gradational colors, dashed lines and question marks indicate uncertainty. (Pa: Paleogene; Ti: Tithonian, CNLOPB, 2012).

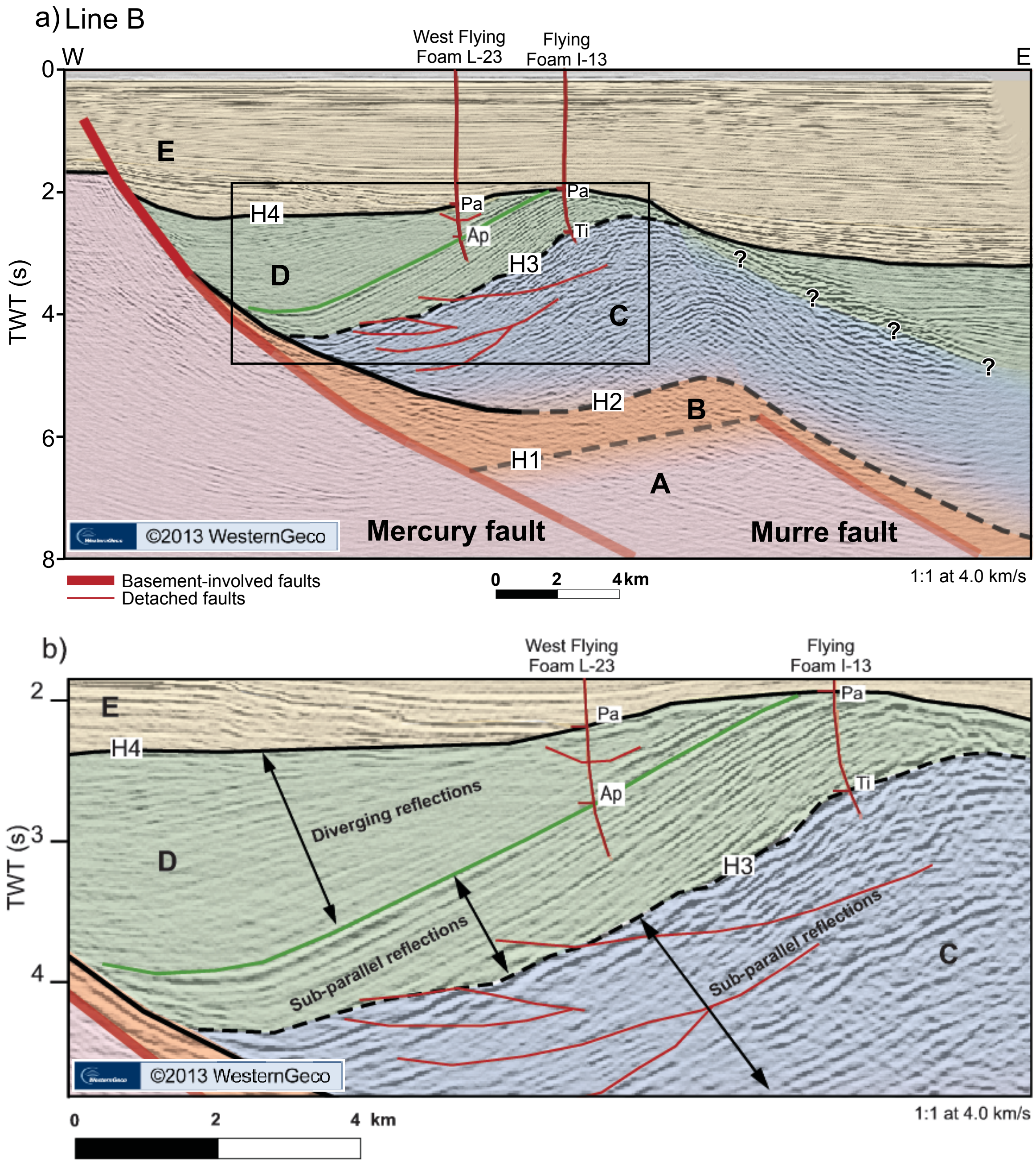

Figure 24. a) Line B highlighting Packages C and D in the hanging wall of the Mercury fault. b) Enlargement shows diverging and sub-parallel reflections in Package D and sub-parallel reflections in Package C. Horizon 3 separates both packages. H1, H2 H3 and H4 are mapped horizons. Other capital letters and colors are tectonostratigraphic packages. Gradational colors, dashed lines and question marks indicate uncertainty. Pa: Paleogene; Ap: Aptian; Ti: Tithonian (CNLOPB, 2012).

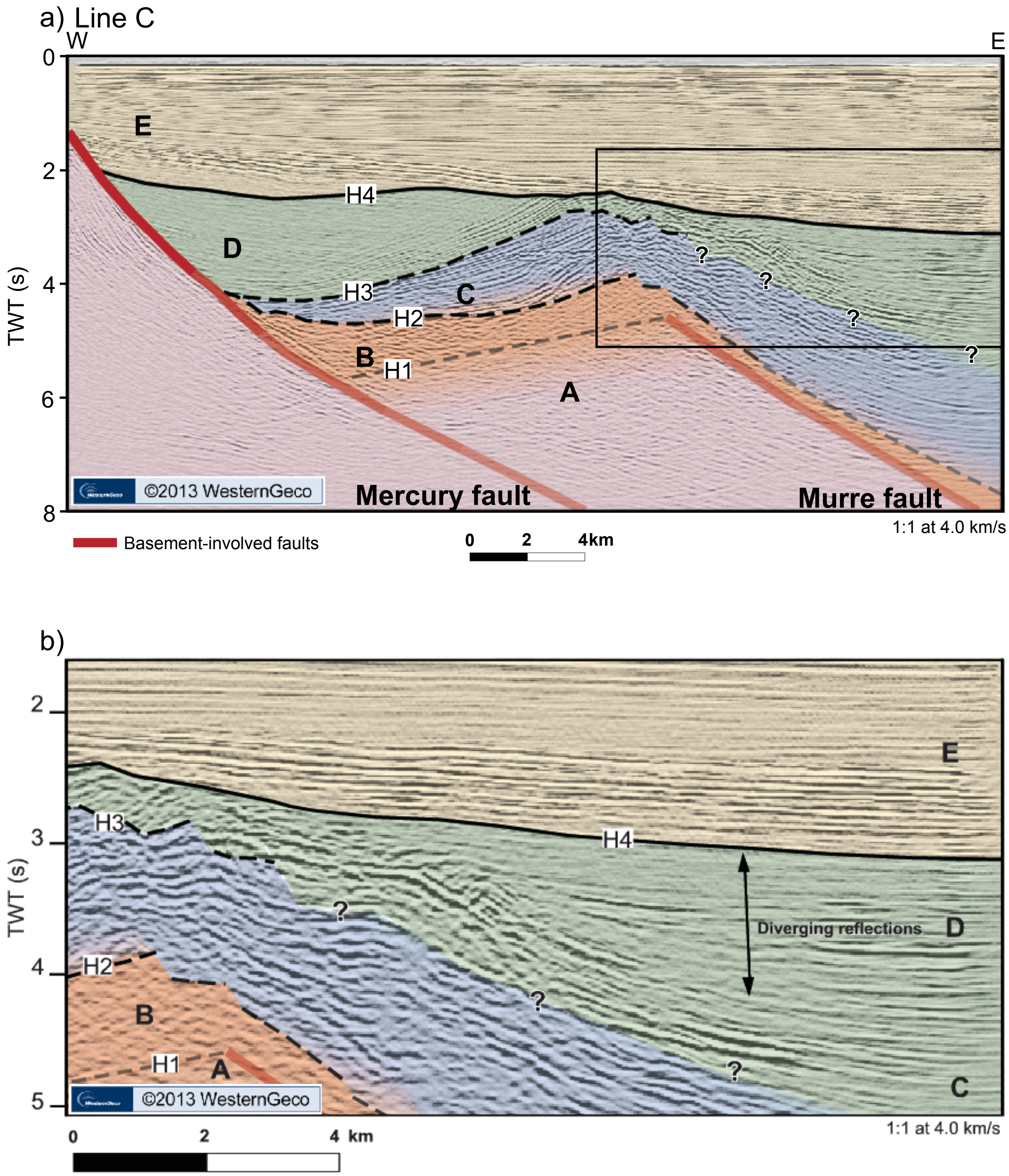

Figure 25. a) Line C highlighting Packages C and D in the hanging wall of the Murre fault. b) Enlargement shows diverging reflections in Package D. H1, H2, H3 and H4 are mapped horizons. Other capital letters and colors are tectonostratigraphic packages. Gradational colors, dashed lines and question marks indicate uncertainty.

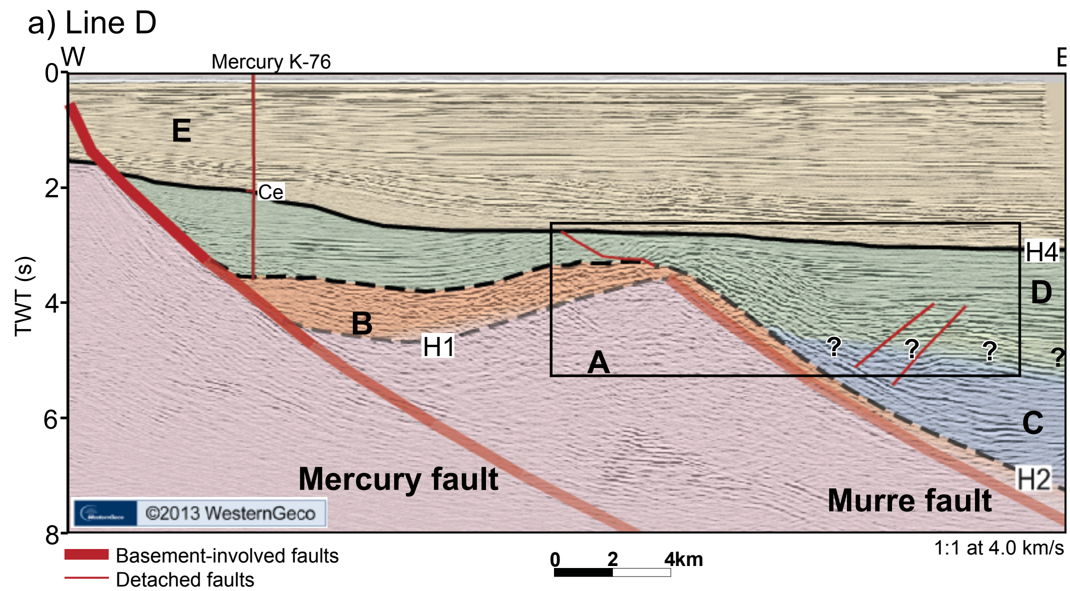

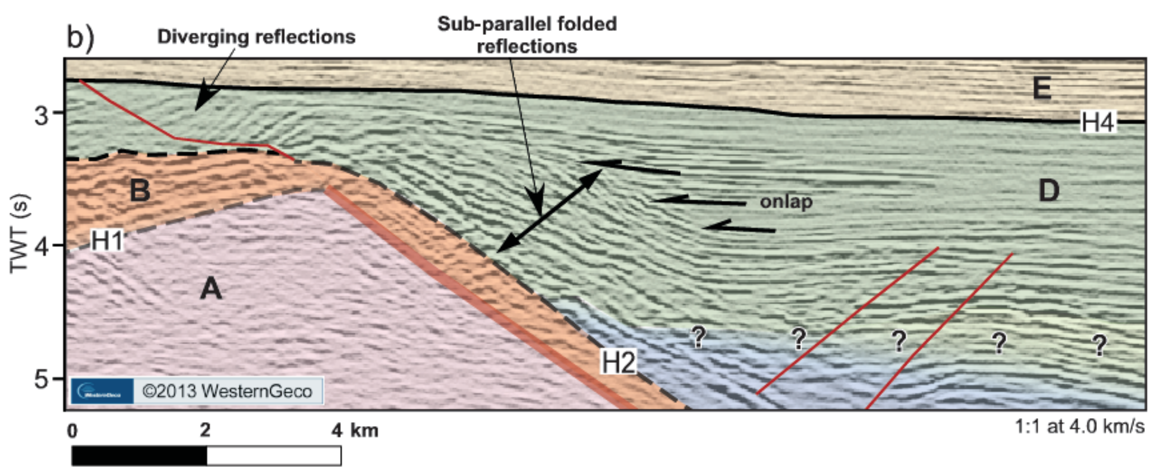

Figure 26. a) Line D highlighting Packages C and D. b) Enlargement showing the characteristics of Package D. Notice the presence of the fault that detaches within Package B. H1, H2, H3 and H4 are mapped horizons. Other capital letters and colors are tectonostratigraphic packages. Gradational colors, dashed lines and question marks indicate uncertainty. Ce: Cenomanian (CNLOPB, 2012).

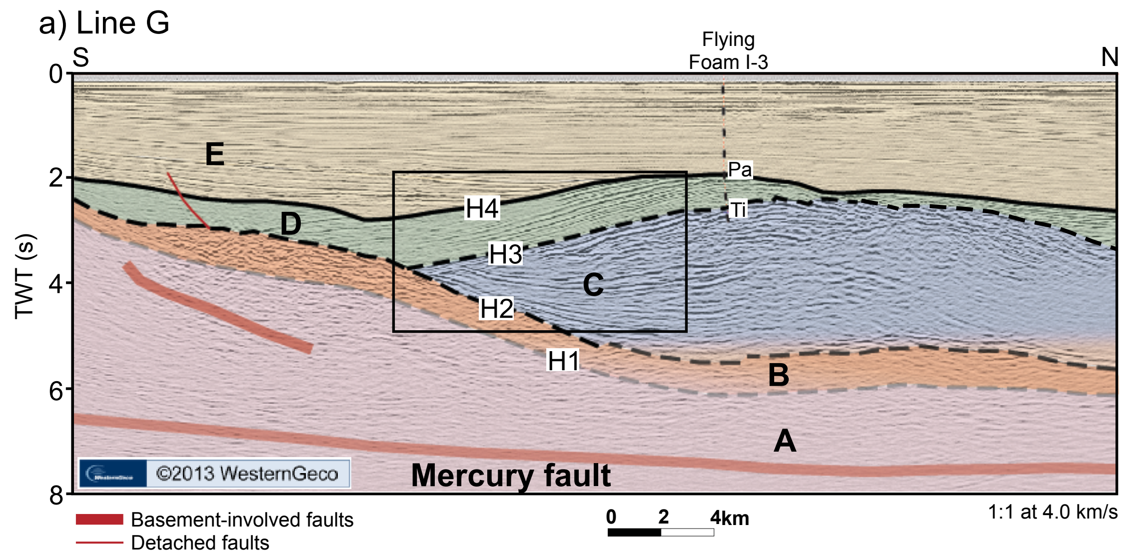

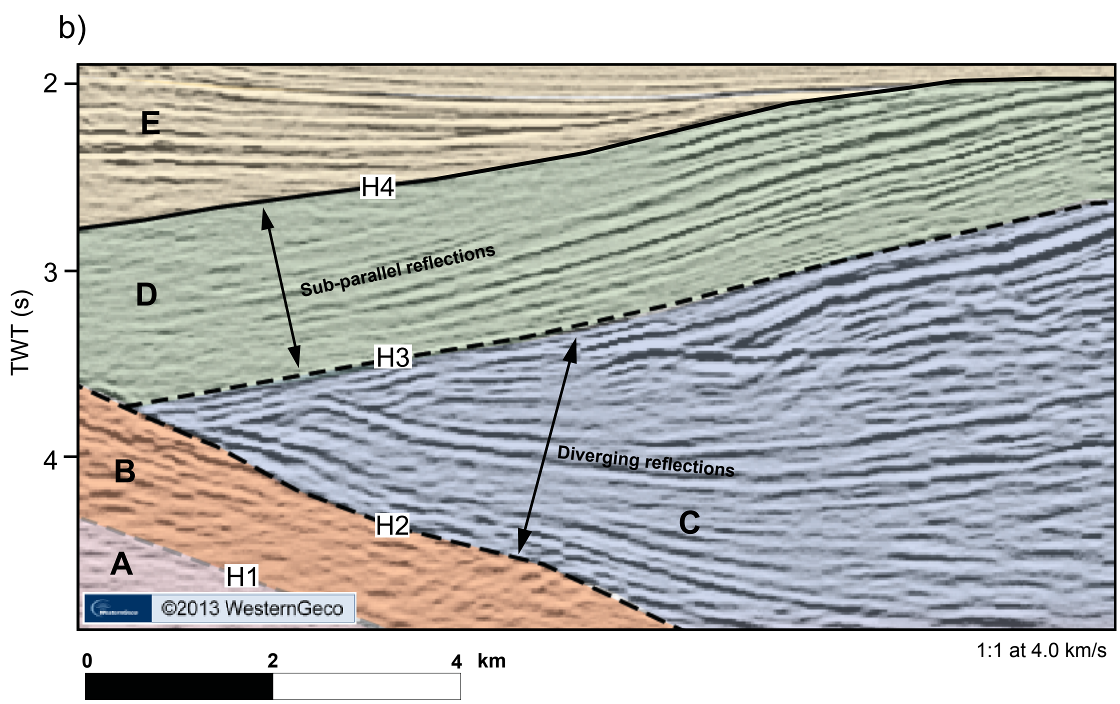

Figure 27. a) Line G highlighting Packages C and D. b) Enlargement showing sub-parallel reflections in Package D and diverging reflections in Package C. Horizon 3 separates both packages. H1, H2, H3 and H4 are mapped horizons. Other capital letters and colors are tectonostratigraphic packages. Gradational colors and dashed lines indicate uncertainty.

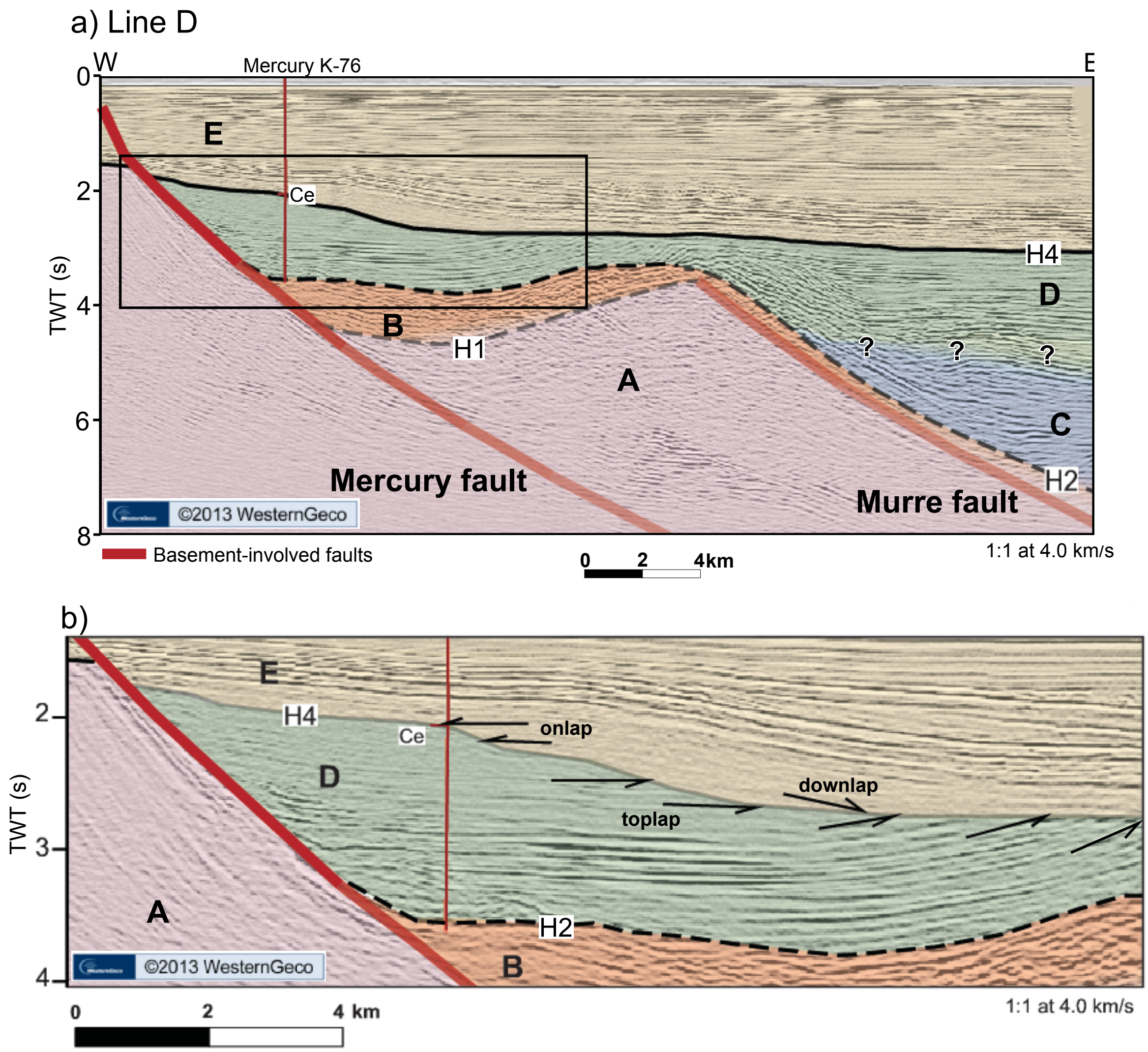

Figure 28. a) Line D highlighting Packages D and E. b) Enlargement showing reflection terminations that define Horizon 4. H1, H2 and H4 are mapped horizons. Other capital letters and colors are tectonostratigraphic packages. Gradational colors, dashed lines and question marks indicate uncertainty. Ce: Cenomanian (CNLOPB, 2012).

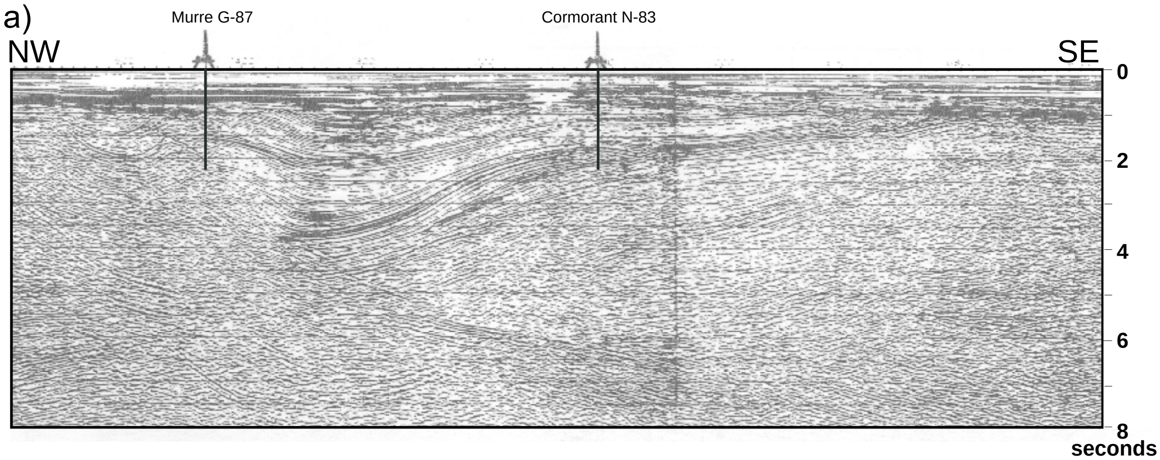

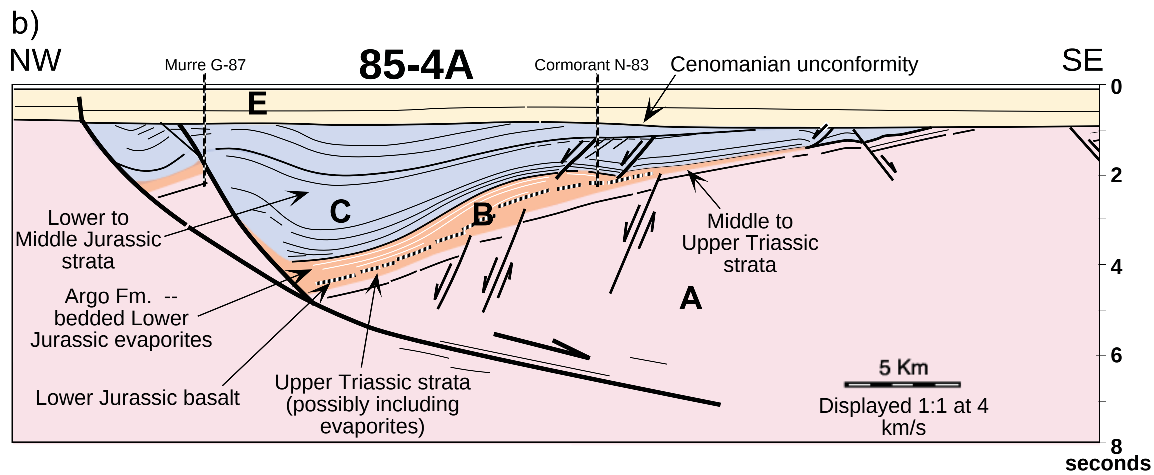

Figure 29. a) Lithoprobe line 85-4A without interpretation showing the location of two wells (modified from Sinclair, 1995). b) Interpreted Lithoprobe line 85-A showing Lower to Middle Jurassic strata thickening toward a basement-involved fault (modified from Withjack and Callaway, 2000). Colors and capital letters are tectonostratigraphic packages. See location of line in Appendix 1.

a) Line G

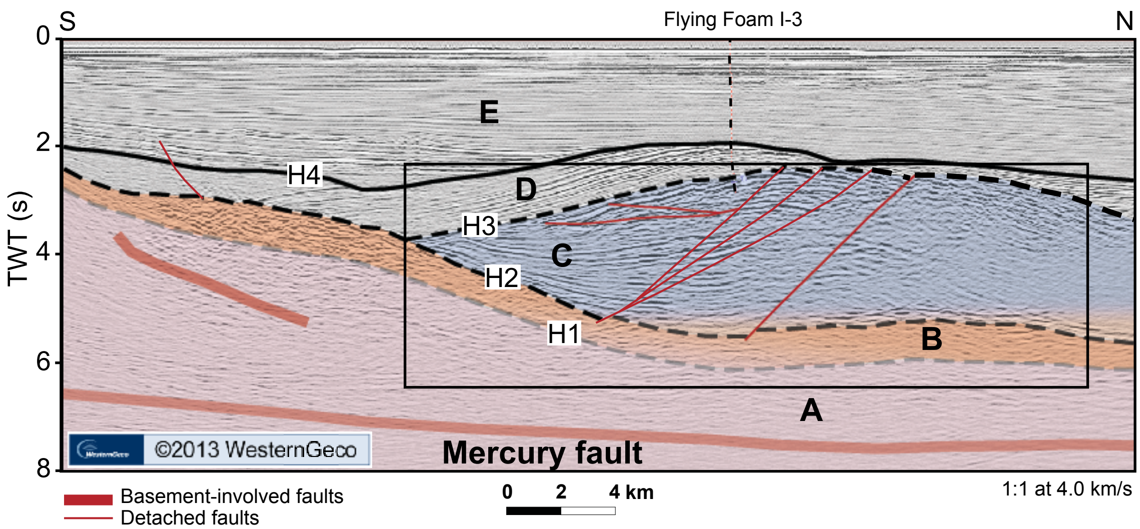

b)

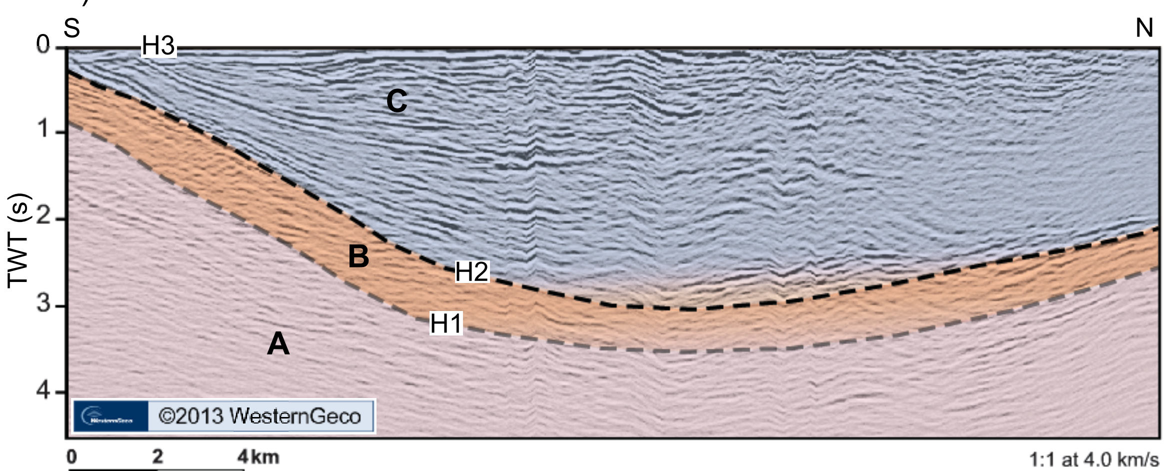

Figure 30. a) Strike view of line G highlighting Package C. b) Enlargement showing the geometry of Package C flattened on H3. H1, H2, H3 and H4 are mapped horizons. Other capital letters are tectonostratigraphic packages. Dashed lines and gradational colors indicate uncertainty.

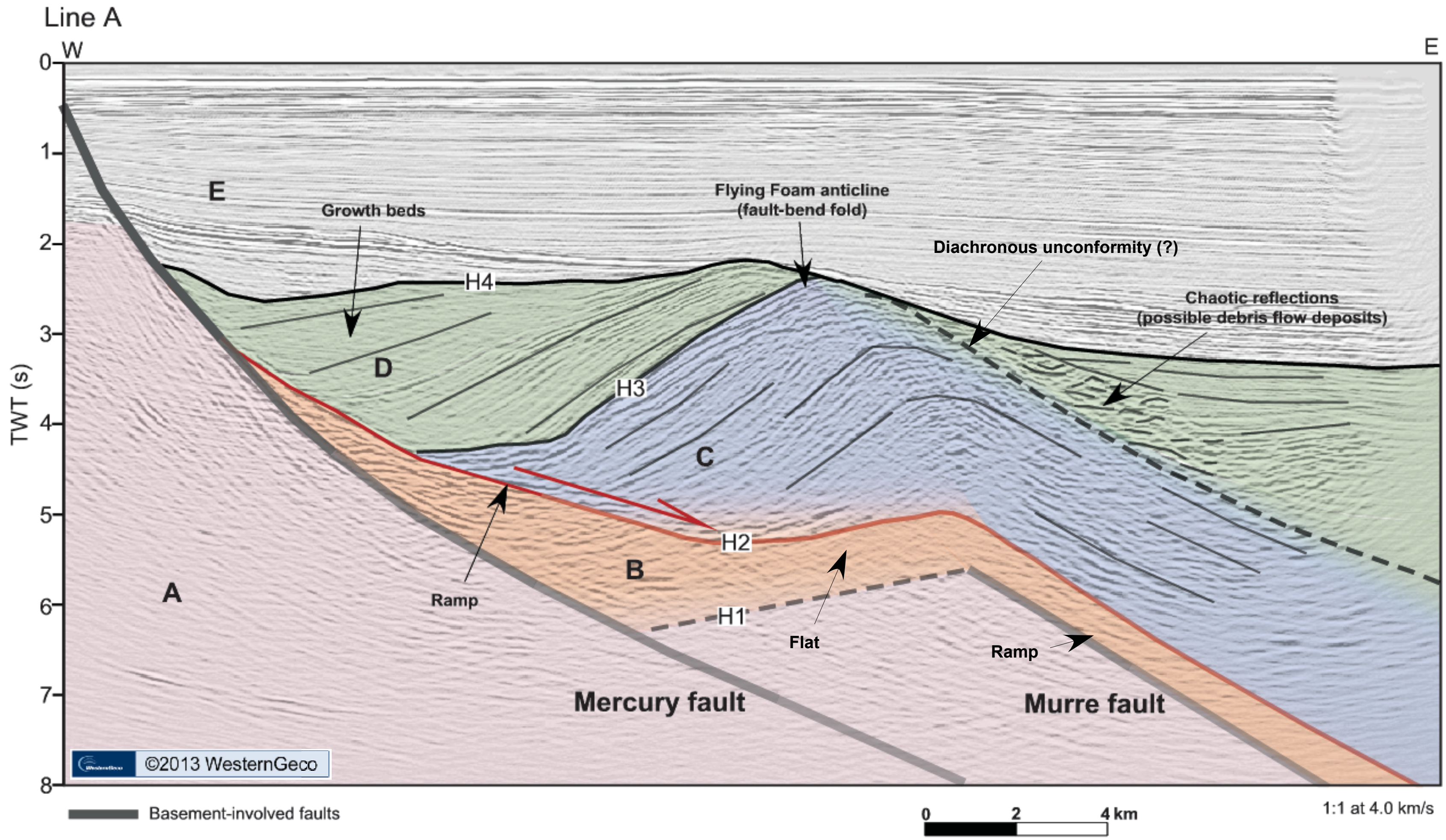

Figure 31. Line A highlighting Packages C and D, the ramp-flat-ramp that Horizon 2 forms and important features. Half arrows indicate direction of movement. H1, H2, H3 and H4 are mapped horizons. Other capital letters and colors are tectonostratigraphic packages. Gradational colors, dashed lines and question marks indicate uncertainty. See full interpretation in Figure 12.

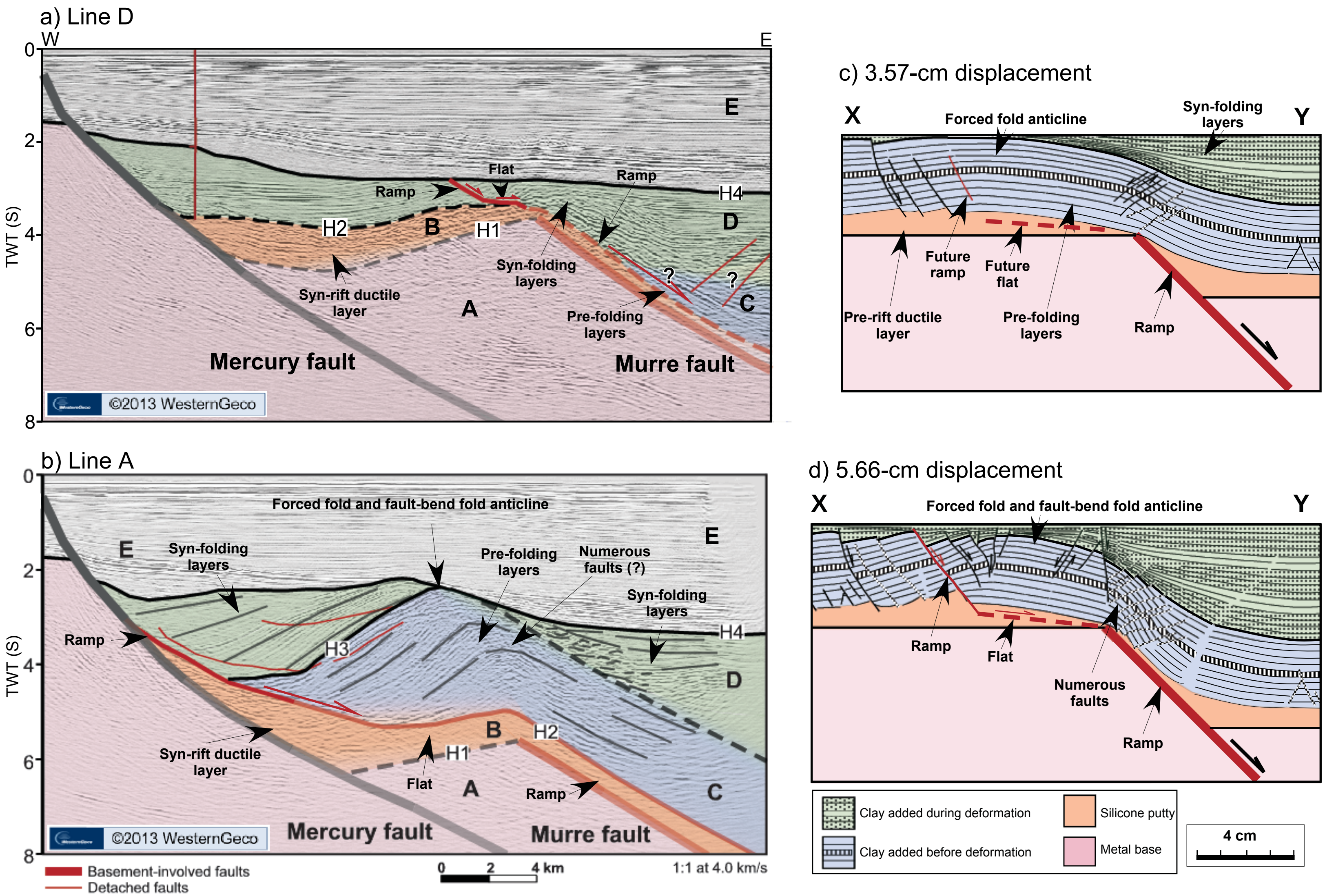
a) Line D
W
E
TWT (S)
0
2
4
6
8
E
H4
D
Flat
Ramp
Ramp
H2
B
H1
Syn-folding layers
Syn-rift ductile layer
A
?
?
C
Pre-folding layers
Mercury fault
Murre fault
©2013 WesternGeco
b) Line A
Forced fold and fault-bend fold anticline
E
E
Syn-folding layers
Pre-folding layers
Numerous faults (?)
Syn-folding layers
Ramp
H3
H4
D
Syn-rift ductile layer
B
H2
H1
Flat
A
Ramp
C
Mercury fault
Murre fault
©2013 WesternGeco
Basement-involved faults
Detached faults
0 2 4 km
1:1 at 4.0 km/s
c) 3.57-cm displacement
X
Y
Forced fold anticline
Syn-folding layers
Future ramp
Future flat
Pre-rift ductile layer
Pre-folding layers
Ramp
d) 5.66-cm displacement
X
Y
Forced fold and fault-bend fold anticline
Ramp
Flat
Numerous faults
Ramp
Clay added during deformation
Clay added before deformation
Silicone putty
Metal base
4 cm

Figure 32. Comparison between lines A and D and analog clay models. a) and b) show that Package C forms a forced fold and a fault-bend fold. Displacement on the Murre on line D is less than on line A. H1, H2, H3 and H4 are mapped horizons. Other capital letters are tectonostratigraphic packages. Dashed lines, gradational colors and question marks indicate uncertainty. See complete lines in Figures 15 and 12. Similarly, c) and d) show experimental clay models with differences in the displacement along a basement-involved fault (modified from Withjack and Callaway, 2000). The colors were chosen to match the colors of the tectonostratigraphic packages of the Flying Foam area.

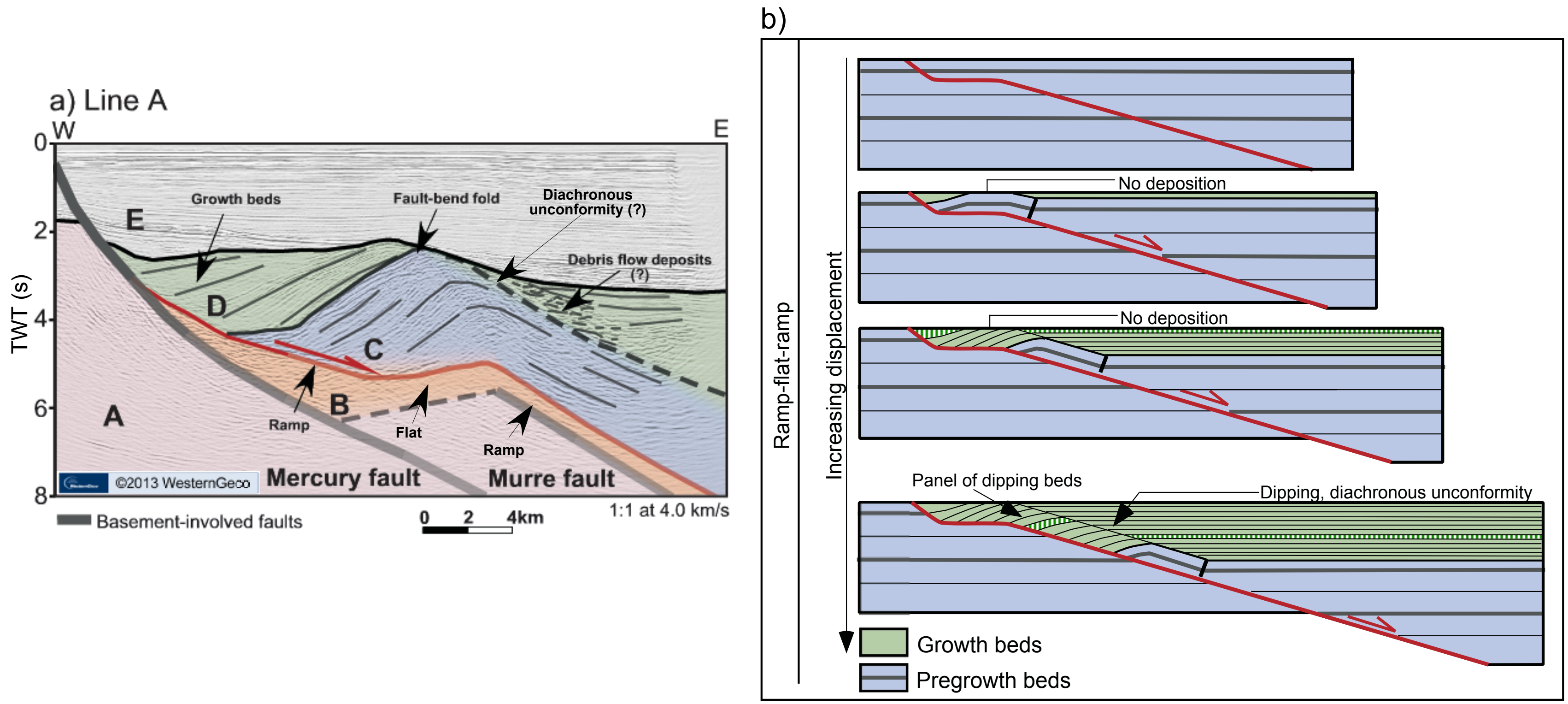

Figure 33. Comparison between line A and a geometric model. a) Line A shows the ramp-flat-ramp geometry of the detached fault on top of Package B (Argo salt). See complete interpretation in Figure 12. Half arrows indicate direction of movement. Capital letters represent tectonostratigraphic packages. b) Geometric model showing the evolution of a fault-bend fold and a diachronous unconformity above a fault with a ramp-flat-ramp geometry (modified from Withjack and Schlische, 2006). Colors were chosen to match the packages in the Flying Foam area.

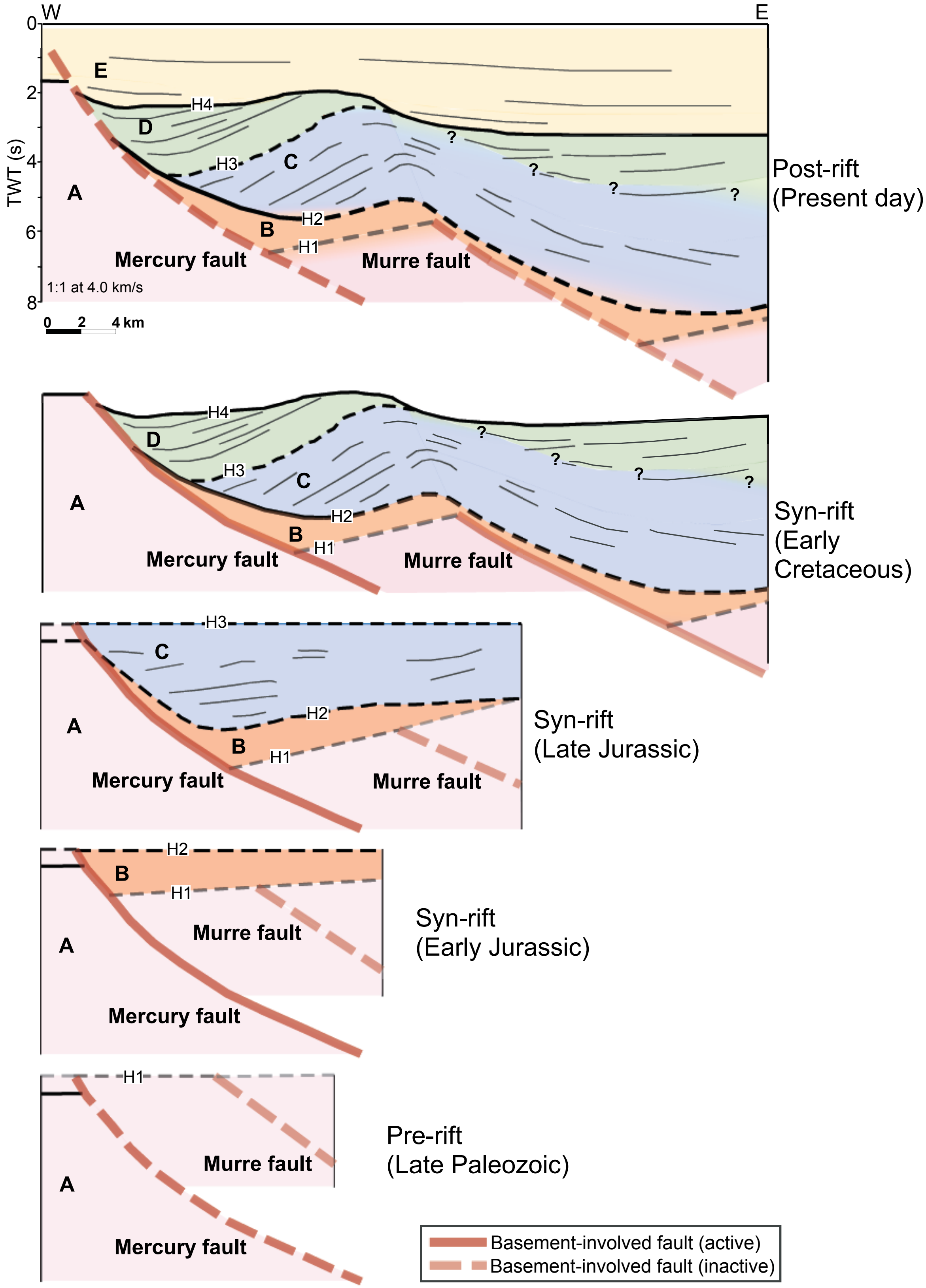
W
E
0
2
4
6
8
TWT (s)
E
H4
D
H3
C
?
?
?
?
A
H2
B
H1
Mercury fault
Murre fault
1:1 at 4.0 km/s
0 2 4 km
Post-rift
(Present day)
H4
D
H3
C
?
?
?
?
A
H2
B
H1
Mercury fault
Murre fault
Syn-rift
(Early
Cretaceous)
H3
C
A
H2
B
H1
Mercury fault
Murre fault
Syn-rift
(Late Jurassic)
H2
B
H1
A
Murre fault
Mercury fault
Syn-rift
(Early Jurassic)
H1
Murre fault
A
Mercury fault
Pre-rift
(Late Paleozoic)
Basement-involved fault (active)
Basement-involved fault (inactive)

Figure 34. Restoration of the Flying Foam area based on line B (Figure 13) and line HBV83-195 (Appendix 3). H1, H2, H3 and H4 are mapped horizons. Other capital letters and colors indicate tectonostratigraphic packages. Dashed lines, gradational colors and question marks indicate uncertainty.

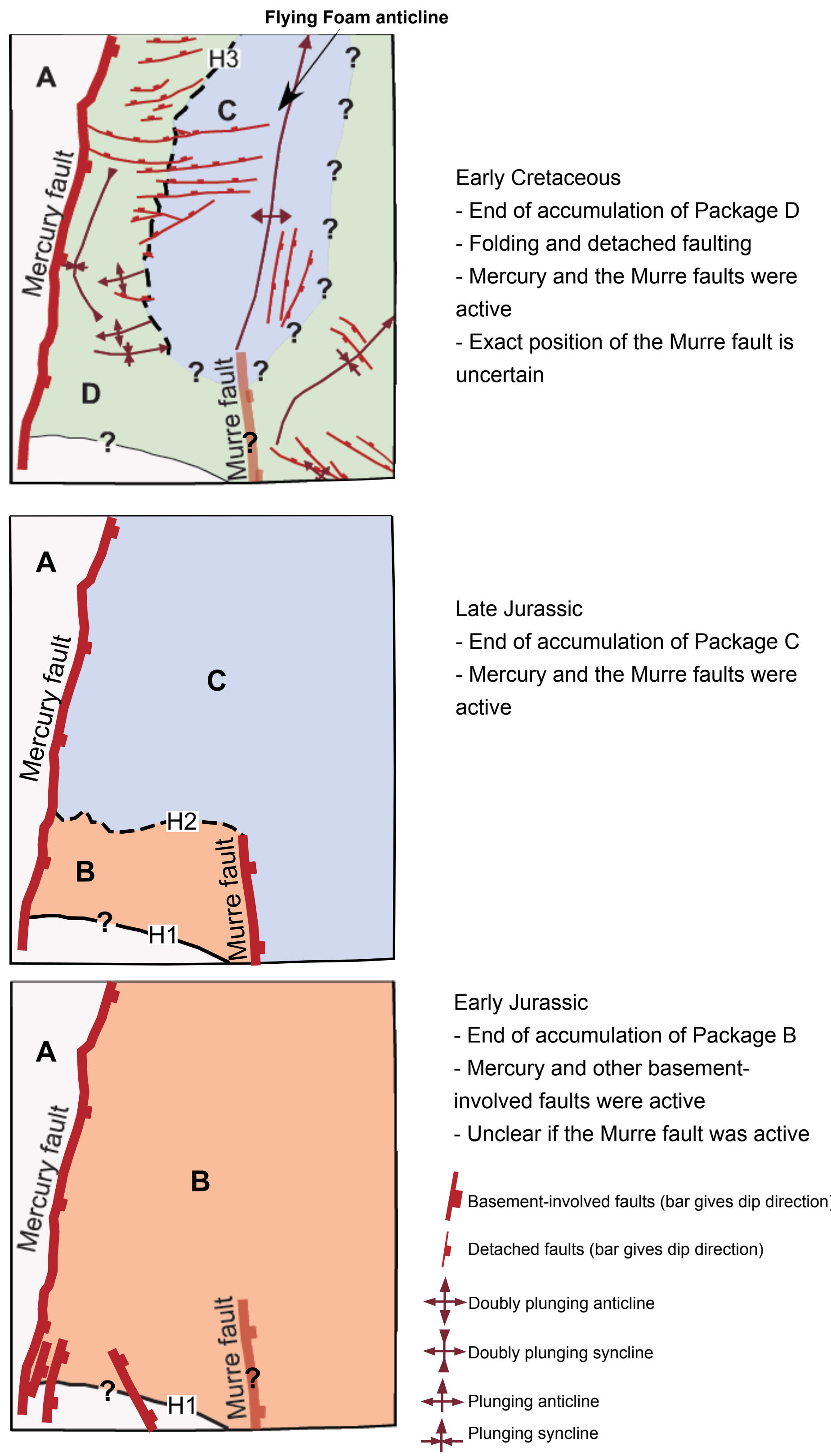

Figure 35. Schematic map-view representation of the syn-rift evolution of the Flying Foam region. H1, H2 and H3 are mapped horizons. Other capital letters are tectonostratigraphic packages. Dashed lines and question marks indicate uncertainty.

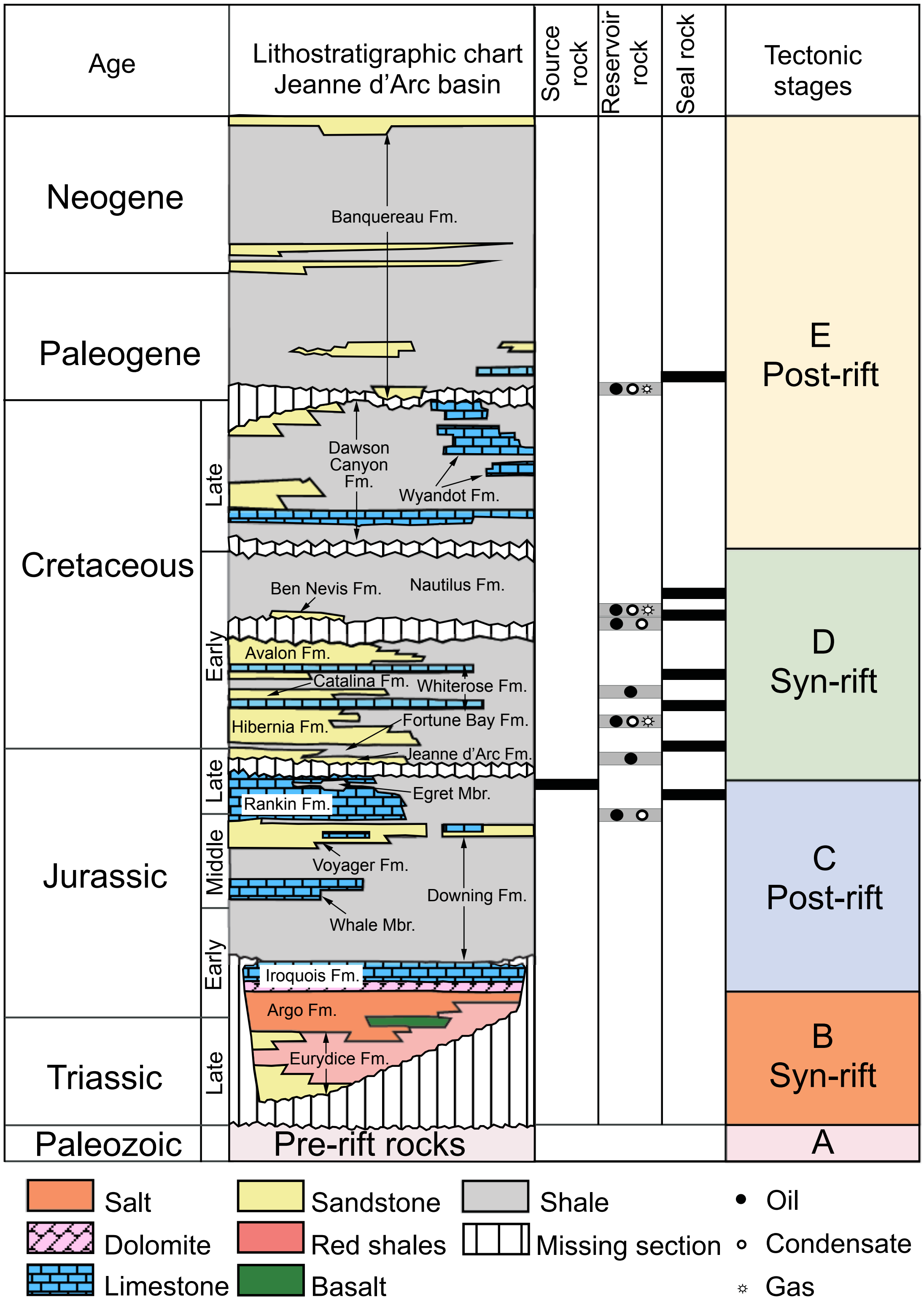

Figure 36. Lithostratigraphic chart of the Jeanne d'Arc basin highlighting tectonostratigraphic packages interpreted in this study (capital letters). Modified from Sinclair *et al*. (1999) and Magoon *et al*. (2005). Results from my thesis work show that Packages B, C and D are all syn-rift units.

Appendix 1: Jeanne d'Arc basin

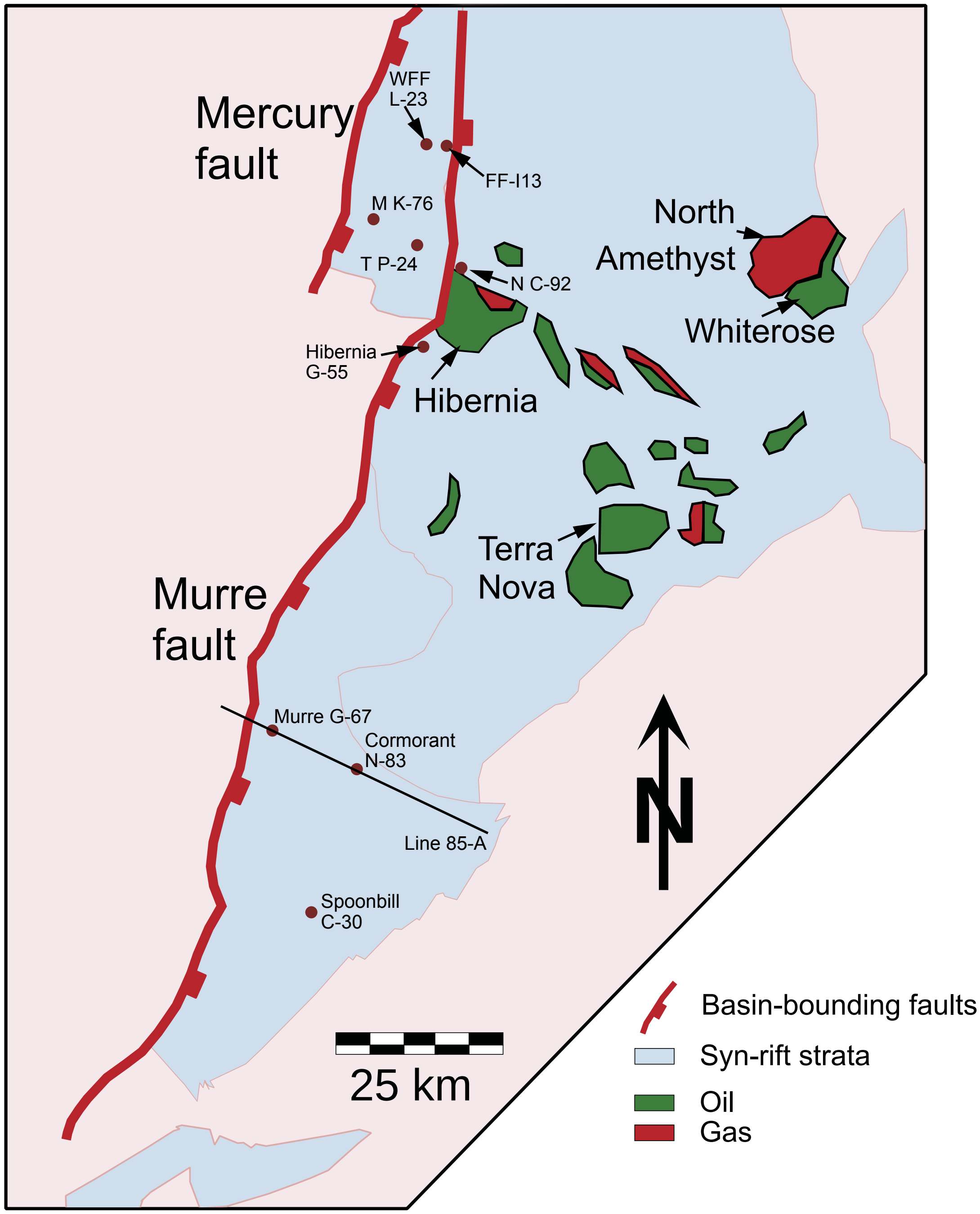

Figure A-1: Map of the Jeanne d'Arc basin showing the main producing hydrocarbon fields,approximate location of wells in the study area and other wells of interest, and Lithoprobe seismic line 85-A. Abbreviations for wells are: WFF: West Flying Foam; FF: Flying Foam; M: Mercury; T: Thorvald; N: Nautilus. Modified from McAlpine (1990), Sinclair (1995) and http://www.worldoil.com/June-2000-International.html.

Schlumberger
Geco-Prakla

1995/6 Marine 3D Survey
Newfoundland Grand Banks
Final Processing Report
for
EXPLORATION SERVICES
Geco-Prakla

by

SCHLUMBERGER
GECO-PRAKLA
1325 South Dairy Ashford
Houston, Texas 77077

1. Introduction

This report summarizes the processing of the Marine 3D survey in GRAND BANKS area, Newfoundland, Canada, by Geco-Prakla, Houston, in 1996. The survey was shot east-west by M/V Geco Diamond. The survey spanned in-lines 11 to 1518 and cross-lines 320 to 2921.

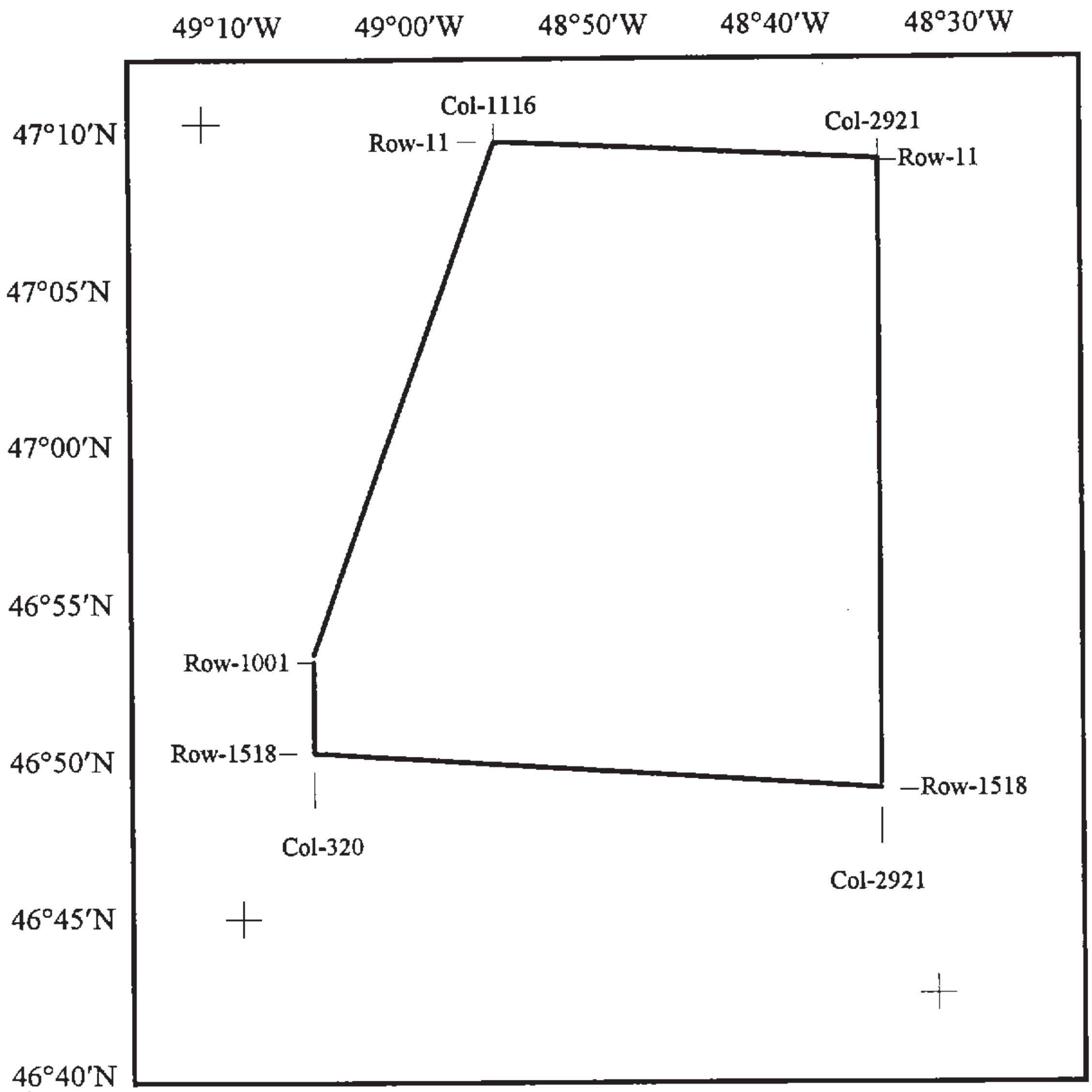

NEWFOUNDLAND GRAND BANKS

2. Acquisition Parameters

Shot by	Geco-Prakla Schlumberger July - September 1995
Boats	M/V Geco Diamond
Navigation	DGPS
Source	
Configuration	Triple Airgun Array Flip/Flop/Flap
Guns/Array	18, subdivided into 3 strings
Volume	5400 cubic inches per array
Pressure	2000 psi
Source Depth	6 meters
Source Separation	50 meters
Shot Interval	25 meters
Pop Interval	75 meters
Streamer	GECO HSSJ
Cable length	4 X 4800 meters
Streamer separation	150 meters
Group Interval	25 meters
Cable Depth	9 meters
Hydrophone per Group	40
Nominal Fold	32
Recording System	NESSIE III
Field Filters	
Low-cut	3 Hz 18 dB/octave slope
High-cut	125 Hz 70 dB/octave slope
Record Length	9.5 seconds
Sampling Interval	2 ms
Processing Record Length	9.0 seconds
Processing Sample Interval	4 ms

3. Processing Resources

3.1 Personnel

Processing Manager	Mark Bull
Processing Supervisor	Tony Johns
Group Supervisor	Catherine Tsai
Geophysicist	Indro Lawu, Mike Fagg

3.2 Software and Hardware

Software	Gecoseis System
Hardware	Fujitsu VPX240, Sun Workstation

4. Processing Parameters

4.1 Grid Orientation

Processing coordinates	
Base Angle	88.34 degrees
Side Angle	178.34 degrees
First in-line number on final migrated volume	1
In-line number increment	1
Distance between adjacent in-lines	25 meters
First cross-line number on final migrated volume	1
Cross-line number increment	1
Distance between adjacent cross-lines	12.5 meters
Spheroid	WGS-84
Projection	UTM
Scale factor on CM	0.9996
Central Meridian	-51.00 degrees
Grid System	TM
Grid Unit	Meters
False Northing	0.0
False Easting	500000
X-coordinate of in-line 1 cross-line 1	645410
Y-coordinate of in-line 1 cross-line 1	5226665

4.2 Processing sequence

4.2.1 Resample

Resample data from 2 ms to 4 ms with a 90 Hz 72 dB/octave high-cut filter.

4.2.2 Editing

Bad traces and/or shots flagged by Field Observers were deleted from the dataset.

4.2.3 Spherical Divergence Correction

Spherical divergence effects were removed by computing a scalar for each time sample from the following formula:

- $Scalar = T*(V_T/V_0)^2$
- T = seismic two-way time in seconds.
- V_0 = RMS velocity at time zero in meters/second.
- V_T = RMS velocity at time T in meters/second.

The following velocity function was used for the above calculation:

Time (sec)	Velocity (m/sec)
0.000	1472
0.500	1647
1.000	1813
1.500	2000
2.000	2221
2.500	2630
3.000	2990
3.500	3274
4.000	3548
4.500	3749
5.000	3920
5.500	4076
6.000	4218
6.500	4335
7.000	4450
7.500	4483
8.000	4509

4.2.4 Exponential Gain Correction

Exponential gain was applied to compensate for amplitude decay with time. The gain applied to the data for a sample at any time was determined by the following functions:

for $0.2 < T < 4.0$

$$Gain = e^{aT}$$

where,

a = (a user specified exponential gain value in dB/sec)*ln(10)/20. The user specified exponential gain value was +3 dB/sec.

$T=t-t_0$, where t is the sample time and t_0 is the start time for the gain function in seconds. The gain calculated at 4.0 seconds was applied to the end of the trace.

4.2.5 Source Signature and Instrument Compensation

An inverse filter was designed by Trilogy to convert the recorded source signature into a band limited minimum phase wavelet. The characteristics of this output wavelet were as follows :

```
Low  cut filter and slope :  6 Hz, 50 dB/octave
High cut filter and slope : 85 Hz, 90 dB/octave
```

This inverse filter was applied to the shot record data for removal of the known component of source wavelet before predictive deconvolution. See Section 12, *Figure 1*, for the production designature operator and *Figure 2* for the conditioned gun signature.

4.2.6 3-D XY Coordinate Merge

Cable position information from the processed navigation data was merged with the seismic data.

4.2.7 Prestack Predictive Deconvolution

Trace by trace predictive deconvolution was applied to further whiten the spectrum and to suppress reverberations. Based on the results of Trilogy testing, the following decon parameters were selected for production processing :

- Design window length: 6000 ms
- Operator length: 320 ms
- Gap length: 4 ms
- Prewhitening: 0.1 %

A job setup for the Deconvolution is attached in Sec. 11.1

4.2.8 Automatic Trace Editing

Data with anonymously large amplitude were edited prior to DMO stacking. From the tests performed, sample values above 10 could be identified as noise spikes for shot data. The near and far windows for this analysis were 1000-9000ms and 4500-9000ms, respectively. Whenever a sample above amplitude 10 was encountered in a window, a mute was applied from the previous sample to the end of the trace.

4.2.9 3-D Elastic Binning

The navigation information was extracted from the merged decon trace headers to generate coverage of the 3-D survey. The coordinates of each data trace were analyzed and each trace was assigned the following information:

- In-line bin number
- Cross-line bin number
- Micro-bin numbers (two values)
  Each bin was subdivided into a 100 X 100 grid. Micro-inline and micro-cross-line numbers were assigned from this micro-grid.
- Offset group (32 offset group numbers defined)
  Offset group 1 being the near, group 32 being the far.

Five values were used to uniquely defined a trace and tabulate binning statistics. From this information five tables were made.

- Total number of traces in each bin with All offset groups 1 - 32.
- Total number of traces in each bin with Nears offset groups 1 - 8.
- Total number of traces in each bin with MidNears offset groups 9 - 16.
- Total number of traces in each bin with MidFars offset groups 17 - 24.
- Total number of traces in each bin with Fars offset groups 25 - 32.

The coverage plots constructed from these tables reflect the actual live seismic data.

Because the binning was constructed from the merged decon trace headers, any missing and edited bad shots and traces were not included in the binning process. Elastic binning and redundancy editing trials were then performed. Each bin was searched in each offset group in an attempt to achieve a nominal 32-fold coverage throughout the survey, with maximum one trace contributing to each of the 32 allowed offset groups. If a particular bin contained more than one trace per offset group, the one trace closest to the bin center was accepted. If a particular bin and offset group contained no traces, adjacent bins were searched for traces in that offset group. If the traces found were within a user specified distance from the boundary of the primary bin, these traces were borrowed and allowed to stack into the bin. The user specified distances were expressed in terms of percentage of cross-line bin size. In this survey the cross-line bin size was 25 meters. A maximum of 2 traces per offset group were allowed in order to obtain nominal 32 fold.

Supergroups were used to describe groups of offset groups to be taken together for flexible redundancy editing. In this survey, the supergroups defined were: offsets 1-8, 9-16, 17-24, and 25-32 with each supergroup having a minimum fold requirement of 8. If normal flexing did not get enough traces in the supergroup to meet the minimum fold requirement, one additional trace from each group (1-32) which has surplus traces was accepted until the minimum fold was met.

Bin expansion tests were conducted at four parts of the survey area at 10, 20, 30 and 40 % respectively. The five coverage plots were once again generated and from these plots the following elastic binning parameters were chosen:

- For all offset groups: 40% bin expansion in cross-line direction. This expanded the cross-line bin size by 10 meters either side, from 25 meters to 45 meters.
- The five coverage plots were once again generated for the final binning table.

4.2.10 Normal Moveout

Normal Moveout was applied to the data using a fully interpolated 3-D velocity cube. See Sec. 10.1 "Stacking Velocity Field".

4.2.11 First Break Suppression

The data was muted in the following manner:

- Offsets up to 575 meters were not muted.
- Offset of 576 meters was muted at 500 ms.
- Offset of 5200 meters was muted at 4200 ms.

Mute times for offsets between the above offsets were calculated by linear interpolation.

4.2.12 3-D DMO and Stack with Elastic Binning

Common azimuth DMO was performed on the data. The procedures were as follows:

The final stack volume was allocated on disk. As traces were used, the DMO operator for each trace was calculated along the source to receiver azimuth.

The primary trace was stacked into the midpoint bin and stacking normalization information was recorded for that bin. The DMO energy traces were stacked into their proper bins but no normalization information was recorded.

As the traces were processed they were checked against the binning information. Redundant traces were discarded and flexed traces were copied if they were flagged as such by the binning information.

When all the data had gone through DMO/stacking procedure the normalization information was utilized to scale each sample of every trace by the inverse of the square root of the number of primary and flexed traces that contributed to the sample in question. This normalization scheme was used to scale down low fold areas that had poor signal to noise ratios. A job setup for 3-D DMO and stack with Elastic Binning is attached in Sec. 11.2.

4.2.13 In-line K-Filter

A k-filter was applied to remove aliased noise in the in-line direction caused by acquisition geometry. The filter was applied fully from 0.0 - 3.0 seconds and tapered off at 4.0 seconds. A job setup for In-line k-filter is attached in Sec. 11.3.

A sample of the Stack Timeslice at 2.0 sec is shown in Section 12, *Figure 3*.

4.2.14 3-D FXY-filter

3-D fxy-filter was applied to attenuate random noise. A job setup for 3-D fxy-filter is attached in Sec. 11.4.

A sample of the Stack Timeslice at 2.0 sec is shown in Section 12, *Figure 4*.

4.2.15 Datuming

A static shift of +12 ms was applied to the stacked data to compensate for the depth of source and the streamers below mean-sea-level.

4.2.16 One Pass Phase Shift Migration

Upon completion of various 2-D migration tests with different velocity reduction percentages of the RMS stacking velocities, the following parameters were used:

Time (seconds)	Percent
0.0	100
4.0	100
6.0	95
9.0	85

The following frequency and dip limits were used :

Time (seconds)	Max Frequency (Hz)
0.0	75

Time (seconds)	Max Dip (degrees)
0.0	60
3.0	60
6.0	40
9.0	10

After the parameters were picked on the 2-D tests, the southern half of the 3-D data-set, (in-line range 780-1532, cross-lines 1-3200), was migrated and provided as a preliminary deliverable to the underwriters on June 30th.

During the QC of the initial 3-D migrated volume there were some regions that were discovered to be slightly under-migrated.

Residual migration tests were performed using 103% and 106% of the above time-variant velocity reduction. These tests indicated that increasing the original reduction by 3% yielded improved imaging.

The following final velocity reductions of the RMS stacking velocities were used for the final 3D migration :

Time (seconds)	Percent
0.0	103
4.0	103
6.0	97.9
9.0	87.6

The phase shift migration uses a spatial operator, which allows accurate treatment of dips and gives a full 3-D operator. Since this operator must be laterally invariant, the data is stretched prior to the migration to accommodate lateral changes in velocity. The stretch function is computed by using a nonlinear optimization method developed at Geco-Prakla. Vertical velocity variations are handled exactly by the phase shift method without stretching.

A spatially and temporally smoothed interval velocity cube was used for input into this optimization algorithm. See Sec. 10.2 "Migration Velocity Field".

The phase shift migration was applied in the following 3 steps:

- The first step reads the unmigrated data by in-lines, stretches the data, and transforms the data into wave number domain over the in-line dimension, after padding to prevent wrap-around. A job setup for Step-I is attached in Sec. 11.5.
- The second step transforms the data in time and in the cross-line direction, performs the migration, and then inverse transforms the data over time and cross-line. A job setup for Step-II is attached in Sec. 11.6.
- The third step reads the data from Step-II by in-lines, inversely transforms the data over the in-line dimension and unstretches the data. A job setup for Step-III is attached in Sec. 11.7

See Section 12, *Figure 5* for the Quicklook cube Migration at 2.0 seconds.
See Section 12, *Figure 6* for the Final Migration timeslice at 2.0 seconds.

5. Final Products

5.1 Film displays

5.1.1 In-line AGC 3-D migration

Every 1500 meters (every 60th in-line) from in-line 61 to 1501 at 1:36,000 scale.

5.1.2 In-line RAP 3-D migration

Every 1500 meters (every 60th in-line) from in-line 61 to 1501 at 1:36,000 scale.

5.1.3 Cross-line AGC 3-D migration

Every 1500 meters (every 120th cross-line) from cross-line 360 to 2880 at 1:36,000 scale.

5.1.4 Cross-line RAP 3-D migration

Every 1500 meters (every 120th cross-line) from cross-line 360 to 2880 at 1:36,000 scale.

5.1.5 Timeslices

Every 200 ms of the final migrated volume from 0.2 - 6.0 sec. and every 1000 ms from 0.5 to 5.5 sec. at 1:48,000 scale.

5.2 Versatec displays

5.2.1 Binning/Index/Grid Plots

All, Nears, MidNears, MidFars, and Fars offset groups for edited and flexed index at 1:48,000 scale.

5.3 Deliverables on Tape

5.3.1 Decon SEGY Tapes

With navigation merge and designature filter applied.

5.3.2 Grid file SEGY Tapes

All, Nears, MidNears, MidFars, and Fars Offset groups from edited and flexed Index.

5.3.3 Binning/Index Offset groups FBKUP tapes

Edited and flexed index.

5.3.4 3-D Stack SEGY tapes

In-line ordered, with K-filter, 3D FXY-filter and +12 ms static shift applied.

5.3.5 3-D Migration SEGY tapes

In-line ordered.

5.3.6 3-D Migration SEGY tapes

Cross-line ordered.

5.3.7 3-D Migration SEGY film tapes

In-line ordered, every 60th in-line, from row 61 through to row 1501.

5.3.8 3-D Migration SEGY film tapes

Cross-line ordered, every 120th cross-line, from column 360 through to column 2880.

5.3.9 3-D DMO Gather SEGY tapes

Used in the velocity analysis for all 47 velocity lines.

5.3.10 Migration Timeslice Gather SEGY tapes.

Gathers are every 200ms from 0.200 - 6.000secs and every 1000ms from 0.500 - 5.500secs.

5.3.11 Migration Velocity Cube Timeslice SEGY tapes.

Every 200ms to 6.000secs.

5.3.12 Stack Velocity Cube Timeslice SEGY tapes.

Every 200ms to 6.000secs.

5.3.13 Following 8 mm velocity tapes:

- Navigation datasets in G2000 format.
- Stacking RMS velocity VBASE - ASCII format
- Stacking RMS velocity VCUBE 200*250 meter grid. i.e. every 8th row & every 20th column - ASCII format.
- Migration interval velocity VCUBE 200*250 meter grid. i.e. every 8th row & every 20th column - ASCII format.
- Migration interval velocity (with percentage reduction scheme applied) VCUBE 200*250 meter grid. i.e. every 8th row & every 20th column - ASCII format.
- Migration Interval velocity VBASE - ASCII format.
- Decon Reel dbase and Edit files.
- Spectra contour, CDP, and MVFS for all 47 velocity lines.

5.3.14 Floppy diskette.

Containing:

- source signature.
- designature operator used in the processing.

6. Line Statistics

Grand total mileage for the entire survey was 62643 kilometers.

System `A'

spint*grpint*noch*fcdp*

75.0 25.0 384 1

seq	punit	navn	rbi	fsp	rei	lsp	freel	lreel	nch	ns	nb	dpt	dir	nav
040	a00	1p0101	1399	1399	2410	2410	D00345	D00348	384	2	1	11	088.	021
042	a01	1i0101	1399	1399	2410	2410	D00365	D00368	384	2	1	11	088.	041
034	a10	1p0113	1395	1395	2409	2409	D00305	D00308	384	2	1	11	088.	021
020	a20	1p0125	1391	1391	2409	2409	D00167	D00170	384	2	1	9	088.	001
032	a21	1i0125	1391	1391	2409	2409	D00285	D00288	384	2	1	11	088.	021
018	a30	1p0137	1387	1387	2410	2410	D00147	D00150	384	2	1	9	088.	001
008	a40	1p0149	1383	1383	2410	2410	D00070	D00073	384	2	1	11	088.	001
010	a50	1p0161	1379	1379	2409	2409	D00088	D00091	384	2	1	11	088.	001
016	a60	2p0173	1375	1375	2409	2409	D00127	D00130	384	2	1	11	088.	001
014	a70	1p0185	1372	1372	2410	2410	D00107	D00110	384	2	1	11	088.	001
024	a71	1i0185	1372	1372	2409	2410	D00205	D00208	384	2	1	9	088.	021
028	a80	1p0197	1368	1368	2409	2409	D00245	D00248	384	2	1	11	088.	021
038	a81	2i0197	1368	1368	2409	2409	D00325	D00329	384	2	1	11	088.	021
026	a90	1p0209	1364	1364	2409	2409	D00225	D00228	384	2	1	9	088.	021
022	b00	1p0221	1360	1360	2410	2410	000534	000558	384	2	1	9	088.	021
005	b10	1p0233	1356	1356	2409	2409	000113	000137	384	2	1	9	088.	001
003	b20	1p0245	1352	1352	2409	2409	000061	000085	384	2	1	11	088.	001
044	b30	1p0257	1348	1348	2409	2409	001105	001130	384	2	1	11	088.	041
047	b31	1i0257	1348	1348	2409	2409	001158	001182	384	2	1	11	088.	041
043	b40	1p0269	2300	2300	1236	1236	001078	001103	384	2	1	11	268.	041
049	b41	1i0269	1345	1345	1950	1950	001212	001226	384	2	1	11	088.	041
041	b50	1p0281	2301	2301	1232	1232	001027	001052	384	2	1	11	268.	041
033	b60	1p0293	2301	2301	1228	1228	000823	000848	384	2	1	9	268.	021
039	b61	1i0293	2301	2301	1228	1228	000977	001002	384	2	1	11	268.	021
031	b70	1p0305	2301	2301	1225	1224	000772	000797	384	2	1	11	268.	021
019	b80	1p0317	2301	2301	1220	1220	000454	000481	384	2	1	9	268.	001
013	b90	1p0329	2301	2301	1218	1216	000299	000324	384	2	1	11	268.	001
004	c00	1p0341	2260	2260	1212	1212	000088	000112	384	2	1	9	268.	001
050	c01	1r0341	2261	2261	2409	2409	001227	001230	384	2	1	11	088.	041
009	c10	1p0353	2301	2301	1209	1209	000197	000222	384	2	1	9	268.	001
011	c20	1p0365	2301	2301	1205	1205	000248	000273	384	2	1	11	268.	001
015	c30	1p0377	2300	2300	1201	1201	000350	000375	384	2	1	11	268.	001
017	c40	1p0389	2301	2301	1197	1197	000402	000427	384	2	1	9	268.	001
021	c50	1p0401	2301	2301	1193	1193	000507	000533	384	2	1	9	268.	021
027	c60	1p0413	2301	2301	1189	1189	000664	000690	384	2	1	9	268.	021
035	c61	1i0413	2301	2301	1189	1189	000873	000899	384	2	1	11	268.	021
023	c70	2p0425	2300	2300	1186	1185	000559	000585	384	2	1	9	268.	021
002	c80	1p0437	2301	2300	1183	1182	000034	000060	384	2	1	11	268.	001
007	c90	1p0449	2301	2301	1178	1178	000144	000171	384	2	1	9	268.	001
046	d00	3p0461	2300	2300	1174	1174	001131	001157	384	2	1	11	268.	041
048	d01	1i0461	2300	2300	1174	1174	001184	001211	384	2	1	11	268.	041
025	d10	1p0473	2300	2300	1170	1170	000611	000638	384	2	1	9	268.	021
030	d20	1p0485	1275	1275	2410	2410	000745	000771	384	2	1	11	088.	021
052	d30	1p0497	1271	1271	2409	2409	001260	001286	384	2	1	11	088.	041
059	d31	1i0497	1271	1271	2409	2409	001420	001446	384	2	1	11	088.	041
124	d32	2i0497	2064	2064	2248	2248	003303	003307	384	2	1	11	088.	121
054	d40	1p0509	1268	1268	2409	2409	001316	001342	384	2	1	11	088.	041
057	d50	1p0521	1264	1264	2410	2410	001374	001401	384	2	1	11	088.	041
061	d60	1p0533	1260	1260	2409	2409	001476	001502	384	2	1	11	088.	061
065	d70	1p0545	1256	1256	2407	2409	001590	001617	384	2	1	11	088.	061
069	d71	1i0545	1256	1256	2409	2409	001704	001731	384	2	1	11	088.	061
071	d72	2i0545	1317	1317	2409	2409	001761	001786	384	2	1	11	088.	061
073	d80	1p0557	1252	1252	2409	2409	001816	001843	384	2	1	11	088.	061
075	d90	1p0569	1248	1248	2380	2380	001874	001900	384	2	1	11	088.	061
081	d91	2p0569	1248	1248	2409	2409	002045	002072	384	2	1	11	088.	061
067	e00	1p0581	1244	1244	2407	2410	001647	001674	384	2	1	11	088.	061
063	e10	1p0593	1241	1241	2410	2410	001533	001560	384	2	1	11	088.	061
077	e20	1p0605	1237	1237	2410	2410	001931	001958	384	2	1	11	088.	061
079	e30	1p0617	1233	1233	2407	2410	001988	002015	384	2	1	11	088.	061
083	e40	1p0629	1229	1229	2410	2410	002101	002128	384	2	1	9	088.	082
082	e50	1p0641	2300	2300	1116	1116	002073	002100	384	2	1	11	268.	082
125	e51	1i0641	2300	2300	1230	1230	003308	003334	384	2	1	11	268.	121
080	e60	1p0653	2301	2301	1112	1112	002016	002043	384	2	1	9	268.	061

078	e70	1p0665	2301	2301	1108	1108	001959	001987	384	2	1	11	268.	061
062	e80	1p0677	2301	2301	1105	1105	001504	001532	384	2	1	11	268.	061
076	e81	1i0677	2301	2301	1105	1105	001902	001930	384	2	1	11	268.	061
051	e90	1p0689	2300	2300	1101	1101	001231	001259	384	2	1	11	268.	041
029	f00	1p0701	2301	2301	1099	1097	000716	000744	384	2	1	11	268.	021
053	f10	1p0713	2301	2301	1094	1093	001287	001315	384	2	1	11	268.	041
055	f20	1p0725	2300	2300	1800	1800	001343	001354	384	2	1	11	268.	041
058	f21	3p0725	1799	1799	1089	1089	001402	001418	384	2	1	11	268.	041
060	f30	1p0737	2301	2301	1086	1085	001447	001475	384	2	1	11	268.	060
064	f31	1i0737	2301	2301	1085	1085	001561	001589	384	2	1	11	268.	061
066	f40	1p0749	2301	2301	1081	1081	001618	001646	384	2	1	11	268.	061
068	f41	1i0749	2301	2301	1081	1081	001675	001703	384	2	1	11	268.	061
070	f50	1p0761	2300	2300	1078	1078	001732	001760	384	2	1	11	268.	061
072	f60	1p0773	2300	2300	1074	1074	001787	001815	384	2	1	11	268.	061
074	f70	1p0785	2301	2301	1070	1070	001844	001872	384	2	1	11	268.	061
129	f71	2i0785	2301	2301	1118	1118	003429	003457	384	2	1	11	268.	082
084	f80	1p0797	2300	2300	1066	1066	002129	002159	384	2	1	9	268.	082
088	f90	1p0809	2245	2245	1063	1062	002253	002281	384	2	1	9	268.	082
112	f91	2p0809	2300	2300	1062	1062	003008	003037	384	2	1	11	268.	101
090	g00	1p0821	2300	2300	1064	1058	002314	002343	384	2	1	9	268.	082
131	g01	1i0821	2005	2005	1058	1058	003491	003518	384	2	1	11	268.	121
098	g10	1p0833	2300	2300	1056	1054	002563	002592	384	2	1	9	268.	082
104	g20	1p0845	2300	2300	1052	1051	002751	002780	384	2	1	11	268.	101
107	g30	1p0857	1156	1156	2407	2409	002845	002876	384	2	1	9	088.	101
093	g40	1p0869	1152	1152	2409	2409	002406	002435	384	2	1	9	088.	082
116	g41	1i0869	1152	1152	2404	2409	003132	003163	384	2	1	11	088.	101
091	g50	1p0881	1148	1148	2409	2410	002344	002373	384	2	1	9	088.	082
087	g60	1p0893	1144	1144	2410	2410	002222	002251	384	2	1	9	088.	082
126	g61	1i0893	1580	1580	2410	2410	003336	003361	384	2	1	11	088.	121
001	g70	1p0905	1140	1140	2406	2410	000001	000032	384	2	1	11	088.	001
085	g80	1p0917	1136	1136	2410	2410	002160	002189	384	2	1	9	088.	082
118	g81	1i0917	1173	1173	2014	2015	003198	003219	384	2	1	11	088.	101
089	g90	1p0929	1133	1133	2410	2410	002282	002313	384	2	1	9	088.	082
095	h00	1p0941	1129	1129	2410	2410	002468	002499	384	2	1	11	088.	095
120	h01	1i0941	1166	1166	2124	2125	003233	003256	384	2	1	11	088.	101
097	h10	1p0953	1125	1125	2409	2410	002532	002562	384	2	1	9	088.	082
105	h20	1p0965	1121	1121	2410	2410	002781	002811	384	2	1	9	088.	101
113	h21	1i0965	1158	1158	2410	2410	003038	003068	384	2	1	11	088.	101
103	h30	1p0977	1117	1117	2410	2410	002720	002750	384	2	1	11	088.	101
101	h40	1p0989	1113	1113	2409	2409	002656	002686	384	2	1	9	088.	101
099	h50	1p1001	1109	1109	2410	2410	002593	002623	384	2	1	9	088.	082
109	h60	1p1013	1106	1106	2409	2410	002909	002940	384	2	1	9	088.	101
128	h61	2i1013	1143	1143	2409	2410	003395	003427	384	2	1	11	088.	121
111	h70	1p1025	1102	1102	2409	2409	002974	003007	384	2	1	11	088.	101
122	h71	1i1025	1380	1380	2408	2409	003270	003295	384	2	1	11	088.	121
130	h80	1p1037	1098	1098	2060	2060	003458	003484	384	2	1	11	088.	121
132	h81	1i1037	1098	1098	2409	2409	003519	003554	384	2	1	11	088.	121
186	h82	2i1037	1600	1600	2409	2409	005330	005349	384	2	1	11	088.	181
108	h90	1p1049	2301	2301	985	985	002877	002908	384	2	1	9	268.	101
086	i00	1p1061	2300	2300	983	981	002190	002221	384	2	1	9	268.	082
092	i10	1p1073	2300	2300	977	977	002374	002405	384	2	1	9	268.	082
188	i11	1i1073	1122	1122	2409	2409	005375	005413	384	2	1	11	088.	181
096	i20	1p1085	2301	2301	974	973	002500	002531	384	2	1	11	268.	082
100	i30	1p1097	2300	2300	970	970	002624	002655	384	2	1	9	268.	082
119	i31	1i1097	1450	1450	970	970	003220	003232	384	2	1	11	268.	101
187	i32	2i1097	2215	2215	1405	1405	005350	005372	384	2	1	11	268.	181
102	i40	1p1109	2300	2300	966	966	002687	002719	384	2	1	11	268.	101
127	i41	1i1109	2263	2263	966	966	003362	003394	384	2	1	11	268.	121
094	i50	1p1121	2300	2300	1451	1451	002436	002456	384	2	1	9	268.	082
121	i51	1r1121	1450	1450	962	962	003257	003269	384	2	1	11	268.	121
106	i60	1p1133	2300	2300	958	958	002812	002844	384	2	1	9	268.	101
110	i70	1p1145	2300	2300	954	954	002941	002973	384	2	1	9	268.	101
114	i80	1p1157	2300	2300	950	950	003069	003101	384	2	1	11	268.	101
117	i81	1i1157	2300	2300	950	950	003164	003197	384	2	1	11	268.	101
133	i90	1p1169	2301	2301	946	946	003555	003587	384	2	1	11	268.	121
137	j00	1p1181	2301	2301	943	943	003694	003728	384	2	1	11	268.	121
139	j01	1i1181	2301	2301	943	943	003765	003798	384	2	1	9	268.	121
145	j10	1p1193	2301	2301	939	939	003973	004006	384	2	1	11	268.	141
135	j20	1p1205	2301	2301	935	935	003622	003657	384	2	1	11	268.	121
151	j21	1i1205	2301	2301	1078	1078	004179	004209	384	2	1	11	268.	141
185	j22	2i1205	1753	1753	1354	1354	005320	005329	384	2	1	11	268.	181
141	j30	1p1217	2301	2301	931	931	003833	003867	384	2	1	9	268.	141
143	j40	1p1229	2301	2301	927	927	003904	003938	384	2	1	9	268.	141
147	j50	1p1241	2301	2301	924	923	004041	004074	384	2	1	11	268.	141
152	j51	1i1241	1032	1032	2410	2410	004210	004243	384	2	1	11	088.	141

148	j60	1p1253	1028	1028	2410	2410	004075	004109	384	2	1	11	088.	141
150	j61	1i1253	1028	1028	2410	2410	004144	004178	384	2	1	11	088.	141
146	j70	1p1265	1025	1025	2410	2410	004007	004040	384	2	1	11	088.	141
134	j80	1p1277	1021	1021	2410	2410	003588	003621	384	2	1	11	088.	121
136	j90	1p1289	1017	1017	2407	2409	003658	003693	384	2	1	11	088.	121
138	k00	1p1301	1013	1013	2410	2410	003729	003764	384	2	1	9	088.	121
140	k01	1i1301	1013	1013	2410	2410	003799	003832	384	2	1	9	088.	121
142	k10	1p1313	1009	1009	2410	2410	003868	003903	384	2	1	9	088.	141
144	k11	1i1313	1009	1009	2410	2410	003939	003972	384	2	1	11	088.	141
154	k20	1p1325	1005	1005	2409	2409	004282	004316	384	2	1	11	088.	141
156	k30	1p1337	1001	1001	2409	2409	004354	004391	384	2	1	11	088.	141
159	k40	1p1349	1001	1001	2409	2410	004470	004504	384	2	1	11	088.	141
161	k41	1i1349	1001	1001	2410	2410	004539	004577	384	2	1	11	088.	161
163	k50	1p1361	1001	1001	2409	2409	004612	004646	384	2	1	11	088.	161
165	k60	1p1373	1001	1001	2409	2409	004681	004714	384	2	1	11	088.	161
167	k70	1p1385	1001	1001	1674	1674	004749	004766	384	2	1	11	088.	161
168	k71	2p1385	1675	1675	2410	2410	004767	004784	384	2	1	11	088.	161
170	k80	1p1397	1001	1001	2409	2409	004821	004855	384	2	1	11	088.	161
172	k81	1i1397	1001	1001	2409	2409	004891	004926	384	2	1	11	088.	161
149	k90	1p1409	2300	2300	892	892	004110	004143	384	2	1	11	268.	141
184	k91	1i1409	1060	1060	1950	1950	005298	005319	384	2	1	11	088.	181
153	l00	1p1421	2301	2301	893	892	004244	004281	384	2	1	11	268.	141
155	l10	1p1433	2301	2301	892	892	004317	004353	384	2	1	11	268.	141
158	l20	1p1445	2300	2300	893	892	004435	004468	384	2	1	11	268.	141
160	l21	1i1445	2300	2300	892	892	004505	004538	384	2	1	11	268.	141
162	l30	1p1457	2301	2301	892	892	004578	004611	384	2	1	11	268.	161
164	l40	1p1469	2301	2301	893	892	004647	004680	384	2	1	11	268.	161
183	l41	1i1469	2301	2301	1630	1630	005278	005297	384	2	1	11	268.	181
166	l50	1p1481	2300	2300	892	892	004715	004748	384	2	1	11	268.	161
169	l60	1p1493	2301	2301	892	892	004785	004820	384	2	1	11	268.	161
171	l70	1p1505	2301	2301	892	892	004856	004890	384	2	1	11	268.	161
173	l80	1p1517	2300	2300	892	892	004927	004960	384	2	1	11	268.	161
175	l81	1i1517	2300	2300	892	892	005003	005036	384	2	1	11	268.	161
177	l90	1p1529	2301	2301	892	892	005073	005106	384	2	1	11	268.	161
179	m00	1p1541	2301	2301	892	892	005145	005179	384	2	1	11	268.	161
181	m10	1p1553	2089	2089	892	892	005214	005242	384	2	1	11	268.	181
182	m11	1i1553	1001	1001	2409	2409	005243	005276	384	2	1	11	088.	181
176	m20	1p1565	1001	1001	2409	2409	005037	005072	384	2	1	11	088.	161
174	m30	1p1577	1001	1001	2410	2410	004961	005002	384	2	1	11	088.	161
178	m40	1p1589	1001	1001	2409	2409	005108	005143	384	2	1	11	088.	161
180	m50	1p1601	1001	1001	2409	2409	005180	005213	384	2	1	11	088.	161

System `B'

seq*punit*navn***ffil*fsp**lfil*lsp**freel**lreel**nch*ns*nb*dpt*dir**nav*

seq	punit	navn	ffil	fsp	lfil	lsp	freel	lreel	nch	ns	nb	dpt	dir	nav
040	a00	1p0101	1399	1399	2410	2410	101003	101026	384	2	1	11	088.	021
042	a01	1i0101	1399	1399	2410	2410	101053	101076	384	2	1	11	088.	041
034	a10	1p0113	1395	1395	2409	2409	100849	100872	384	2	1	11	088.	021
020	a20	1p0125	1391	1391	2409	2409	100482	100505	384	2	1	9	088.	001
032	a21	1i0125	1391	1391	2409	2409	100798	100822	384	2	1	11	088.	021
018	a30	1p0137	1387	1387	2410	2410	100429	100453	384	2	1	9	088.	001
008	a40	1p0149	1383	1383	2410	2410	100172	100196	384	2	1	11	088.	001
010	a50	1p0161	1379	1379	2409	2409	100223	100247	384	2	1	11	088.	001
016	a60	2p0173	1375	1375	2409	2409	100377	100401	384	2	1	11	088.	001
014	a70	1p0185	1372	1372	2410	2410	100325	100349	384	2	1	11	088.	001
024	a71	1i0185	1372	1372	2409	2410	100586	100610	384	2	1	9	088.	021
028	a80	1p0197	1368	1368	2409	2409	100691	100715	384	2	1	11	088.	021
038	a81	2i0197	1368	1368	2409	2409	100952	100976	384	2	1	11	088.	021
026	a90	1p0209	1364	1364	2409	2409	100639	100663	384	2	1	9	088.	021
022	b00	1p0221	1360	1360	2410	2410	100534	100558	384	2	1	9	088.	021
005	b10	1p0233	1356	1356	2409	2409	100113	100137	384	2	1	9	088.	001
003	b20	1p0245	1352	1352	2409	2409	100061	100085	384	2	1	11	088.	001
044	b30	1p0257	1348	1348	2409	2409	101105	101130	384	2	1	11	088.	041
047	b31	1i0257	1348	1348	2409	2409	101158	101182	384	2	1	11	088.	041
043	b40	1p0269	2300	2300	1236	1236	101078	101103	384	2	1	11	268.	041
049	b41	1i0269	1345	1345	1950	1950	101212	101226	384	2	1	11	088.	041
041	b50	1p0281	2301	2301	1232	1232	101027	101052	384	2	1	11	268.	041
033	b60	1p0293	2301	2301	1229	1228	100823	100848	384	2	1	9	268.	021
039	b61	1i0293	2301	2301	1228	1228	100977	101002	384	2	1	11	268.	021
031	b70	1p0305	2301	2301	1225	1224	100772	100797	384	2	1	11	268.	001
019	b80	1p0317	2301	2301	1220	1220	100454	100481	384	2	1	9	268.	001
013	b90	1p0329	2301	2301	1218	1216	100299	100324	384	2	1	11	268.	001
004	c00	1p0341	2260	2260	1212	1212	100088	100112	384	2	1	9	268.	001
050	c01	1r0341	2261	2261	2409	2409	101227	101230	384	2	1	11	088.	041
009	c10	1p0353	2301	2301	1209	1209	100197	100222	384	2	1	9	268.	001
011	c20	1p0365	2301	2301	1205	1205	100248	100273	384	2	1	11	268.	001

015	c30	1p0377	2300	2300	1201	1201	100350	100375	384	2	1	11	268.	001
017	c40	1p0389	2301	2301	1197	1197	100402	100427	384	2	1	9	268.	001
021	c50	1p0401	2301	2301	1193	1193	100507	100533	384	2	1	9	268.	021
027	c60	1p0413	2301	2301	1189	1189	100664	100690	384	2	1	9	268.	021
035	c61	1i0413	2301	2301	1189	1189	100873	100899	384	2	1	11	268.	021
023	c70	2p0425	2300	2300	1186	1185	100559	100585	384	2	1	9	268.	021
002	c80	1p0437	2301	2300	1183	1182	D00015	D00019	384	2	1	11	268.	001
007	c90	1p0449	2301	2301	1178	1178	100144	100171	384	2	1	9	268.	001
046	d00	3p0461	2300	2300	1174	1174	101131	101157	384	2	1	11	268.	041
048	d01	1i0461	2300	2300	1174	1174	101184	101211	384	2	1	11	268.	041
025	d10	1p0473	2300	2300	1170	1170	100611	100638	384	2	1	9	268.	021
030	d20	1p0485	1275	1275	2410	2410	100745	100771	384	2	1	11	088.	021
052	d30	1p0497	1271	1271	2409	2409	101260	101286	384	2	1	11	088.	041
059	d31	1i0497	1271	1271	2409	2409	101420	101446	384	2	1	11	088.	041
124	d32	2i0497	2064	2064	2248	2248	103303	103307	384	2	1	11	088.	121
054	d40	1p0509	1268	1268	2409	2409	101316	101342	384	2	1	11	088.	041
057	d50	1p0521	1264	1264	2410	2410	101374	101401	384	2	1	11	088.	041
061	d60	1p0533	1260	1260	2409	2409	101476	101502	384	2	1	11	088.	061
065	d70	1p0545	1256	1256	2408	2409	101590	101617	384	2	1	11	088.	061
069	d71	1i0545	1256	1256	2409	2409	101704	101731	384	2	1	11	088.	061
071	d72	2i0545	1317	1317	2409	2409	101761	101786	384	2	1	11	088.	061
073	d80	1p0557	1252	1252	2409	2409	101816	101843	384	2	1	11	088.	061
075	d90	1p0569	1248	1248	2380	2380	101874	101900	384	2	1	11	088.	061
081	d91	2p0569	1248	1248	2409	2409	102045	102072	384	2	1	11	088.	061
067	e00	1p0581	1244	1244	2408	2410	101647	101674	384	2	1	11	088.	061
063	e10	1p0593	1241	1241	2410	2410	101533	101560	384	2	1	11	088.	061
077	e20	1p0605	1237	1237	2410	2410	101931	101958	384	2	1	11	088.	061
079	e30	1p0617	1233	1233	2408	2410	101988	102015	384	2	1	11	088.	061
083	e40	1p0629	1229	1229	2410	2410	102101	102128	384	2	1	9	088.	082
082	e50	1p0641	2300	2300	1116	1116	102073	102100	384	2	1	11	268.	082
125	e51	1i0641	2300	2300	1230	1230	103308	103334	384	2	1	11	268.	121
080	e60	1p0653	2301	2301	1112	1112	102016	102043	384	2	1	9	268.	061
078	e70	1p0665	2301	2301	1108	1108	101959	101987	384	2	1	11	268.	061
062	e80	1p0677	2301	2301	1105	1105	101504	101532	384	2	1	11	268.	061
076	e81	1i0677	2301	2301	1105	1105	101902	101930	384	2	1	11	268.	061
051	e90	1p0689	2300	2300	1101	1101	101231	101259	384	2	1	11	268.	041
029	f00	1p0701	2301	2301	1099	1097	100716	100744	384	2	1	11	268.	021
053	f10	1p0713	2301	2301	1094	1093	101287	101315	384	2	1	11	268.	041
055	f20	1p0725	2300	2300	1800	1800	101343	101354	384	2	1	11	268.	041
058	f21	3p0725	1799	1799	1089	1089	101402	101418	384	2	1	11	268.	041
060	f30	1p0737	2301	2301	1085	1085	101447	101475	384	2	1	11	268.	060
064	f31	1i0737	2301	2301	1085	1085	101561	101589	384	2	1	11	268.	061
066	f40	1p0749	2301	2301	1081	1081	101618	101646	384	2	1	11	268.	061
068	f41	1i0749	2301	2301	1081	1081	101675	101703	384	2	1	11	268.	061
070	f50	1p0761	2300	2300	1078	1078	101732	101760	384	2	1	11	268.	061
072	f60	1p0773	2300	2300	1074	1074	101787	101815	384	2	1	11	268.	061
074	f70	1p0785	2301	2301	1070	1070	101844	101872	384	2	1	11	268.	061
129	f71	2i0785	2301	2301	1118	1118	103429	103457	384	2	1	11	268.	121
084	f80	1p0797	2300	2300	1066	1066	102129	102159	384	2	1	9	268.	082
088	f90	1p0809	2257	2245	1075	1062	102253	102281	384	2	1	9	268.	082
112	f91	2p0809	2300	2300	1062	1062	103008	103037	384	2	1	11	268.	101
090	g00	1p0821	2300	2300	1065	1058	102314	102343	384	2	1	9	268.	082
131	g01	1i0821	2005	2005	1058	1058	103491	103518	384	2	1	11	268.	121
098	g10	1p0833	2300	2300	1056	1054	102563	102592	384	2	1	9	268.	082
104	g20	1p0845	2300	2300	1052	1051	102751	102780	384	2	1	11	268.	101
107	g30	1p0857	1156	1156	2407	2409	102845	102876	384	2	1	9	088.	101
093	g40	1p0869	1152	1152	2409	2409	102406	102435	384	2	1	9	088.	082
116	g41	1i0869	1152	1152	2409	2409	103132	103163	384	2	1	11	088.	101
091	g50	1p0881	1148	1148	2410	2410	102344	102373	384	2	1	9	088.	082
087	g60	1p0893	1144	1144	2410	2410	102222	102251	384	2	1	9	088.	082
126	g61	1i0893	1580	1580	2410	2410	103336	103361	384	2	1	11	088.	121
001	g70	1p0905	1140	1140	2407	2410	100001	100032	384	2	1	11	088.	001
085	g80	1p0917	1136	1136	2410	2410	102160	102189	384	2	1	9	088.	082
118	g81	1i0917	1173	1173	2014	2015	103198	103218	384	2	1	11	088.	101
089	g90	1p0929	1133	1133	2410	2410	102282	102313	384	2	1	9	088.	082
095	h00	1p0941	1129	1129	2410	2410	102468	102499	384	2	1	11	088.	095
120	h01	1i0941	1166	1166	2124	2125	103233	103256	384	2	1	11	088.	101
097	h10	1p0953	1125	1125	2410	2410	102532	102562	384	2	1	9	088.	082
105	h20	1p0965	1121	1121	2410	2410	102781	102811	384	2	1	9	088.	101
113	h21	1i0965	1158	1158	2410	2410	103038	103068	384	2	1	11	088.	101
103	h30	1p0977	1117	1117	2410	2410	102720	102750	384	2	1	11	088.	101
101	h40	1p0989	1113	1113	2409	2409	102656	102686	384	2	1	9	088.	101
099	h50	1p1001	1109	1109	2410	2410	102593	102623	384	2	1	9	088.	082
109	h60	1p1013	1106	1106	2409	2410	102909	102940	384	2	1	9	088.	101
128	h61	2i1013	1143	1143	2410	2410	103395	103428	384	2	1	11	088.	121

111	h70	1p1025	1102	1102	2409	2409	102974	103007	384	2	1	11	088.	101
122	h71	1i1025	1380	1380	2408	2409	103270	103295	384	2	1	11	088.	121
130	h80	1p1037	1098	1098	2060	2060	103458	103484	384	2	1	11	088.	121
132	h81	1i1037	1098	1098	2409	2409	103519	103554	384	2	1	11	088.	121
186	h82	2i1037	1600	1600	2409	2409	105330	105349	384	2	1	11	088.	181
108	h90	1p1049	2301	2301	985	985	102877	102908	384	2	1	9	268.	101
086	i00	1p1061	2300	2300	982	981	102190	102221	384	2	1	9	268.	082
092	i10	1p1073	2300	2300	977	977	102374	102405	384	2	1	9	268.	082
188	i11	1i1073	1122	1122	2409	2409	105374	105413	384	2	1	11	088.	181
096	i20	1p1085	2301	2301	974	973	102500	102531	384	2	1	11	268.	082
100	i30	1p1097	2300	2300	970	970	102624	102655	384	2	1	9	268.	082
119	i31	1i1097	1450	1450	970	970	103220	103232	384	2	1	11	268.	101
187	i32	2i1097	2215	2215	1405	1405	105350	105372	384	2	1	11	268.	181
102	i40	1p1109	2300	2300	966	966	102687	102719	384	2	1	11	268.	101
127	i41	1i1109	2263	2263	966	966	103362	103394	384	2	1	11	268.	121
094	i50	1p1121	2300	2300	1451	1451	102436	102456	384	2	1	9	268.	082
121	i51	1r1121	1450	1450	962	962	103257	103269	384	2	1	11	268.	121
106	i60	1p1133	2300	2300	958	958	102812	102844	384	2	1	9	268.	101
110	i70	1p1145	2300	2300	954	954	102941	102973	384	2	1	9	268.	101
114	i80	1p1157	2300	2300	950	950	103069	103101	384	2	1	11	268.	101
117	i81	1i1157	2300	2300	950	950	103164	103197	384	2	1	11	268.	101
133	i90	1p1169	2301	2301	946	946	103555	103587	384	2	1	11	268.	121
137	j00	1p1181	2301	2301	943	943	103694	103728	384	2	1	11	268.	121
139	j01	1i1181	2301	2301	943	943	103765	103798	384	2	1	9	268.	121
145	j10	1p1193	2301	2301	939	939	103973	104006	384	2	1	11	268.	141
135	j20	1p1205	2301	2301	935	935	103622	103657	384	2	1	11	268.	121
151	j21	1i1205	2301	2301	1078	1078	104179	104209	384	2	1	11	268.	141
185	j22	2i1205	1753	1753	1354	1354	105320	105329	384	2	1	11	268.	181
141	j30	1p1217	2301	2301	931	931	103833	103867	384	2	1	9	268.	141
143	j40	1p1229	2301	2301	927	927	103904	103938	384	2	1	9	268.	141
147	j50	1p1241	2301	2301	924	923	104041	104074	384	2	1	11	268.	141
152	j51	1i1241	1032	1032	2410	2410	104210	104243	384	2	1	11	088.	141
148	j60	1p1253	1028	1028	2410	2410	104075	104109	384	2	1	11	088.	141
150	j61	1i1253	1028	1028	2410	2410	104144	104178	384	2	1	11	088.	141
146	j70	1p1265	1025	1025	2410	2410	104007	104040	384	2	1	11	088.	141
134	j80	1p1277	1021	1021	2410	2410	103588	103621	384	2	1	11	088.	121
136	j90	1p1289	1017	1017	2408	2409	103658	103693	384	2	1	11	088.	121
138	k00	1p1301	1013	1013	2410	2410	103729	103764	384	2	1	9	088.	121
140	k01	1i1301	1013	1013	2410	2410	103799	103832	384	2	1	9	088.	121
142	k10	1p1313	1009	1009	2410	2410	103868	103903	384	2	1	9	088.	141
144	k11	1i1313	1009	1009	2410	2410	103939	103972	384	2	1	11	088.	141
154	k20	1p1325	1005	1005	2409	2409	104282	104316	384	2	1	11	088.	141
156	k30	1p1337	1001	1001	2409	2409	104354	104391	384	2	1	11	088.	141
159	k40	1p1349	1001	1001	2409	2410	104470	104504	384	2	1	11	088.	141
161	k41	1i1349	1001	1001	2410	2410	104539	104577	384	2	1	11	088.	161
163	k50	1p1361	1001	1001	2409	2409	104612	104646	384	2	1	11	088.	161
165	k60	1p1373	1001	1001	2409	2409	104681	104714	384	2	1	11	088.	161
167	k70	1p1385	1001	1001	1674	1674	104749	104766	384	2	1	11	088.	161
168	k71	2p1385	1675	1675	2410	2410	104767	104784	384	2	1	11	088.	161
170	k80	1p1397	1001	1001	2409	2409	104821	104855	384	2	1	11	088.	161
172	k81	1i1397	1001	1001	2409	2409	104891	104926	384	2	1	11	088.	161
149	k90	1p1409	2300	2300	892	892	104110	104143	384	2	1	11	268.	141
184	k91	1i1409	1060	1060	1950	1950	105298	105319	384	2	1	11	088.	181
153	l00	1p1421	2301	2301	893	892	104244	104281	384	2	1	11	268.	141
155	l10	1p1433	2301	2301	892	892	104317	104353	384	2	1	11	268.	141
158	l20	1p1445	2300	2300	893	892	104435	104468	384	2	1	11	268.	141
160	l21	1i1445	2300	2300	892	892	104505	104538	384	2	1	11	268.	141
162	l30	1p1457	2301	2301	892	892	104578	104611	384	2	1	11	268.	161
164	l40	1p1469	2301	2301	893	892	104647	104680	384	2	1	11	268.	161
183	l41	1i1469	2301	2301	1630	1630	105278	105297	384	2	1	11	268.	181
166	l50	1p1481	2300	2300	892	892	104715	104748	384	2	1	11	268.	161
169	l60	1p1493	2301	2301	892	892	104785	104820	384	2	1	11	268.	161
171	l70	1p1505	2301	2301	892	892	104856	104890	384	2	1	11	268.	161
173	l80	1p1517	2300	2300	892	892	104927	104960	384	2	1	11	268.	161
175	l81	1i1517	2300	2300	892	892	105003	105036	384	2	1	11	268.	161
177	l90	1p1529	2301	2301	892	892	005073	005106	384	2	1	11	268.	161
179	m00	1p1541	2301	2301	892	892	105145	105179	384	2	1	11	268.	161
181	m10	1p1553	2089	2089	892	892	105214	105242	384	2	1	11	268.	181
182	m11	1i1553	1001	1001	2409	2409	105243	105276	384	2	1	11	088.	181
176	m20	1p1565	1001	1001	2409	2409	105037	105072	384	2	1	11	088.	161
174	m30	1p1577	1001	1001	2410	2410	104961	105002	384	2	1	11	088.	161
178	m40	1p1589	1001	1001	2409	2409	105108	105144	384	2	1	11	088.	161
180	m50	1p1601	1001	1001	2409	2409	105180	105213	384	2	1	11	088.	161

7. Processing Time Line

Decon	August-December 1995
Elastic Binning	April - May 1996
Velocity	January - April 1996
DMO Stack	May - June 1996
Migration	July 1996

8. Notable Processing Problems and Solutions

The benefits from the decision to rebuild the Index from seismic headers instead of using the G2000 navigation files delivered from the Calgary center were not realised until stack production. After 34% of the southern priority area was stacked, it was discovered that the 'dpr' files generated from the G2000 did not agree with the seismic trace headers which created the index file. This discrepancy caused a significant amount of traces to be dropped from the stack. After discussing the problem with the DP support group, stack production resumed by using a processor `dmbgf' which circumvented the input of dpr files. As a consequence, an initial delay of 1 week was encountered, but was later recovered from the assignment of additional cpu resources.

9. Conclusion

Houston DP inherited this project from the Calgary DP Center in late March 1996 when the original deadline was due. After reviewing the previous processing, it soon became obvious that the Index had to be rebuilt from scratch and the velocities had to be partially re-run and completely re-picked. However, with the support of the DP management and from the great effort of the processing group, we were able to deliver the Migrated Volume of the Southern priority area of the survey on June 30, while continuing to stack the Northern half. Finally, by the end of July 1996, as promised, the final migration of the entire volume was delivered.

Due to the wide spread deployment of the four streamer and triple source array, the shallow data was heavily contaminated by aliased noise. In fact, the data volume as a whole had a relatively poor signal/noise ratio. It was deemed necessary to apply, post-stack, a shallow in-line K-filter in conjunction with a 3-D FXY noise attenuation filter over the entire record length.

Figures 3 & 4 in Section 12 illustrate the results with and without the 3-D FXY noise attenuation filter.

Also shown in Section 12, Figures 5 and 6 are the timeslices from the QuickLook Cube migration (QLC) and the Final migrated volume, respectively. These timeslices are both at 2.0secs and clearly demonstrate the improvements attained from the final processing sequence.

10. 3-D Velocity Fields

10.1 Stacking Velocity Field

The 3-D stacking velocity field was generated using velocities derived by performing 3-D velocity analysis at selected in-line locations on the 3-D grid. The velocities were to be calculated on an 800 X 800 meter grid. Since the data was acquired with a subsurface line spacing of 25 meters, this required that every 32nd row location be processed in 3-D mode as a velocity line, starting with row 25. The following is a list of the velocity lines that were used for this survey.

Rows 25, 57, 89, 121, 153, 185, 217, 249, 281, 313, 345, 377, 409, 441, 473, 505, 537, 569, 601, 633, 665, 697, 729, 761, 793, 825, 857, 889, 921, 953, 985, 1017, 1049, 1081, 1113, 1145, 1177, 1209, 1241, 1273, 1305, 1337, 1369, 1401, 1433, 1465, and 1497.

The DMO gathers were created on Fujitsu for above velocity lines and transferred to the Geco-Prakla Sun Workstation for velocity analysis. Finally, 2-D DMO stacks were generated to verify velocity interpretation. The stacks were created by using data acquired closest to the velocity row location, merging data with navigation and then stacking into 3-D grid which was allocated with wide bins.

Once all the velocities analyses had been interpreted and approved, a 3-D velocity database was constructed. According to the grid definition, the in-line position and the cross-line position, each velocity location was assigned the proper X, Y coordinate. In order for our program to properly build a velocity cube, the input grid of velocity cube completely covered the survey, the rectangular grid was defined to cover cross-line 1 through 3200 and in-line 1 through 1532. The first and last functions for each velocity line were repeated to cover this area. Once this velocity database was built, velocities were interpolated in time and space.

Temporal resampling to a regular time increment was done first, such that each function now had 76 velocity picks (i.e. 76 velocity timeslices). Each timeslice was then interpolated to fill in all intermediate points. Interpolation of the timeslices was done in the following manner:

1. Calculate the midpoint bin number of the four velocities on the regular rectangle bounded input velocities $V_{i,j}$ $V_{i+1,j}$ $V_{i,j+1}$ $V_{i+1,j+1}$, where i is the in-line number and j is the cross-line number.
2. Calculate the average velocity of these four velocities weighted by the inverse of the distance to the midpoints.
3. Linearly interpolate between known input points in the in-line direction.
4. Linearly interpolate between known input points in the cross-line direction.
5. Linearly interpolate the midpoints calculated in step 2 in the in-line direction.
6. Linearly interpolate the midpoints calculated in step 2 in the cross-line direction.
7. Linearly interpolate points along every 64 cross-line.
8. Linearly interpolate remaining points in the in-line direction.

10.2 Migration Velocity Field

The migration velocity field was constructed in a similar fashion. This procedure started with the temporally resampled database that was used for the stacking velocity cube. Before spatial interpolation of the functions, the velocities were converted to interval velocities. In addition, these interval velocity functions were temporally smoothed by fitting the time velocity points to a ninth order polynomial. This ensured that there were no unreasonably large temporal velocity changes in the interval velocity functions. These smoothed interval velocity functions were then spatially interpolated as above. After spatial interpolation, a four-pass recursive smoothing filter was applied to the velocity cube. This recursive filter operated in the following manner:

1. Each bin was summed with the previous bin in the cross-line direction with the following weights: 0.1 for the current bin and 0.9 for the previous bin. The resultant velocity was immediately written back to the current location. This procedure was repeated at next location and continued until all bins were mixed. The direction of mixing was from highest in-line number to lowest in-line number.
2. Same as in 1, but done from lowest in-line number to highest in-line number.
3. Same as 1, but in the in-line direction from highest cross-line number to lowest cross-line number.
4. Same as 3, but from lowest cross-line number to highest cross-line number.

11. Job Setups for Main Processing Steps

11.1 A job setup for Deconvolution

```
/job      acct '7263 nflp0557 explserv segystbd'
          trdcntl '/proj/nav/cntl/g2s0731.cntl'

/seisin   format segd datafmt 8015
          data 1 9000 2 384 0
          dens hc
          exthdr 12
          extprint
          errtyp 2
          nodummy conskip 999999 totskip 999999
          reel 1816
          reel 1817
          reel 1818
          reel 1819
          reel 1820
          reel 1821
          reel 1822
          reel 1823
          reel 1824
          reel 1825
          reel 1826
          reel 1827
          reel 1828
          reel 1829
          reel 1830
          reel 1831
          reel 1832
          reel 1833
          reel 1834
          reel 1835
          reel 1836
          reel 1837
          reel 1838
          reel 1839
          reel 1840
          reel 1841
          reel 1842
          reel 1843
          bi 1252 ei 2409
          (revfiles
          device 'rmt1'
          ftraces d9,200,1 d201,392,1
(port          ftraces d1,192,1 d201,392,1
          reseq 1

/deadset

/filter   butterwo lowpass minimum filt 90 72 nfpts 121
/resamp   sro 4 noalias

(@zero
/zero ftraces 208
```

```
/zero ffiles 1278 1353 2219
(          1         2         3         4         5         6
(234567890123456789012345678901234567890123456789012345678901234567890
(nf-1p0557     FSP       LSP        1.0  FTR  LTR
(nf-1p0557                               200  200
(nf-1p0557     1278      1278       1.0
(nf-1p0557     1353      1353       1.0
(nf-1p0557     2219      2219       1.0
(234567890123456789012345678901234567890123456789012345678901234567890

( add 384 to port cable only to match p190s and make each kfldtn unique:
/glmod    add kfldtn -8 0
(port /glmod    ftraces d201,392,1 add kfldtn -8 0
(port /glmod    add kfldtn 384 0
/sphdiv   vel
          1.  1472.   500.  1647.  1000.  1813.  1500.  2000.
       2000.  2221.  2500.  2630.  3000.  2990.  3500.  3274.
       4000.  3548.  4500.  3749.  5000.  3920.  5500.  4076.
       6000.  4218.  6500.  4335.  7000.  4450.  7500.  4483.
       8000.  4509.  8500.  4509.  9000.  4509
          tstop 8000

/expgain  begtime 1 200 9999 200 endtime 1 4000 9999 4000 expfunc +3.0
/filter   filename '/data11/desig/designature'

/merg3d   mxtrskip 300000
          detnum   768
          usefldtr
          navshots 1252 2409
          mxspskip 999
          mxsptdlt 30
          timediff 2
          todmerge
          (sidfmt '(i8,2x)'
          line 'nf_1p0557    ' (these blank spaces are needed to make it
work..

/preddcon zone 1
          operator    1 6000 320    4
          operator 9999
          design      1 260 400  5050 4700
          design   9999
          apply      1 260 0  5050 0
          apply    9999
          prewhite 0.1
          byfile

/glmod set kgrrow 0557,0
/glmod setlid nf1p kgrrow
(this is optional to stop /output putting all reel numbers as "SCRTCH":
/hdrsegy  cardnum 3
 contents 'C 3 REEL NO 1p0557  DAY_START OF REEL     YEAR      OBSERVER'
/output   lname '1p0557' dens hc segyhead gecostrd
          device rmt2
          segyhist '/proj/gss/jobs/segy/newf_template'
          noreseq
/eoj
```

11.2 A job setup for 3-D DMO and Stack with Elastic Binning

```
/job        acct     '0489 g30a nfgb   dms'
            (runcode 0
            (system  vpx220
            (division  f
            (region 84 Mb
/jobtick    submitby 'group11'
            runtime   5.0
            inreel 'D00987'
            inreel 'D00988'
            inreel 'D00989'
            inreel 'D00990'
            inreel 'D00991'
            process 'dmbtd'
            userinst '**** NEW FOUNDLAND **'
            userinst '                      '
            userinst 'RUN ONE JOB AT A TIME'
            userinst '*** dmo stack *******'
            dsn '/prod/dmstk/b4dmstkg30a.s'
/trdfile    use stack  ctrlname '/SDP248/grp11/p489/stack.cntl'
            use index  ctrlname '/SDP366/grp11/p489/index.cntlall'
            jobrows    759  797
            jobcols    1    3200
/seisin     data 5 9000 4 384  0
            eofcount 2
            dens silo
            reel D00987
            reel D00988
            reel D00989
            reel D00990
            reel D00991
            byfield
            reseq 1
/deadset
/grdit      getrwcl
            xorigin   645410   yorigin   5226665
            basangle   88.34   sidangle   178.34
            rowsize     25.0   colsize     12.50
            nombinsx     100   nombinsy      100
            maxgrdcl    3200
            setcdp             setsta
/dmbgf      contfile '/SDP213/grp11/p489/dmbtd.cntl'
            xorigin   645410   yorigin   5226665
            basangle   88.34   sidangle   178.34
            rowsize     25.0   colsize     12.50
            newline '1p0857 A  '
            print  30
/dmbcd      contfile '/SDP213/grp11/p489/dmbtd.cntl'
            mappedtr 1200
            firstrow  763
            lastrow   793
            firstcol    1
            lastcol  3200
            xorigin   645410   yorigin   5226665
            basangle   88.34   sidangle   178.34
            rowsize     25.0   colsize     12.50
```

```
/tranalys
          offset       265 5040 thres 10.0 firstspk
          nearwind    1000 9000
          farwind     4500 9000
          taper        200
/zvelocit threed
          rmsvels
          notintrp
          rdthreed   0 100 9000 100
          maxrow     1532
          maxcol     3200
          vcubenam 'dsn=/SDP238/grp11/p489/vcub489.cntl;'
/nmo
/mute    fmute       1  0+0 575+0 576+500  5200+4200
         fmute 9999999  0+0 575+0 576+500  5200+4200
         taper 20
/deadset useglcom
         (fmute and tmute in headers applied to trace samples
/dmbtd
         stkcntl  '/SDP248/grp11/p489/stack.cntl'
         contfile '/SDP213/grp11/p489/dmbtd.cntl'
         filetype stack
         (restart
         boundary  1  1  1532  1 1532  3200  1 3200
                   1  1
         firstrow  763
         lastrow   793
         firstcol  1
         lastcol   3200
         feather    200
         numbins   5500
         unnorm
         (printbnd   use for first dmo run only
/eoj
```

11.3 A job setup for In-line k-filter

```
/job        acct '0489 norm nfgb    dms'
            (runcode 0
            (system  vpx220
            (priority  8
            (division  e
/jobtick    submitby 'cathy'
            runtime  3.5
            process  'norm'
            userinst '*** NEW FOUNDLAND**'
            userinst ' DMO STACK      '
            userinst ' NORMALIZE CUBE'
            userinst ' row 001-200       '
            userinst '*******************'
            dsn      'gss/jobs/prod/norm/b1normala.s'
/trdfile    use stack
            ctrlname  '/SDP248/grp11/p489/stack.cntl'
            jobrows  001 200
            jobcols  1   3200
/stkin      data 4 9000 4 1 0
            rows 1  200 1
            cols 1 3200 1
            use  stack
            root
            xorigin  645410    yorigin   5226665
            basangle  88.34    sidangle  178.34
            rowsize      25    colsize   12.5

/deadset
/glmod      set kcdp 1  1

/filtwod
            nxfilt 25 ntfilt 1
            timegate 0 0 3000 4000
            kfilt  -43  -38  -28  -23
            reject  costaper
/filtwod
            nxfilt 25 ntfilt 1
            timegate 0 0 3000 4000
            kfilt  -76  -71  -61  -56
            reject  costaper
/filtwod
            nxfilt 25 ntfilt 1
            timegate 0 0 3000 4000
            kfilt  -110  -105  -95  -90
            reject  costaper

/deadset    useglcom
/stkout     client 'exp services'
            area   'n foundland'
            use stack
            firstrow  1       lastrow  779
            firstcol  1       lastcol  3200

/eoj
```

11.4 A job setup for 3-D FXY-filter

```
/job        acct '0489 rowqc nfgb dms' plotevry 1
            (runcode 0
            (system  vpx220
            (division e
            (priority 8
            (region 60 Mb
/jobtick    submitby 'indro'
            runtime  1.30
            process  'fxy'
            userinst '***newfoundland***'
            userinst 'fxy dcn             '
            userinst '******************'
            dsn      'gss/jobs/test/b0fxy1.s'
/trdfile    use stack
            ctrlname  '/SDP248/grp11/p489/stack.cntl'
            jobrows 211    278
            jobcols 1533   3200
/stkin      data 4 9000 4 1 0
            rows  211    278  1    (insert correct row range
            cols  1533   3200 1
            root
            bycol
            xorigin  645410    yorigin   5226665
            basangle  88.34    sidangle  178.34
            rowsize    25      colsize   12.5

/deadset
/renumber   firstcdp  1

/fxyfilt
            ilwind 20
            xlwind 20
            lenfil 5 (default 3 ,recomm
            ilovlp 10
            xlovlp 10
            lowfreq  0
            highfreq 75
            nscalwin 10
            bycol

/deadset useglcom
/stkout     client 'exp services'
            area   'n foundland'
            use stack
            firstrow   1       lastrow  1532
            firstcol   1       lastcol  3200
/eoj
```

11.5 A job setup for Migration Step-I

```
/job        acct '0489 1225 nfgb mig'
     (runcode 0
           (system   vpx220
           (priority 8
           (region 110Mb
           (division E
/jobtick    submitby 'nicholas'
            runtime   5.00
            inreel   'disk'
            outreel  'no/op'
            process  'mig'
            userinst '******nfgb*****'
            userinst 'migration step 1        '
            userinst '!!! check memory before'
            userinst 'starting job!!          '
            userinst '******nfgb*****'
            dsn      'N/A'
/trdfile    use mig
            ctrlname '/SDP248/grp11/p489/mig.cntl'
            jobrows 1051 1225 (reading in 175 in-lines
            jobcols 1 3750 (full range including padded zone
/stkin      data 4 9000 6 1 0 (without stretch
            use mig
            rows 1051 1225 1 (reading in 175 inlines
            cols 1 3200 1 (full range excluding padded zone
/renumber   firstcdp 1
/deadset
/mgtda      qc
            unit     '3380  '
            volser   'SDP388'
            resfile  '/SDP388/grp11/p489/mgtdap1_1225.log'
            wrkfile  '/SDP388/grp11/p489/mgtdap1_1225.wrk'
            hdrfile  '/SDP388/grp11/p489/mgtdap1_1225.hdr'
            atap      20 (default is 30
            vmax      0  (0 for steps 1 and 3 otherwise 5000.0
            use mig
            flagtd
            byrows            (byrows or bycols
            firstrow  1051    (first row forjob
            lastrow   1225    (last row forjob
            firstcol  1
            lastcol   3200    (excluding padding
            delrow    25.0
            delcol    12.5
            anone     0.5
            antwo     1.5
            anthree   65
            (anfour    75 2.0 70 4.0 50 6.0 40 9.0 30
            anfour    75
            angm      60 3.0 60 6.0 40 9.0 10
            (bmem      0.4
            padt      2.0
            interval
            fracv     3.0
            dtrms     200
            ivpt      1       (step number 1 2 or 3
```

```
        nrows      1532     (total rows
        ncols      3200     (total, excluding padding
        ncolsb     3750     (total, including padding
        knsmpa     1501     (based on 9000ms same for all 3 steps
        knsmpb     1617     (based on 9700ms same for all 3 steps
        minrow     1
        mincol     1
        oppam      0 4 4 4
        opcoef
2.6885530025518318e-12
-1.5643384297873967e-10
2.1290515836198131e-09
9.8991836409524095e-10
-3.1765299123544911e-10
1.7937876643132595e-08
-2.5513263531331779e-07
5.8315702273087551e-07
6.5697373079858209e-09
-3.7729275820553167e-07
5.7157588556168815e-06
-2.9293642775904404e-05
-1.9393565181001961e-08
1.5356500315522706e-06
-3.0044565226616910e-05
2.0466111784319987e-04
-4.6059397877277321e-11
2.2498468580708324e-09
-2.0560394654967973e-08
-1.1887344421262180e-07
5.0196558319867309e-09
-2.6580428720523643e-07
3.2847062992355365e-06
-7.8541951852597136e-07
-1.0053347633009887e-07
5.6454287584597702e-06
-8.0992933789517047e-05
3.4944739663473836e-04
2.3097712487347025e-07
-2.1946018446472336e-05
4.3855936018693099e-04
-1.5231606720904691e-03
1.9308953322115055e-10
-6.0785162295568208e-09
-3.9673038335757044e-08
1.5050571147391096e-06
-1.9009562222806280e-08
8.3932435472912061e-07
-5.7555177273305824e-06
-8.2047805427580000e-05
3.3276832198055027e-07
-1.7517174728528716e-05
2.2245527911552334e-04
-4.8666418329775061e-04
8.7828068061426891e-09
4.8522394112172528e-05
-1.2590824440579876e-03
5.6091735027792361e-04
2.9426077435090765e-11
-7.1375725480455047e-09
2.4061149572508669e-07
```

```
-8.3096238541784616e-07
2.0173669271152617e-09
1.2334199172536735e-07
-8.4742999246973462e-06
1.0141919557191004e-04
-7.0234471937942906e-10
-9.0518773823712036e-07
1.2399309386829978e-05
-4.6301647641408615e-04
-1.0515828579203047e-06
3.3027604263354205e-05
1.4688985990807825e-04
1.8936469985501221e-02
(pilot interval velocities follow
vpilot (reduced pilot velocity function
1561.48 ( at 0.00000000e+00  milliseconds
1591.35 ( at 199.99992  milliseconds
1701.56 ( at 399.99976  milliseconds
1849.88 ( at 599.99976  milliseconds
1992.02 ( at 799.99976  milliseconds
2135.19 ( at 999.99976  milliseconds
2314.41 ( at 1199.9998  milliseconds
2520.41 ( at 1399.9995  milliseconds
2755.25 ( at 1599.9993  milliseconds
3005.54 ( at 1799.9990  milliseconds
3257.89 ( at 1999.9990  milliseconds
3504.06 ( at 2199.9998  milliseconds
3735.81 ( at 2399.9995  milliseconds
3953.14 ( at 2599.9993  milliseconds
4163.26 ( at 2799.9990  milliseconds
4332.18 ( at 2999.9990  milliseconds
4475.35 ( at 3199.9988  milliseconds
4617.49 ( at 3399.9995  milliseconds
4724.61 ( at 3599.9993  milliseconds
4818.34 ( at 3799.9990  milliseconds
4916.19 ( at 3999.9990  milliseconds
4727.63 ( at 4199.9961  milliseconds
4775.36 ( at 4399.9961  milliseconds
4828.32 ( at 4599.9961  milliseconds
4890.72 ( at 4799.9961  milliseconds
4930.20 ( at 4999.9961  milliseconds
4994.20 ( at 5199.9961  milliseconds
5043.84 ( at 5399.9961  milliseconds
5064.38 ( at 5599.9961  milliseconds
5100.93 ( at 5799.9961  milliseconds
5110.71 ( at 5999.9961  milliseconds
4915.52 ( at 6199.9961  milliseconds
4882.66 ( at 6399.9961  milliseconds
4838.82 ( at 6599.9961  milliseconds
4757.56 ( at 6799.9961  milliseconds
4663.44 ( at 6999.9961  milliseconds
4574.28 ( at 7199.9961  milliseconds
4454.18 ( at 7399.9961  milliseconds
4353.84 ( at 7599.9961  milliseconds
4260.69 ( at 7799.9961  milliseconds
4190.87 ( at 7999.9961  milliseconds
4106.28 ( at 8199.9961  milliseconds
4021.91 ( at 8399.9961  milliseconds
3930.85 ( at 8599.9961  milliseconds
3838.66 ( at 8799.9961  milliseconds
```

```
 3746.56 ( at 8999.9961  milliseconds
 3746.56 (repeat last velocity for stretch
 3746.56 (9400 milliseconds
 3746.56 (9600 milliseconds
 3746.56 (9800 milliseconds
/stkout   use mig
          client 'expl'
          area 'nfgb'
          firstrow 1051 lastrow 1225
          firstcol 1 lastcol 3750 (including padding
/eoj
```

11.6 A job setup for Migration Step-II

```
/job        acct '0489 3000 nfgb mig'
            (runcode 0
            (system   vpx220
            (priority 8
            (region 110Mb
            (division G
/jobtick    submitby 'nicholas'
            runtime   6.00
            inreel   'disk'
            outreel  'no/op'
            process  'mig'
            userinst '******nfgb*****'
            userinst 'migration step 2        '
            userinst '!!! check memory before'
            userinst 'starting job!!          '
            userinst '******nfgb*****'
            dsn      'N/A'
/trdfile    use mig
            ctrlname '/SDP248/grp11/p489/mig.cntl'
            jobrows 1 1532 (reading in 1532 inlines
            jobcols 2851 3000 (150 cols, last job includes padded zone
/syndata    sr 6 msi 9700 ntr 1 nrecs 1 datatype shot type 5
/mgtda      qc
            unit     '3380  '
            volser   'SDP388'
            resfile  '/SDP388/grp11/p489/mgtdap2_3000.log'
            wrkfile  '/SDP388/grp11/p489/mgtdap2_3000.wrk'
            hdrfile  '/SDP388/grp11/p489/mgtdap2_3000.hdr'
            atap      20 (default is 30
            vmax      5200  (0 for steps 1 and 3 otherwise 5200.0
            use mig
            flagtd
            bycols          (byrows or bycols
            firstrow  1     (first row forjob
            lastrow   1532  (last row forjob
            firstcol  2851  (first col for job
            lastcol   3000  (last job includes padding
            delrow    25.0
            delcol    12.5
            anone     0.5
            antwo     1.5
            anthree   65
            anfour    75
            angm      60 3.0 60 6.0 40 9.0 10
            (bmem      0.4
            padt      2.0
            interval
            fracv     3.0
            dtrms     200
            ivpt      2      (step number 1 2 or 3
            nrows     1532   (total rows
            ncols     3200   (total, excluding padding
            ncolsb    3750   (total, including padding
            knsmpa    1501   (based on 9000ms same for all 3 steps
            knsmpb    1617   (based on 9700ms same for all 3 steps
```

```
          minrow    1
          mincol    1
          oppam     0 4 4 4
          opcoef
2.6885530025518318e-12
-1.5643384297873967e-10
2.1290515836198131e-09
9.8991836409524095e-10
-3.1765299123544911e-10
1.7937876643132595e-08
-2.5513263531331779e-07
5.8315702273087551e-07
6.5697373079858209e-09
-3.7729275820553167e-07
5.7157588556168815e-06
-2.9293642775904404e-05
-1.9393565181001961e-08
1.5356500315522706e-06
-3.0044565226616910e-05
2.0466111784319987e-04
-4.6059397877277321e-11
2.2498468580708324e-09
-2.0560394654967973e-08
-1.1887344421262180e-07
5.0196558319867309e-09
-2.6580428720523643e-07
3.2847062992355365e-06
-7.8541951852597136e-07
-1.0053347633009887e-07
5.6454287584597702e-06
-8.0992933789517047e-05
3.4944739663473836e-04
2.3097712487347025e-07
-2.1946018446472336e-05
4.3855936018693099e-04
-1.5231606720904691e-03
1.9308953322115055e-10
-6.0785162295568208e-09
-3.9673038335757044e-08
1.5050571147391096e-06
-1.9009562222806280e-08
8.3932435472912061e-07
-5.7555177273305824e-06
-8.2047805427580000e-05
3.3276832198055027e-07
-1.7517174728528716e-05
2.2245527911552334e-04
-4.8666418329775061e-04
8.7828068061426891e-09
4.8522394112172528e-05
-1.2590824440579876e-03
5.6091735027792361e-04
2.9426077435090765e-11
-7.1375725480455047e-09
2.4061149572508669e-07
-8.3096238541784616e-07
2.0173669271152617e-09
1.2334199172536735e-07
-8.4742999246973462e-06
1.0141919557191004e-04
```

```
-7.0234471937942906e-10
-9.0518773823712036e-07
1.2399309386829978e-05
-4.6301647641408615e-04
-1.0515828579203047e-06
3.3027604263354205e-05
1.4688985990807825e-04
1.8936469985501221e-02
(pilot interval velocities follow
vpilot (reduced pilot velocity function
1561.48 ( at 0.00000000e+00  milliseconds
1591.35 ( at 199.99992  milliseconds
1701.56 ( at 399.99976  milliseconds
1849.88 ( at 599.99976  milliseconds
1992.02 ( at 799.99976  milliseconds
2135.19 ( at 999.99976  milliseconds
2314.41 ( at 1199.9998  milliseconds
2520.41 ( at 1399.9995  milliseconds
2755.25 ( at 1599.9993  milliseconds
3005.54 ( at 1799.9990  milliseconds
3257.89 ( at 1999.9990  milliseconds
3504.06 ( at 2199.9998  milliseconds
3735.81 ( at 2399.9995  milliseconds
3953.14 ( at 2599.9993  milliseconds
4163.26 ( at 2799.9990  milliseconds
4332.18 ( at 2999.9990  milliseconds
4475.35 ( at 3199.9988  milliseconds
4617.49 ( at 3399.9995  milliseconds
4724.61 ( at 3599.9993  milliseconds
4818.34 ( at 3799.9990  milliseconds
4916.19 ( at 3999.9990  milliseconds
4727.63 ( at 4199.9961  milliseconds
4775.36 ( at 4399.9961  milliseconds
4828.32 ( at 4599.9961  milliseconds
4890.72 ( at 4799.9961  milliseconds
4930.20 ( at 4999.9961  milliseconds
4994.20 ( at 5199.9961  milliseconds
5043.84 ( at 5399.9961  milliseconds
5064.38 ( at 5599.9961  milliseconds
5100.93 ( at 5799.9961  milliseconds
5110.71 ( at 5999.9961  milliseconds
4915.52 ( at 6199.9961  milliseconds
4882.66 ( at 6399.9961  milliseconds
4838.82 ( at 6599.9961  milliseconds
4757.56 ( at 6799.9961  milliseconds
4663.44 ( at 6999.9961  milliseconds
4574.28 ( at 7199.9961  milliseconds
4454.18 ( at 7399.9961  milliseconds
4353.84 ( at 7599.9961  milliseconds
4260.69 ( at 7799.9961  milliseconds
4190.87 ( at 7999.9961  milliseconds
4106.28 ( at 8199.9961  milliseconds
4021.91 ( at 8399.9961  milliseconds
3930.85 ( at 8599.9961  milliseconds
3838.66 ( at 8799.9961  milliseconds
3746.56 ( at 8999.9961  milliseconds
3746.56 (repeat last velocity for stretch
3746.56 (9400 milliseconds
3746.56 (9600 milliseconds
/eoj
```

11.7 A job setup for Migration Step-III

```
/job        acct '0489 1225 nfgb mig'
            (runcode 0
            (system   vpx220
            (priority 8
            (region 110Mb
            (division E
/jobtick    submitby 'nicholas'
            runtime   6.00
            inreel    'disk'
            outreel   'no/op'
            process   'mig'
            userinst  '******nfgb*****'
            userinst  'migration step 3       '
            userinst  '!!! check memory before'
            userinst  'starting job!!         '
            userinst  '******nfgb*****'
            dsn       'N/A'
/trdfile    use mig
            ctrlname '/SDP248/grp11/p489/mig.cntl'
            jobrows 1051 1225 (reading in 175 inlines
            jobcols 1 3750 (full range including padded zone
/stkin      data 4 9700 6 1 0 (with stretch
            use mig
            rows 1051 1225 1 (reading in 175 inlines
            cols 1 3750 1 (full range including padded zone
/renumber   firstcdp 1
/mgtda      qc
            unit      '3380  '
            volser    'SDP388'
            resfile   '/SDP388/grp11/p489/mgtdap3_1225.log'
            wrkfile   '/SDP388/grp11/p489/mgtdap3_1225.wrk'
            hdrfile   '/SDP388/grp11/p489/mgtdap3_1225.hdr'
            atap       20 (default is 30
            vmax       0  (0 for steps 1 and 3 otherwise 5000.0
            use mig
            flagtd
            byrows              (byrows or bycols
            firstrow  1051      (first row forjob
            lastrow   1225      (last row forjob
            firstcol  1
            lastcol   3750      (including padding
            delrow    25.0
            delcol    12.5
            anone     0.5
            antwo     1.5
            anthree   65
            (anfour    75 2.0 70 4.0 50 6.0 40 9.0 30
            anfour    75
            angm      60 3.0 60 6.0 40 9.0 10
            (bmem      0.4
            padt      2.0
            interval
            fracv     3.0
            dtrms     200
            ivpt      3        (step number 1 2 or 3
```

```
            nrows      1532    (total rows
            ncols      3200    (total, excluding padding
            ncolsb     3750    (total, including padding
            knsmpa     1501    (based on 9000ms same for all 3 steps
            knsmpb     1617    (based on 9700ms same for all 3 steps
            minrow     1
            mincol     1
            oppam      0 4 4 4
            opcoef
2.6885530025518318e-12
-1.5643384297873967e-10
2.1290515836198131e-09
9.8991836409524095e-10
-3.1765299123544911e-10
1.7937876643132595e-08
-2.5513263531331779e-07
5.8315702273087551e-07
6.5697373079858209e-09
-3.7729275820553167e-07
5.7157588556168815e-06
-2.9293642775904404e-05
-1.9393565181001961e-08
1.5356500315522706e-06
-3.0044565226616910e-05
2.0466111784319987e-04
-4.6059397877277321e-11
2.2498468580708324e-09
-2.0560394654967973e-08
-1.1887344421262180e-07
5.0196558319867309e-09
-2.6580428720523643e-07
3.2847062992355365e-06
-7.8541951852597136e-07
-1.0053347633009887e-07
5.6454287584597702e-06
-8.0992933789517047e-05
3.4944739663473836e-04
2.3097712487347025e-07
-2.1946018446472336e-05
4.3855936018693099e-04
-1.5231606720904691e-03
1.9308953322115055e-10
-6.0785162295568208e-09
-3.9673038335757044e-08
1.5050571147391096e-06
-1.9009562222806280e-08
8.3932435472912061e-07
-5.7555177273305824e-06
-8.2047805427580000e-05
3.3276832198055027e-07
-1.7517174728528716e-05
2.2245527911552334e-04
-4.8666418329775061e-04
8.7828068061426891e-09
4.8522394112172528e-05
-1.2590824440579876e-03
5.6091735027792361e-04
2.9426077435090765e-11
-7.1375725480455047e-09
2.4061149572508669e-07
```

```
-8.3096238541784616e-07
2.0173669271152617e-09
1.2334199172536735e-07
-8.4742999246973462e-06
1.0141919557191004e-04
-7.0234471937942906e-10
-9.0518773823712036e-07
1.2399309386829978e-05
-4.6301647641408615e-04
-1.0515828579203047e-06
3.3027604263354205e-05
1.4688985990807825e-04
1.8936469985501221e-02
(pilot interval velocities follow
vpilot (reduced pilot velocity function
1561.48 ( at 0.00000000e+00  milliseconds
1591.35 ( at 199.99992  milliseconds
1701.56 ( at 399.99976  milliseconds
1849.88 ( at 599.99976  milliseconds
1992.02 ( at 799.99976  milliseconds
2135.19 ( at 999.99976  milliseconds
2314.41 ( at 1199.9998  milliseconds
2520.41 ( at 1399.9995  milliseconds
2755.25 ( at 1599.9993  milliseconds
3005.54 ( at 1799.9990  milliseconds
3257.89 ( at 1999.9990  milliseconds
3504.06 ( at 2199.9998  milliseconds
3735.81 ( at 2399.9995  milliseconds
3953.14 ( at 2599.9993  milliseconds
4163.26 ( at 2799.9990  milliseconds
4332.18 ( at 2999.9990  milliseconds
4475.35 ( at 3199.9988  milliseconds
4617.49 ( at 3399.9995  milliseconds
4724.61 ( at 3599.9993  milliseconds
4818.34 ( at 3799.9990  milliseconds
4916.19 ( at 3999.9990  milliseconds
4727.63 ( at 4199.9961  milliseconds
4775.36 ( at 4399.9961  milliseconds
4828.32 ( at 4599.9961  milliseconds
4890.72 ( at 4799.9961  milliseconds
4930.20 ( at 4999.9961  milliseconds
4994.20 ( at 5199.9961  milliseconds
5043.84 ( at 5399.9961  milliseconds
5064.38 ( at 5599.9961  milliseconds
5100.93 ( at 5799.9961  milliseconds
5110.71 ( at 5999.9961  milliseconds
4915.52 ( at 6199.9961  milliseconds
4882.66 ( at 6399.9961  milliseconds
4838.82 ( at 6599.9961  milliseconds
4757.56 ( at 6799.9961  milliseconds
4663.44 ( at 6999.9961  milliseconds
4574.28 ( at 7199.9961  milliseconds
4454.18 ( at 7399.9961  milliseconds
4353.84 ( at 7599.9961  milliseconds
4260.69 ( at 7799.9961  milliseconds
4190.87 ( at 7999.9961  milliseconds
4106.28 ( at 8199.9961  milliseconds
4021.91 ( at 8399.9961  milliseconds
3930.85 ( at 8599.9961  milliseconds
3838.66 ( at 8799.9961  milliseconds
```

```
 3746.56 ( at 8999.9961  milliseconds
 3746.56 (repeat last velocity for stretch
 3746.56 (9400 milliseconds
 3746.56 (9600 milliseconds
 3746.56 (9800 milliseconds
/renumber firstcdp 1
/glcom    grrows 1051 1225
/expgain  begtime 1 5000 999999 5000
          endtime 1 9000 999999 9000
          expfunc +2.0
/stkout   use mig
          client 'expl'
          area 'nfgb'
          firstrow 1051 lastrow 1225
          firstcol 1 lastcol 3200 (excluding padding
/eoj
```

12. Figures

Figure 1 : GRAND BANKS production designature operator

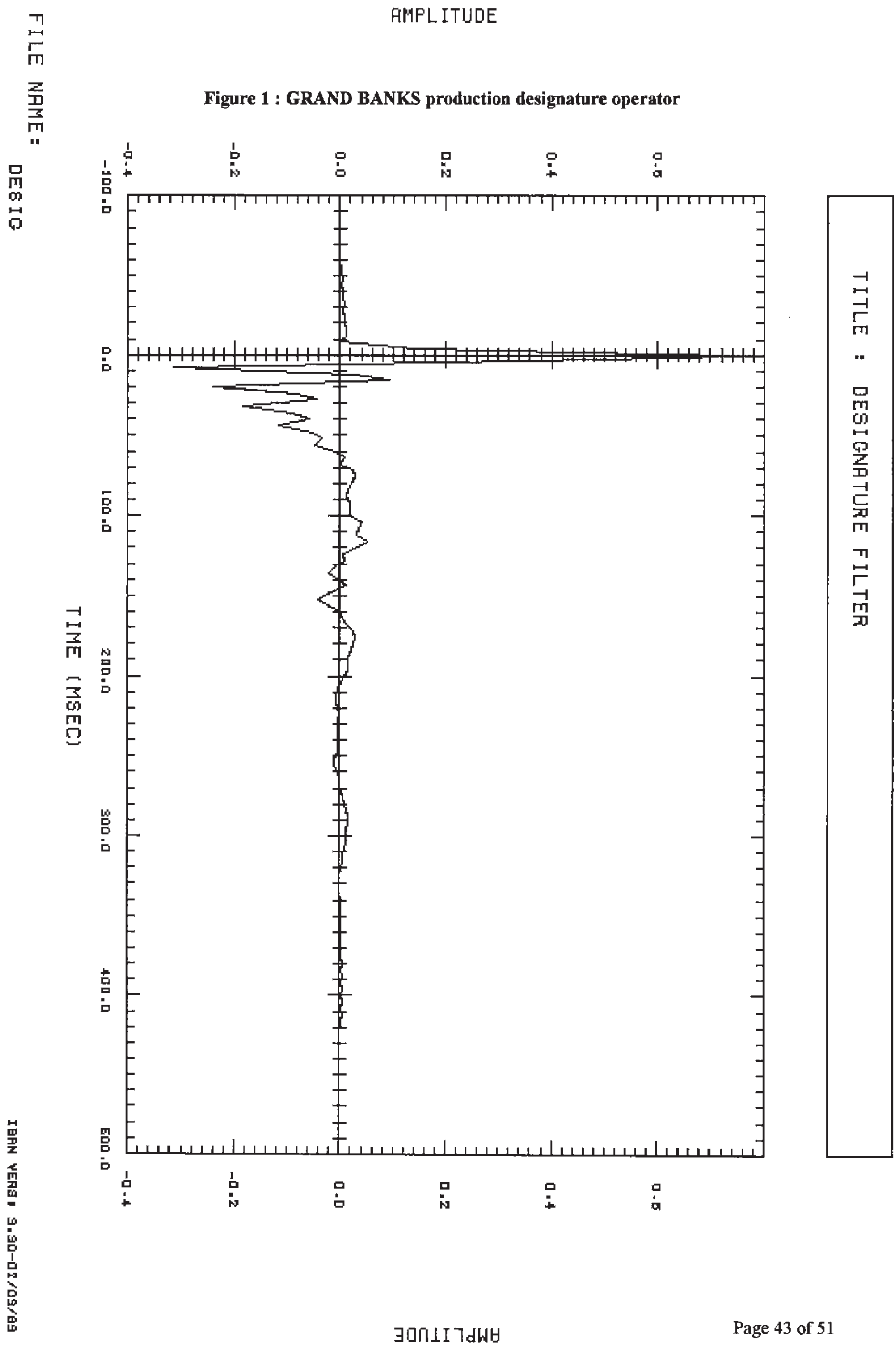

Figure 2 : GRAND BANKS conditioned gun signature

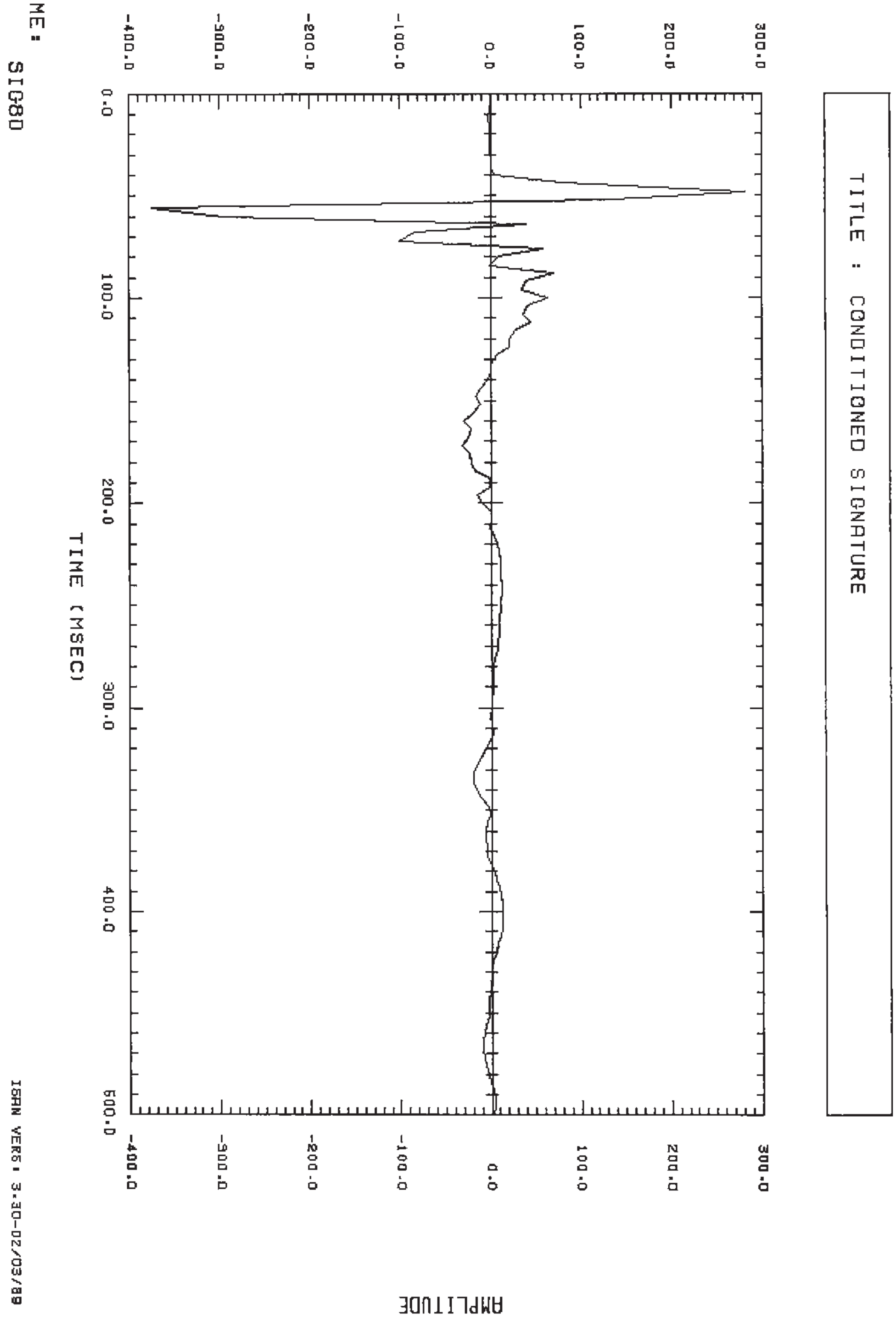

Figure 3 : K-Filter Stack Timeslice 2.0 sec

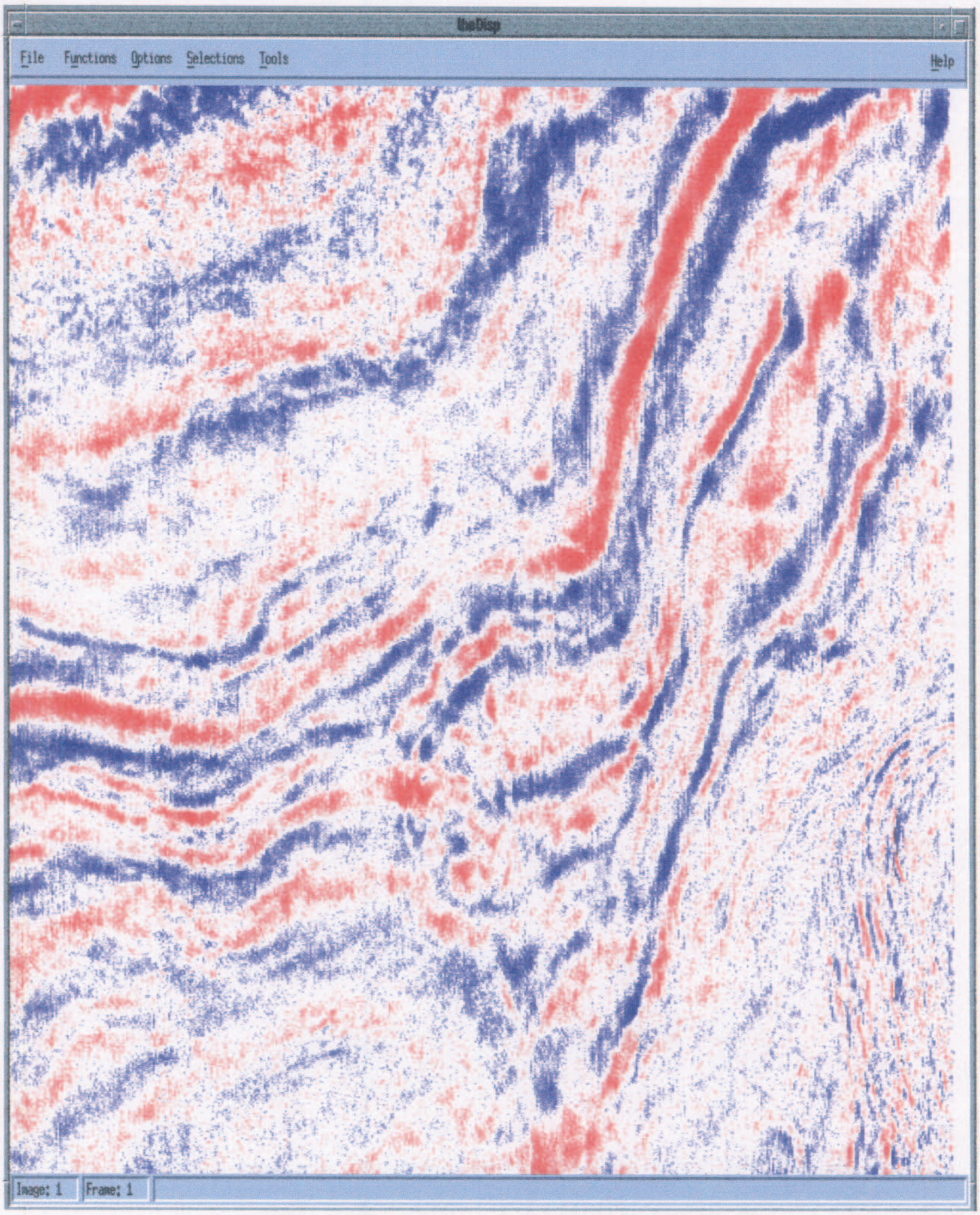

Figure 4 : 3D FXYFILT Stack Timeslice 2.0 sec

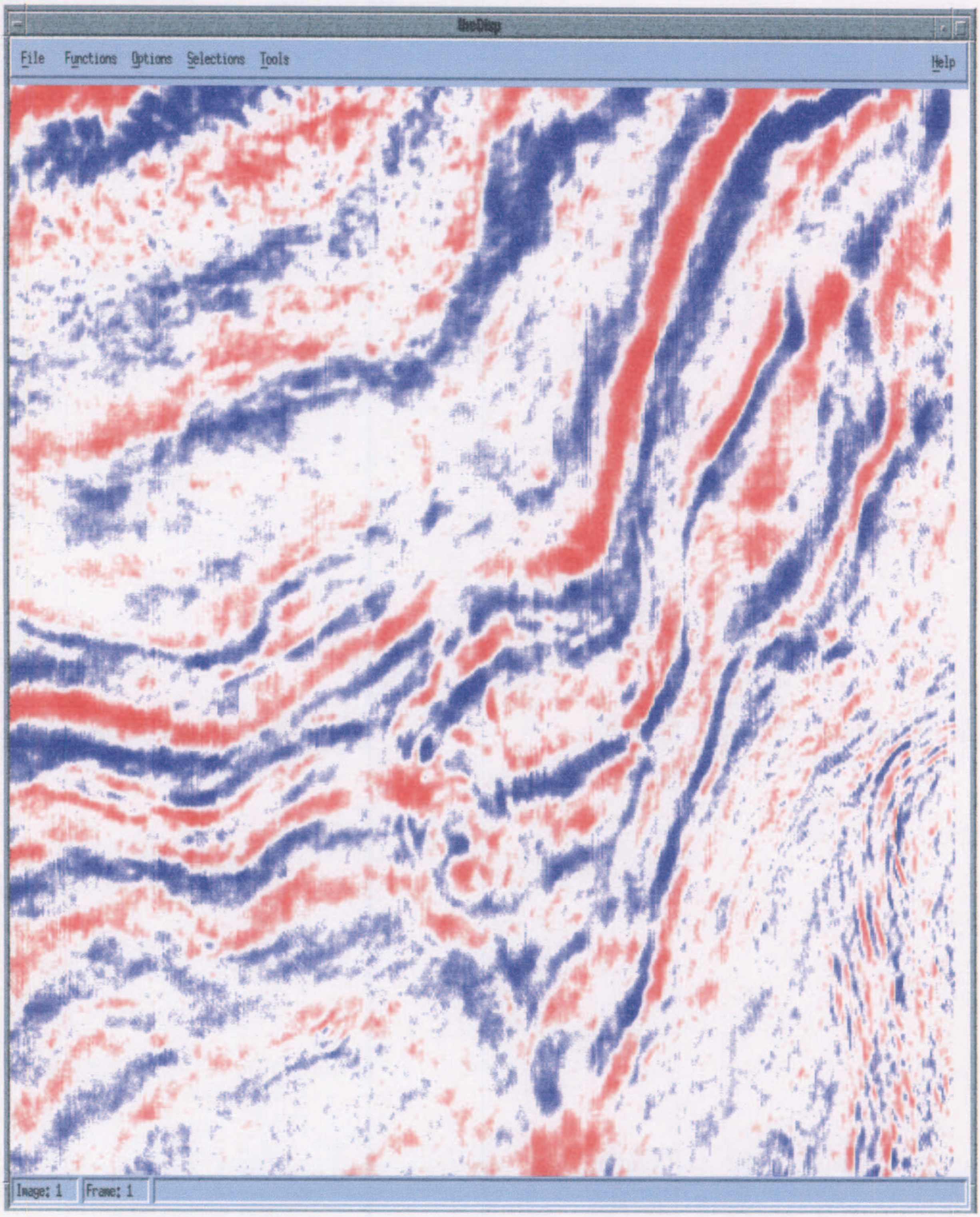

Figure 5 : Quick Look Cube Migration Timeslice 2.0 sec

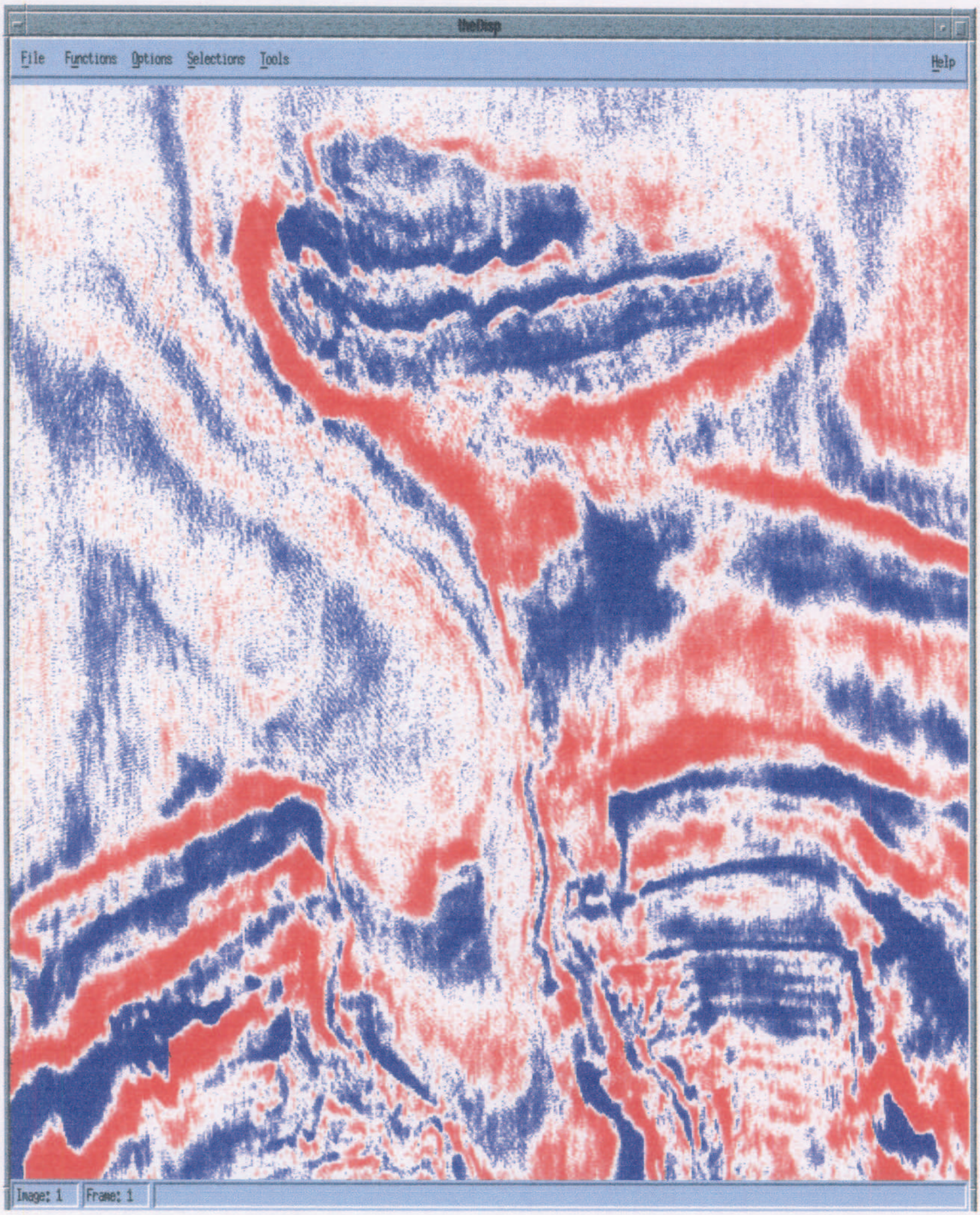

Figure 6 : Final Migration Timeslice 2.0 sec

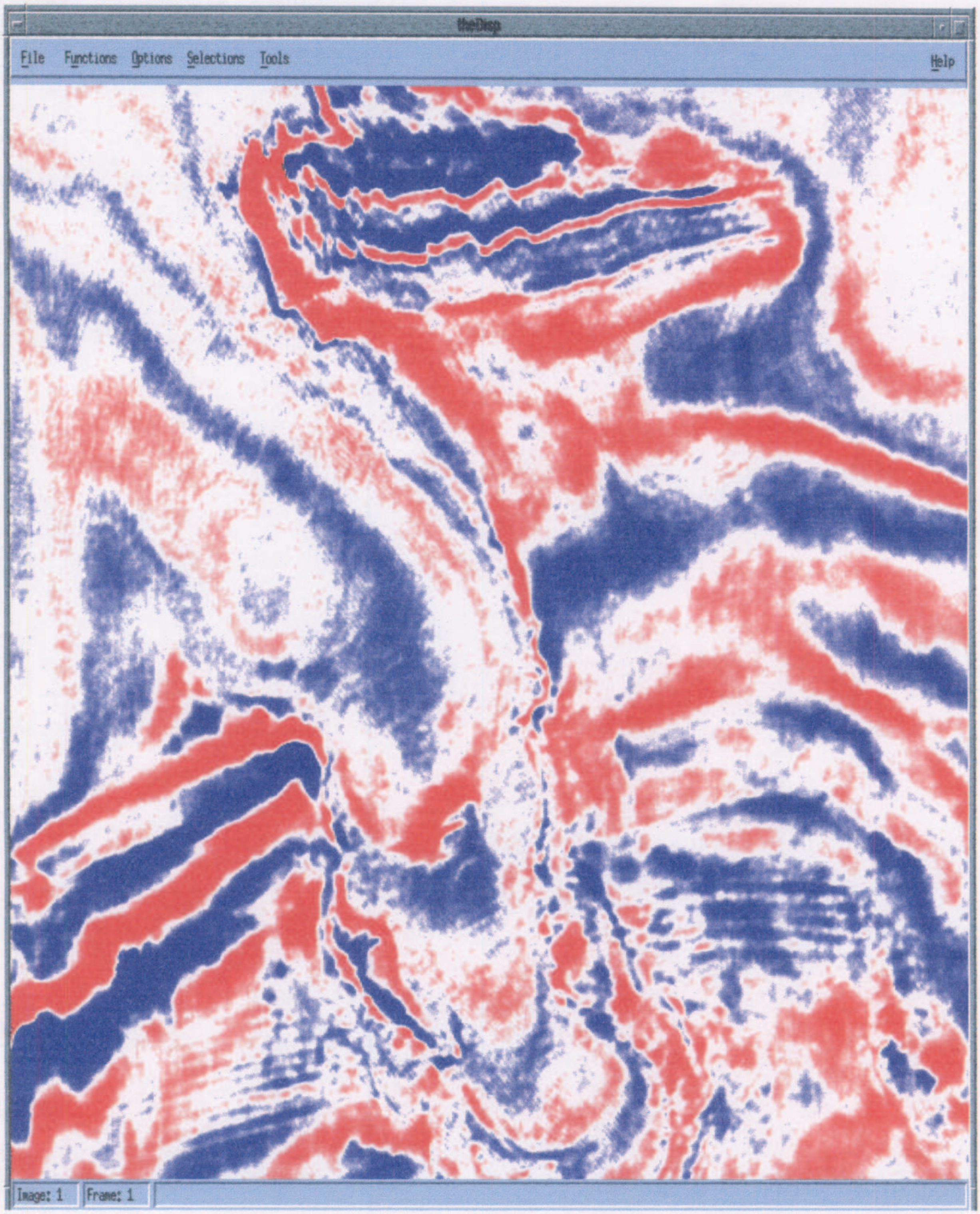

13. Appendix

13.1 Average Amplitude Report

after	10 traces.	mn/av/mx	-2.9757	0.24983	5.1008	samp	1: 1501
after	20 traces.	mn/av/mx	-2.9757	0.26086	5.6896	samp	1: 1501
after	30 traces.	mn/av/mx	-3.5370	0.27447	5.8874	samp	1: 1501
after	40 traces.	mn/av/mx	-3.8205	0.28321	5.8874	samp	1: 1501
after	50 traces.	mn/av/mx	-3.8205	0.28813	5.8874	samp	1: 1501
		cdp	51				
after	60 traces.	mn/av/mx	-3.8205	0.29130	5.8874	samp	1: 1501
after	70 traces.	mn/av/mx	-3.8205	0.29214	5.8874	samp	1: 1501
after	80 traces.	mn/av/mx	-3.8205	0.29232	5.8874	samp	1: 1501
after	90 traces.	mn/av/mx	-3.8205	0.29432	5.8874	samp	1: 1501
after	100 traces.	mn/av/mx	-3.8205	0.29570	5.8874	samp	1: 1501
		cdp	101				
after	110 traces.	mn/av/mx	-3.8205	0.29648	5.8874	samp	1: 1501
after	120 traces.	mn/av/mx	-3.8205	0.30070	5.8874	samp	1: 1501
after	130 traces.	mn/av/mx	-3.8205	0.30416	5.8874	samp	1: 1501
after	140 traces.	mn/av/mx	-3.8205	0.30628	5.8874	samp	1: 1501
after	150 traces.	mn/av/mx	-3.8205	0.30971	5.8874	samp	1: 1501
		cdp	151				
after	160 traces.	mn/av/mx	-3.8205	0.31184	5.8874	samp	1: 1501
after	170 traces.	mn/av/mx	-3.8205	0.31369	5.8874	samp	1: 1501
after	180 traces.	mn/av/mx	-3.8205	0.31572	6.5053	samp	1: 1501
after	190 traces.	mn/av/mx	-3.8205	0.31695	6.5053	samp	1: 1501
after	200 traces.	mn/av/mx	-3.8205	0.31682	6.5053	samp	1: 1501
		cdp	201				
after	210 traces.	mn/av/mx	-3.8205	0.31812	6.5053	samp	1: 1501
after	220 traces.	mn/av/mx	-3.8205	0.31883	6.5053	samp	1: 1501
after	230 traces.	mn/av/mx	-3.8205	0.31920	6.5053	samp	1: 1501
after	240 traces.	mn/av/mx	-3.8205	0.32017	6.5053	samp	1: 1501
after	250 traces.	mn/av/mx	-4.2455	0.32153	6.5053	samp	1: 1501
		cdp	251				
after	260 traces.	mn/av/mx	-4.4773	0.32264	6.5053	samp	1: 1501
after	270 traces.	mn/av/mx	-4.4773	0.32424	6.5053	samp	1: 1501
after	280 traces.	mn/av/mx	-4.4773	0.32576	6.5053	samp	1: 1501
after	290 traces.	mn/av/mx	-4.4773	0.32604	6.5053	samp	1: 1501
after	300 traces.	mn/av/mx	-4.4773	0.32712	6.5053	samp	1: 1501
		cdp	301				
after	310 traces.	mn/av/mx	-4.4773	0.32850	6.5053	samp	1: 1501
after	320 traces.	mn/av/mx	-4.4773	0.32981	6.5053	samp	1: 1501
after	330 traces.	mn/av/mx	-4.4773	0.33099	6.5053	samp	1: 1501
after	340 traces.	mn/av/mx	-4.4773	0.33178	6.5053	samp	1: 1501
after	350 traces.	mn/av/mx	-4.4773	0.33398	6.5053	samp	1: 1501
		cdp	351				
after	360 traces.	mn/av/mx	-4.5997	0.33540	6.5053	samp	1: 1501
after	370 traces.	mn/av/mx	-4.5997	0.33567	6.5053	samp	1: 1501
after	380 traces.	mn/av/mx	-5.7632	0.33632	6.5053	samp	1: 1501
after	390 traces.	mn/av/mx	-5.7707	0.33718	6.5053	samp	1: 1501
after	400 traces.	mn/av/mx	-5.7707	0.33747	6.5053	samp	1: 1501
		cdp	401				

```
after 410 traces. mn/av/mx -5.7707  0.33797  6.5053 samp 1: 1501
after 420 traces. mn/av/mx -5.7707  0.33795  6.5053 samp 1: 1501
after 430 traces. mn/av/mx -5.7707  0.33767  6.5053 samp 1: 1501
after 440 traces. mn/av/mx -5.7707  0.33741  6.5053 samp 1: 1501
after 450 traces. mn/av/mx -5.7707  0.33730  6.5053 samp 1: 1501
                      cdp 451
after 460 traces. mn/av/mx -5.7707  0.33782  6.5053 samp 1: 1501
after 470 traces. mn/av/mx -5.7707  0.33875  6.5053 samp 1: 1501
after 480 traces. mn/av/mx -5.7707  0.33930  6.5053 samp 1: 1501
after 490 traces. mn/av/mx -5.7707  0.33936  6.5053 samp 1: 1501
after 500 traces. mn/av/mx -5.7707  0.33927  6.5053 samp 1: 1501
                      cdp 501
after 510 traces. mn/av/mx -5.7707  0.33911  6.5053 samp 1: 1501
after 520 traces. mn/av/mx -5.7707  0.33853  6.5053 samp 1: 1501
after 530 traces. mn/av/mx -5.7707  0.33766  6.5053 samp 1: 1501
after 540 traces. mn/av/mx -5.7707  0.33762  6.5053 samp 1: 1501
after 550 traces. mn/av/mx -5.7707  0.33778  6.5053 samp 1: 1501
                      cdp 551
after 560 traces. mn/av/mx -5.7707  0.33742  6.5053 samp 1: 1501
after 570 traces. mn/av/mx -5.7707  0.33710  6.5053 samp 1: 1501
after 580 traces. mn/av/mx -5.7707  0.33672  6.5053 samp 1: 1501
after 590 traces. mn/av/mx -5.7707  0.33622  6.5053 samp 1: 1501
after 600 traces. mn/av/mx -5.7707  0.33583  6.5053 samp 1: 1501
                      cdp 601
after 610 traces. mn/av/mx -5.7707  0.33600  6.5053 samp 1: 1501
after 620 traces. mn/av/mx -5.7707  0.33583  6.5053 samp 1: 1501
after 630 traces. mn/av/mx -5.7707  0.33555  6.5053 samp 1: 1501
after 640 traces. mn/av/mx -5.7707  0.33525  6.5053 samp 1: 1501
after 650 traces. mn/av/mx -5.7707  0.33538  6.5053 samp 1: 1501
                      cdp 651
after 660 traces. mn/av/mx -5.7707  0.33537  6.5053 samp 1: 1501
after 670 traces. mn/av/mx -5.7707  0.33523  6.5053 samp 1: 1501
after 680 traces. mn/av/mx -5.7707  0.33487  6.5053 samp 1: 1501
after 690 traces. mn/av/mx -5.7707  0.33463  6.5053 samp 1: 1501
after 700 traces. mn/av/mx -5.7707  0.33426  6.5053 samp 1: 1501
                      cdp 701
after 710 traces. mn/av/mx -5.7707  0.33394  6.5053 samp 1: 1501
after 720 traces. mn/av/mx -5.7707  0.33353  6.5053 samp 1: 1501
after 730 traces. mn/av/mx -5.7707  0.33315  6.5053 samp 1: 1501
after 740 traces. mn/av/mx -5.7707  0.33284  6.5053 samp 1: 1501
after 750 traces. mn/av/mx -5.7707  0.33280  6.5053 samp 1: 1501
                      cdp 751
after 760 traces. mn/av/mx -5.7707  0.33277  6.5053 samp 1: 1501
after 770 traces. mn/av/mx -5.7707  0.33304  6.5053 samp 1: 1501
after 780 traces. mn/av/mx -5.7707  0.33307  6.5053 samp 1: 1501
after 790 traces. mn/av/mx -5.7707  0.33335  6.5053 samp 1: 1501
after 800 traces. mn/av/mx -5.7707  0.33374  6.5053 samp 1: 1501
                      cdp 801
after 810 traces. mn/av/mx -5.7707  0.33397  6.5053 samp 1: 1501
after 820 traces. mn/av/mx -5.7707  0.33403  6.5053 samp 1: 1501
after 830 traces. mn/av/mx -5.7707  0.33422  6.5053 samp 1: 1501
after 840 traces. mn/av/mx -5.7707  0.33427  6.5053 samp 1: 1501
after 850 traces. mn/av/mx -5.7707  0.33418  6.5053 samp 1: 1501
                      cdp 851
```

after 860 traces. mn/av/mx -5.7707	0.33428	6.5053	samp	1: 1501
after 870 traces. mn/av/mx -5.7707	0.33446	6.5053	samp	1: 1501
after 880 traces. mn/av/mx -5.7707	0.33474	6.5053	samp	1: 1501
after 890 traces. mn/av/mx -5.7707	0.33478	6.5053	samp	1: 1501
after 900 traces. mn/av/mx -5.7707	0.33467	6.5053	samp	1: 1501
cdp 901				
after 910 traces. mn/av/mx -5.7707	0.33460	6.5053	samp	1: 1501
after 920 traces. mn/av/mx -5.7707	0.33458	6.5053	samp	1: 1501
after 930 traces. mn/av/mx -5.7707	0.33454	6.5053	samp	1: 1501
after 940 traces. mn/av/mx -5.7707	0.33467	6.5053	samp	1: 1501
after 950 traces. mn/av/mx -5.7707	0.33474	6.5053	samp	1: 1501
cdp 951				
after 960 traces. mn/av/mx -5.7707	0.33498	6.5053	samp	1: 1501
after 970 traces. mn/av/mx -5.7707	0.33529	6.5053	samp	1: 1501
after 980 traces. mn/av/mx -5.7707	0.33540	6.5053	samp	1: 1501
after 990 traces. mn/av/mx -5.7707	0.33574	6.5053	samp	1: 1501
after 1000 traces. mn/av/mx -5.7707	0.33608	6.5053	samp	1: 1501

after a total of 1000 traces with live data between samples 1 and 1501 **avg = 0.3360797**

Appendix 3: Line HBV83-195

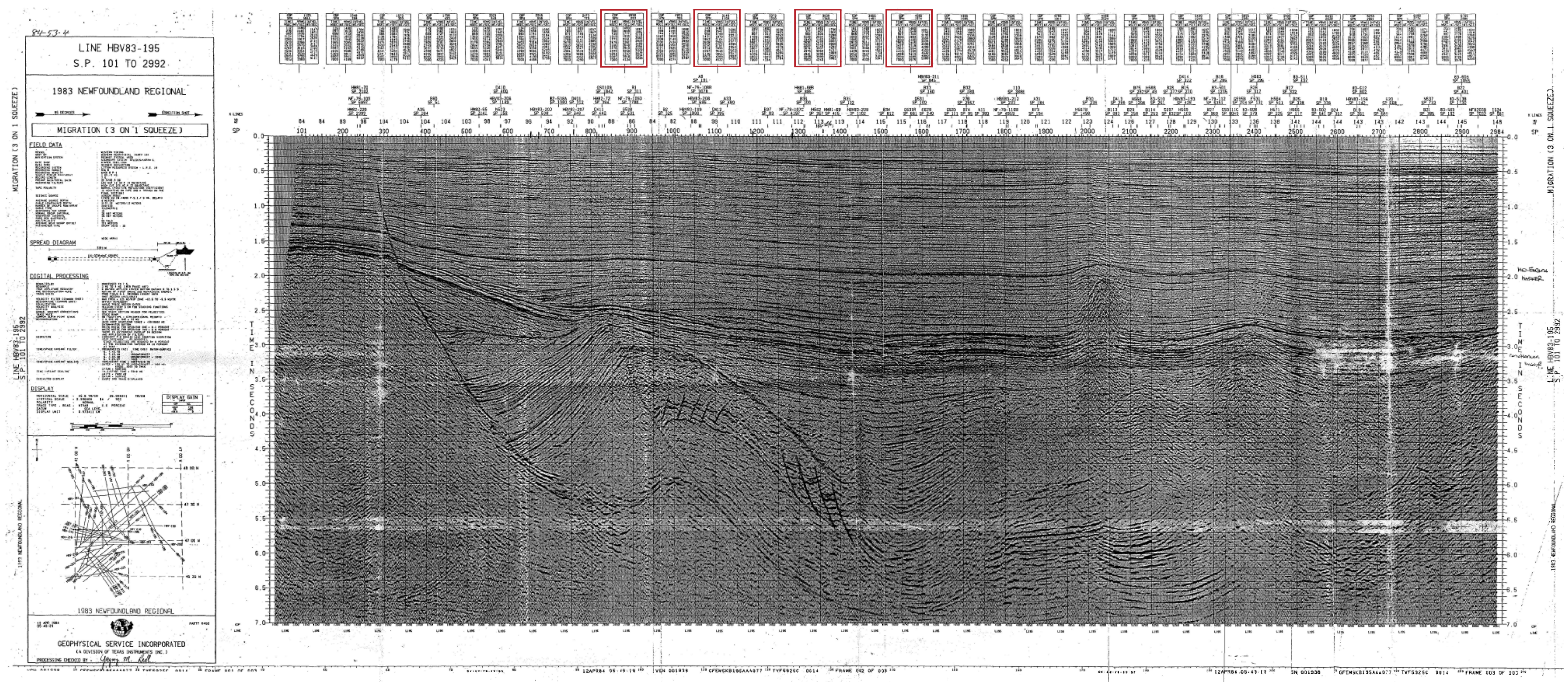

Figure A3-1: 2D seismic line HBV83-195. Red rectangles highlight selected velocity surveys shown in Appendix 4. Vertical exaggeration 3:1

APPENDIX 4

Root mean square velocities (V_{RMS}) from some velocity surveys from line HBV83-195 used to calculate the average velocity of the sedimentary section.

Velocity survey	Time (ms)	V_{RMS} (m/s)
CDP 2698	6005	3910
CDP 3148	6012	4289
CDP 3630	5998	3899
CDP 4080	5999	3689
	Average	3946 (~4.0 km/s)

CDP: 2698		
Time (ms)	V_{RMS} (m/s)	Vint (m/s)
117	1480	1687
300	1609	1885
735	1777	2118
1319	1935	2682
1773	2151	2823
2476	2361	3489
3166	2648	4004
3776	2910	5320
4222	3250	5236
5204	3707	5034
6005	3910	5233
7000	4124	

CDP: 3148		
Time (ms)	V_{RMS} (m/s)	Vint (m/s)
143	1480	1606
299	1547	1859
802	1749	2221
1431	1970	2516
1842	2104	2977
2606	2393	3895
3252	2757	4854
3714	3096	5623
4297	3546	5217
5126	3955	5859
6012	4289	5796
7000	4532	

CDP: 3630		
Time (ms)	V_{RMS} (m/s)	Vint (m/s)
167	1480	1730
327	1607	1916
862	1805	2298
1526	2034	2580
1940	2162	3032
2836	2470	3948
3328	2739	4293
3874	3007	4737
4375	3252	4959
4941	3490	5416
5998	3899	5882
7000	4240	

CDP: 4080		
Time (ms)	V_{RMS} (m/s)	Vint (m/s)
157	1480	1601
351	1548	1796
907	1704	2132
1550	1893	2694
2000	2100	3039
2963	2445	4030
3437	2719	4299
3907	2954	4593
4439	3195	4632
5088	3412	4960
5999	3689	5380
7000	3975	

APPENDIX 5

List of formation tops from available wells. Depths are in meters and measured depths. From the BASIN database website (http://basin.gdr.nrcan.gc.ca/wells/index_e.php) (2012)

Well Flying Foam I-13

Year	Author	Depth Type	Top	Bottom	Units	Formation
2007	CNLOPB	MD		2115.5	M	BANQUEREAU FM
2007			744	768	M	(OLIGOCENE SANDSTONE - UPPER)
2007			940.5	948	M	(OLIGOCENE SANDSTONE - LOWER)
2007			2115.5	2115.5	M	(BASE TERTIARY UNCONFORMITY)
2007			2115.5	2487	M	WHITEROSE FM
2007			2115.5	2467	M	CATALINA
2007			2467	2487	M	"B" MARKER MB
2007			2487	3114	M	HIBERNIA FM
2007			2487	2847	M	SHALE EQUIV OF HIBERNIA UPPER ZONE
2007			2847	3114	M	HIBERNIA LOWER ZONE
2007			3114	3268	M	FORTUNE BAY FM
2007			3268	3268	M	(TITHONIAN UNCONFORMITY)
2007			3268	3683.2	M	RANKIN FM
2007			3281	3353	M	EGRET MB
2007			3592.5	3683.2	M	PORT AU PORT MB
1989	MCALPINE,K.D.			2116	M	BANQUEREAU FM
1989			2116	2116	M	(UNCONFORMITY)
1989			2116	2467	M	CATALINA FM
1989			2467	2487	M	("B" MARKER)
1989			2487	2847	M	WHITEROSE SHALE (LOWER)
1989			2847	3114	M	HIBERNIA FM
1989			3114	3194	M	FORTUNE BAY SHALE
1989			3194	3269	M	JEANNE D'ARC FM
1989			3269	3269	M	(UNCONFORMITY)
1989			3269	3683	M	RANKIN FM
1989			3281	3353	M	EGRET MB
1987	WADE,J.A. & SHERWIN,D.F.				FT	BANQUEREAU FM
1987			6941	6941		(AVALON UNCONFORMITY)
1987			6941	8170		MISSISAUGA EQUIV
1987			8170	10488		VERRILL CANYON FM ?
1987			10488	12084		ABENAKI/MIC MAC ?
1985	MCALPINE,K.D.					(SEE UPDATED REPORT)
1980	WADE,J.A.					(SEE MCALPINE REPORT)

Well West Flying Foam L-23

Year	Author	Depth Type	Top	Bottom	Units	Formation
2007	CNLOPB	MD		2496	M	BANQUEREAU FM
2007			755	780	M	(OLIGOCENE SANDSTONE - UPPER)
2007			962	968	M	(OLIGOCENE SANDSTONE - LOWER)
2007			2464	2496	M	SOUTH MARA MB
2007			2483	2490	M	(LIMESTONE)
2007			2496	2496	M	(BASE TERTIARY UNCONFORMITY)
2007			2496	3430	M	NAUTILUS FM
2007			3430	3471	M	BEN NEVIS FM
2007			3471	3471	M	(APTIAN UNCONFORMITY)
2007			3471	3580	M	AVALON FM
2007			3493	3564	M	(SHALE TONGUE)
2007			3564	3580	M	"A" MARKER MB
2007			3580	3760	M	WHITEROSE FM
2007			3760	4292	M	CATALINA FM
2007			4167	4292	M	"B" MARKER MB
2007			4292	4553.8	M	HIBERNIA FM
2007			4292	4553.8	M	SHALE EQUIV OF HIBERNIA UPPER ZONE
1989	MCALPINE,K.D.			2496	M	BANQUEREAU FM
1989			2407	2407	M	(UNCONFORMITY)
1989			2407	2496	M	SOUTH MARA UNIT
1989			2496	2496	M	(UNCONFORMITY)
1989			2496	2516	M	DAWSON CANYON FM
1989			2516	3090	M	NAUTILUS SHALE
1989			2570	2570	M	(UNCONFORMITY)
1989			3090	3090	M	
1989			3090	3189	M	AVALON FM
1989			3189	3189	M	(UNCONFORMITY)
1989			3189	3760	M	WHITEROSE SHALE
1989			3760	4554	M	CATALINA FM
1987	WADE,J.A. & SHERWIN,D.F.		2293		M	(UPPER CRETACEOUS "K" MARKER)
1987			2483		M	(PETREL LIMESTONE MARKER)
1987			2517	2517	M	(MIDDLE CRETACEOUS UNCONFORMITY)
1985	MCALPINE,K.D.					(SEE UPDATED REPORT)
1982	MOBIL OIL CANADA LTD		2292.8		M	("K" MARKER)
1982			2482.8		M	(PETREL LIMESTONE "P" MARKER)
1982			2516.8		M	(UNCONFORMITY)
1982			2746.8		M	

Mercury K-76

Year	Author	Depth Type	Top	Bottom	Units	Formation
2007	CNLOPB	MD		1594	M	BANQUEREAU FM
2007			618	636	M	(OLIGOCENE SANDSTONE - UPPER)
2007			772	796	M	(OLIGOCENE SANDSTONE - LOWER)
2007			1565	1594	M	TILTON MB
2007			1594	1594	M	(BASE TERTIARY UNCONFORMITY)
2007			1594	2362	M	DAWSON CANYON FM
2007			1594	1620	M	FOX HARBOUR MB
2007			1705	1906	M	OTTER BAY MB
2007			1836	1875	M	PETREL MB
2007			2362	2362	M	(CENOMANIAN UNCONFORMITY)
2007			2362	2668	M	NAUTILUS FM
2007			2668	5212.8	M	BEN NEVIS FM
2007			4077	5212.8	M	GAMBO MB
1989	MCALPINE,K.D.			1594	M	BANQUEREAU FM
1989			1565	1565	M	(UNCONFORMITY)
1989			1565	1594	M	SOUTH MARA UNIT
1989			1594	1594	M	(UNCONFORMITY)
1989			1594	1875	M	DAWSON CANYON FM
1989			1836	1874	M	PETREL MB
1989			1875	2362	M	EIDER FM
1989			2362	2362	M	(UNCONFORMITY)
1989			2362	2668	M	NAUTILUS SHALE
1989			2668	2668	M	(UNCONFORMITY)
1989			2668	3848	M	BEN NEVIS FM
1989			3848	3848	M	(UNCONFORMITY)
1989			3848	4270	M	AVALON FM
1989			4270	4270	M	(UNCONFORMITY)
1989			4270	5213	M	EASTERN SHOALS FM
1986	MOBIL OIL CANADA LTD		1594	1594	M	(BASE TERTIARY UNCONFORMITY)
1986			1836		M	PETREL LIMESTONE
1986			2362	2362	M	(MID-CRETACEOUS UNCONFORMITY)
1986			2668		M	AVALON SANDSTONE
1986			4041	4041	M	(APTIAN UNCONFORMITY)

Thorvald P-24

Year	Author	Depth Type	Top	Bottom	Units	Formation
2008	CNLOPB	MD		2050	M	BANQUEREAU FM
2008			659	683	M	(OLIGOCENE SANDSTONE - UPPER)
2008			834	855	M	(OLIGOCENE SANDSTONE - LOWER)
2008			1822	1893	M	SOUTH MARA MB - UPPER
2008			1916	1937	M	SOUTH MARA MB - MIDDLE
2008			1996	2031	M	SOUTH MARA MB - LOWER
2008			2031	2050	M	TILTON MB
2008			2050	2050	M	(BASE TERTIARY UNCONFORMITY)
2008			2050		M	DAWSON CANYON FM
2008			2363	2383	M	WYANDOT FM
2008			2526	2537	M	OTTER BAY MB
2008			2545	2607	M	PETREL MB
2008			2858	2858	M	(CENOMANIAN UNCONFORMITY)
2008			2858	2945	M	(UNNAMED SANDSTONE)
2008			3031	3076	M	NAUTILUS FM
2008			3076	3810	M	BEN NEVIS FM
2003	DEPTUCK,M.E.		659	855	M	THORVALD MB
1991	D'EON-MILLER & ASSOC LTD		570	2050	M	BANQUEREAU FM
1991			659	683	M	(UPPER OLIGOCENE SANDSTONE)
1991			834	855	M	(LOWER OLIGOCENE SANDSTONE)
1991			1386	1386	M	(MID-EOCENE MARKER)
1991			1822	2031	M	(PLUTO SEQUENCE)
1991			1852	1893	M	(UPPER SAND)
1991			1996	2031	M	(LOWER SAND)
1991			2031	2050	M	(DANIAN SILT)
1991			2050	2050	M	(BASE TERTIARY UNCONFORMITY)
1991			2050	3030	M	DAWSON CANYON FM
1991			2363	2383	M	WYANDOT MB
1991			2526	2537	M	OTTER BAY SAND MB
1991			2539	2606	M	PETREL MB
1991			3030	3030	M	(CENOMANIAN UNCONFORMITY)
1991			3030	3076	M	NAUTILUS FM
1991			3076	3810	M	BEN NEVIS FM

Nautilus C-92

Year	Author	Depth Type	Top	Bottom	Units	Formation
2007	CNLOPB	MD		2166	M	BANQUEREAU FM
2007			1996	2166	M	TILTON MB
2007			2166	2166	M	(BASE TERTIARY UNCONFORMITY)
2007			2166		M	DAWSON CANYON FM
2007			2166	2234	M	FOX HARBOUR MB
2007			2461	2512	M	WYANDOT FM
2007			2559	2663	M	PETREL MB
2007			2846	2846	M	(CENOMANIAN UNCONFORMITY)
2007			2846	3237	M	NAUTILUS FM
2007			2978	2978	M	(FAULT)
2007			3237	3337	M	BEN NEVIS FM
2007			3337	3337	M	(APTIAN UNCONFORMITY)
2007			3337	3448	M	AVALON FM
2007			3347	3436	M	(SHALE TONGUE)
2007			3436	3448	M	"A" MARKER MB
2007			3448		M	WHITEROSE FM
2007			3825	4095	M	CATALINA FM
2007			3965	3965	M	(FAULT)
2007			4119	4186	M	"B" MARKER MB
2007			4186	4646	M	HIBERNIA FM
2007			4186	4503	M	SHALE EQUIV OF HIBERNIA UPPER ZONE
2007			4503	4646	M	HIBERNIA LOWER ZONE
2007			4646	4801	M	FORTUNE BAY FM
2007			4801	5116.7	M	JEANNE D'ARC FM
1989	MCALPINE,K.D.			2174	M	BANQUEREAU FM
1989			1996	1996	M	(UNCONFORMITY)
1989			1996	2174	M	SOUTH MARA UNIT
1989			2174	2174	M	(UNCONFORMITY)
1989			2174	2668	M	DAWSON CANYON FM
1989			2559	2663	M	PETREL MB
1989			2668	3285	M	NAUTILUS SHALE
1989			2847	2847	M	
1989			3048	3048	M	(UNCONFORMITY)
1989			3285	3285	M	
1989			3285	3345	M	AVALON FM
1989			3345	3345	M	(UNCONFORMITY)
1989			3345	3866	M	WHITEROSE SHALE (UPPER)
1989			3436	3448	M	("A" MARKER)
1989			3866	4119	M	CATALINA FM
1989			4119	4186	M	("B" MARKER)
1989			4186	4549	M	WHITEROSE SHALE (LOWER)
1989			4549	4647	M	HIBERNIA FM
1989			4647	4802	M	FORTUNE BAY SHALE
1989			4802	5117	M	JEANNE D'ARC FM

1987	WADE,J.A. & SHERWIN,D.F.	2166		M	("K" MARKER)
1987		2462		M	PETREL MB
1987		2883	2883	M	(AVALON UNCONFORMITY)
1987		3319		M	AVALON SANDSTONE
1987		3873		M	CATALINA SAND
1987		4120		M	("B" LIMESTONE)
1987		4504		M	HIBERNIA SAND
1987		4806		M	("J" MARKER)
1985	MCALPINE,K.D.				(SEE UPDATED REPORT)
1983	MOBIL OIL CANADA LTD	2165.4		M	("K" MARKER)
1983		2461.4		M	PETREL LIMESTONE
1983		2882.4	2882.4	M	(UNCONFORMITY)
1983		3318.4		M	("A" SANDSTONE)
1983		3872.4		M	("B" SANDSTONE)
1983		4124.4		M	("B" LIMESTONE)
1983		4503.4		M	HIBERNIA SANDSTONE
1983		4805.4		M	("J" MARKER)

Appendix 6: Tie of well data to seismic line B

a) CDP 2698 from Line HBV83-195

TIME (s)	V_{RMS} (m/s)	X(m)
0.117	1480	86.58
0.300	1609	241.35
0.735	1777	653.05
1.319	1935	1276.13
1.773	2151	1906.86
2.476	2361	2922.92
3.166	2648	4191.78
3.776	2910	5494.08
4.222	3250	6860.75
5.204	3707	9645.61
6.005	3910	11739.78
7.000	4124	14434.00

b) Time vs. depth graph from the velocity survey

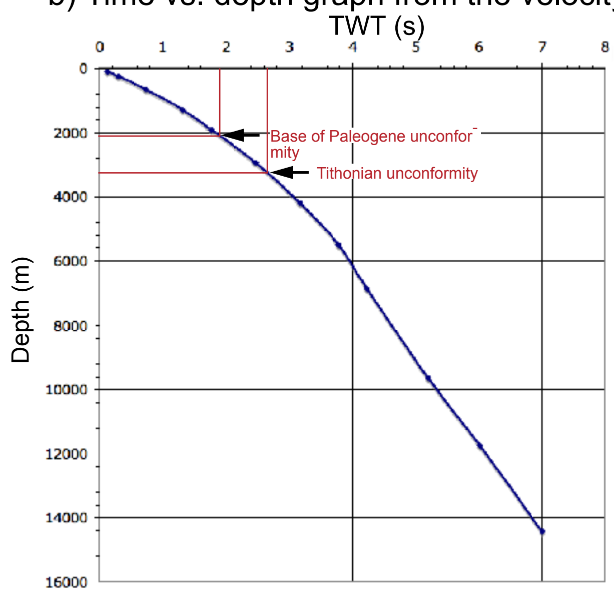

c) Conversion to time for the Flying Foam I-13 well

Depth (m)	TWT (s)	Unconformity
2115.50	1.92	Base of Paleogene
3268.00	2.65	Tithonian

Figure A6-1: a) Velocity survey from the 2D line HBV83-195 and distance in meters (third column) from the Dix equation. The velocity data are from the top of the Flying Foam anticline (see Appendix 3), in approximately the same structural position as that the Flying Foam I-13 well (see Figure 11). b) Time vs. depth graph for the table in a. The graph helps find the TWT for the unconformitties reported in the Flying Foam I-13 well. c) The table shows the conversion to time for the unconformities reported in the Flying Foam I-13 well (CNLOPB, 2012).

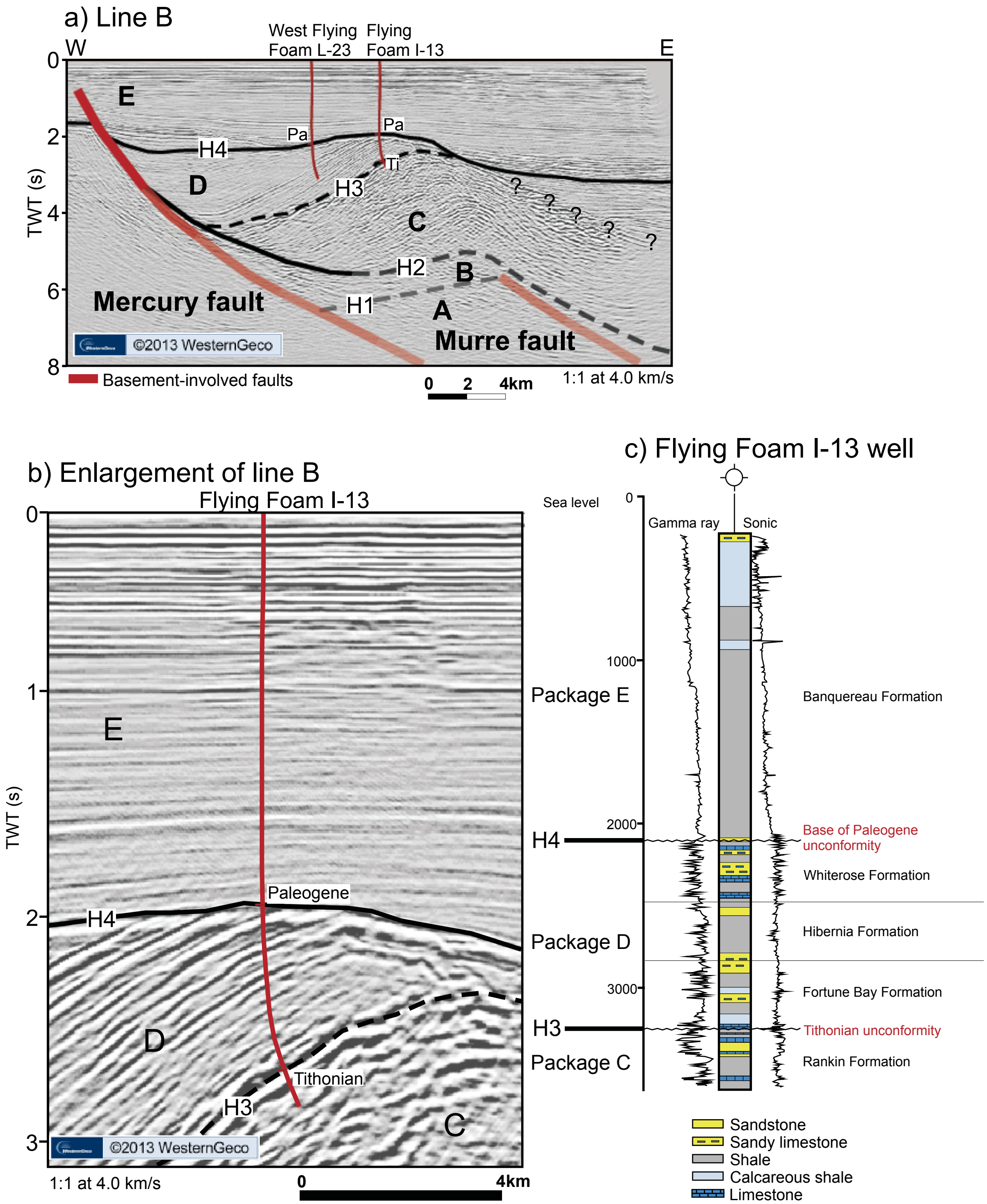

Figure A6-2: a) Seismic line B showing key structural features and tectonostratigraphic packages (other capital letters). H1, H2, H3 and H4 are mapped horizons. b) Enlarged area highlighting the Flying Foam I-13 well. c) Flying Foam I-13 well showing horizons, tectonostratigraphic packages, gamma ray/sonic log, lithologies, formation tops and unconformities. Gamma ray/sonic log and lithologies modified from McAlpine (1990). Unconformities and formation tops modified from CNLOPB (2012).